UC San Diego
UC San Diego Electronic Theses and Dissertations

Title
Bioengineering approaches to study human pluripotent stem cells and their derivatives

Permalink
https://escholarship.org/uc/item/9dj4c6vn

Author
Kumar, Nathan Lee

Publication Date
2015

Peer reviewed|Thesis/dissertation

UNIVERSITY OF CALIFORNIA, SAN DIEGO

Bioengineering approaches to study human pluripotent stem cells and their derivatives

A dissertation submitted in partial satisfaction of the
requirements for the degree Doctor of Philosophy

in

Bioengineering

by

Nathan Lee Kumar

Committee in Charge:

Professor Shu Chien, Co-Chair
Professor Karl Willert, Co-Chair
Professor David Brafman
Professor Karen Christman
Professor Adam Engler
Professor Maike Sander

2015

The dissertation of Nathan Lee Kumar is approved and it is acceptable in

quality and form for publication on microfilm and electronically:

_____

_____

_____

_____

_____

                                                                    Co-Chair

_____

                                                                    Co-Chair

University of California, San Diego

2015

Dedication

To my eternally supportive grandparents

Table of Contents

List of Abbreviations

ACME   Arrayed Cellular Microenvironment

ACT   Activin

BMP   BMP4

CHR   CHIR98014

COL I   Collagen I

COL III   Collagen III

COL IV   Collagen IV

COL V   Collagen V

CYC   Cyclopamine

DKK   Dkk-1

DSM   Dorsomorphin

ECMP   Extracellular Matrix Protein

EGF   EGF

FGF   FGF

FN   Fibronectin

GF   Growth Factor

hES   Human Embryonic Stem

hiPS   Human Induced Pluripotent Stem

hPS   Human Pluripotent Stem

IWP   IWP-2

KGF   KGF

LN   Laminin

NOG   Noggin

PFSC   Posterior foregut stem cell

RSP   R-Spondin

SB4   SB 431542

SHH   SHH

SM   Small Molecule

VGF   VEGF

VN=VTN   Vitronectin

WNT   Wnt3a

List of Figures

List of Tables

Acknowledgements

First, I'd like to thank the people that have been most influential in my graduate career, my advisors, Karl Willert and David Brafman. They have shaped my way of thinking and my approach to scientific questions which has not only made me a better scientist, but also a better person. The invaluable lessons I have learned from them will stay with me through the rest of my scientific career.

Second, I would like to thank my committee members: Shu Chien, Karen Christman, Adam Engler, and Maike Sander for their time, input, and guidance. Despite their busy schedules, they were always willing to chat. It has been very helpful to have successful scientists offering their perspective, allowing me to grow as an independent researcher.

Next, I'd like to thank both past and present Willert and Brafman lab members and friends. I am lucky to have been part of such a friendly, supportive, and intelligent group of people. In particular, Anne Conway, Stephanie Grainger, Antonio Fernandez, Ian Huggins, Eric O'Connor, Karl Marquez, Nisha Patel, Jenna Richter, and Jason Ross were always there to provide any help they could towards my endeavors, whether science-related or not. Others, including Julia Busch, Matt Bauer, Josh Cutts, Ellen Mintz, Angeline Puranen, Kelly Ross, Olivia Gaylord, Crystal, and Nikki were wonderful colleagues throughout the years. They were never too busy to provide scientific insight, patiently taught me so much of what I know now, and were extremely supportive when I needed it most. More importantly, these were my friends, my lab family, and this experience would have been far emptier without them alongside me every day. I would like to thank my friends outside of the lab, both near and far, for being incredibly encouraging and supportive through this journey. Most were not scientists, but were always interested in hearing about my work, often

moreso than I was willing to talk about it at that moment, and always championed my progress. I am so grateful to be supported by my community.

I thank my family, Mom, Pops, and Rachel, for their unwavering encouragement and confidence that I can succeed at whatever I set out to do.   I love you all so much, you've given me everything.

Lastly, I'd like to thank the building personnel at the Sanford Consortium. These hard-working individuals worked as security officers, janitors, building management, and mail couriers. They were always willing to listen to me babble on about science while they shared their smiles. I feel so lucky to have worked in a facility as abundant and luxurious as the Sanford Consortium and I must thank all those that worked towards keeping it that way.

Vita

Education

2009   Bachelor of Science in Biomedical Engineering, *summa cum laude*,

Georgia Institute of Technology, Atlanta, GA

Minor in Finance, Georgia Institute of Technology, Atlanta, GA

2015   Doctor of Philosophy in Bioengineering, University of California, San

Diego, CA

Association Memberships

2007 – 2009   *Alpha Eta Mu Beta*, President (2008-2009)

2007 – 2009   Biomedical Student Advisory Board

2006 – 2009   *Sigma Chi*, Recruitment Chair (2007-2008)

2005   Boy Scouts of America, Eagle Scout

Professional Experience

2008   Horizons Leadership Training, Snowbird, UT

2009   Licensed Georgia Real Estate Salesperson

2009   Research Associate, Life Technologies, Carlsbad, CA

Professional Presentations

2011 – 2013   Stem Cell Meeting on the Mesa, Salk Institute, San Diego, CA

Publications

N Kumar. (2009) Sustained Delivery of Thermally Stabilized chABC by Lipid Microtubules. Georgia Institute of Technology, Department of Biomedical Engineering Undergraduate Theses.

DA Brafman, C Phung, N Kumar, K Willert. (2013) Regulation of endodermal differentiation of human embryonic stem cells through integrin-ECM interactions. *Cell Death & Differentiation* 20(3), 369-381. Provided in Appendix with related experiments described in Chapter 3.

N Kumar, DA Brafman, K Willert. (2015) Generation of an expandable intermediate mesoderm restricted progenitor cell line from human pluripotent stem cells. *Under Review*. A modified version of this manuscript is provided in Chapter 4.

N Kumar, E O'Connor, K Willert. (2015) Endoderm Differentiation from Human Pluripotent Stem Cells. *Working with Stem Cells - Quick and easy methodologies and applications.* An adapted version of this book chapter is provided in Chapter 2.

ABSTRACT OF THE DISSERTATION

Bioengineering approaches to study human pluripotent stem cells and

their derivatives

by

Nathan Lee Kumar

Doctor of Philosophy in Bioengineering

University of California, San Diego, 2015

Professor Shu Chien, Co-Chair

Professor Karl Willert, Co-Chair

Human pluripotent stem (hPS) cells revolutionized tissue engineering with their ability to indefinitely self-renew whilst retaining the potential to differentiate into all mature cell types of the human body. However, the use of hPS cells in regenerative medicine is hindered by contamination with unwanted cell types, which includes

undifferentiated cells capable of forming tumors upon transplantation. In addition, differentiated cell populations are often impure and contain cell types derived from multiple lineages. To overcome these problems requires a complete understanding of differentiation conditions so that hPS cell derivatives are restricted to a single lineage. In addition, to advance the use of hPS cells in regenerative medicine it would be desirable to develop derivative expandable cell populations with restricted differentiation potential. Here I describe a systematic approach to identify conditions that support the derivation and propagation of cell populations associated with specific developmental lineages. Specifically, I will describe approaches to derive and expand multipotent progenitors with either endodermal or mesodermal properties. Employing hPS reporter lines, I based self-renewal of endodermal or mesodermal cells on proliferative capacity and maintenance of gene markers specific to each lineage. Iterative protein screens using a high throughput screening approach referred to as Arrayed Cellular Microenvironments (ACME) identified a fully defined and optimized culture condition that supports the derivation and propagation of a homogenous progenitor cell population with mesodermal properties. This study presents a framework for defining the culture requirements for expanding progenitor populations derived from hPS cells.

Chapter 1. Introduction- Progenitor Expansion

Introduction

Background

Human pluripotent stem cells (hPS cells; including human embryonic stem [hES] cells and human induced pluripotent stem [hiPS] cells) have the potential to generate the various cell types of the adult body. Therefore, hPS cells provide a potentially unlimited source of mature cell types that can be used for disease modeling, drug discovery, and regenerative medicine purposes. Current methods for generating these therapeutically relevant cell types follow a linear approach in which hPS cells are sequentially exposed to soluble growth factors and thusly differentiated in incremental, discrete steps mimicking the sequence of events occurring during development. The initial stage in these protocols typically involves specification of hPS cells into one of the three embryonic germ layers—ectoderm, endoderm, or mesoderm. As such, several protocols have been developed for the generation of hPS cell-derived tissues including neural cell types (Kirkeby et al., 2012; Xi et al., 2012), liver (Touboul et al., 2010), endothelial cells (James et al., 2010), pancreatic islets (D'Amour et al., 2006; Kelly et al., 2011; Kroon et al., 2008; Nostro et al., 2011), cardiovascular cells (Yang et al., 2008), and hematopoietic stem cells (Ledran et al., 2008), to name a few. These studies demonstrate the broad potential of hPS cells for cell replacement therapies but also harbor significant drawbacks: while mature cell types can be generated with variable efficiencies, the resulting populations are heterogeneous and often capable of tumorogenesis when transplanted, which impedes their clinical application. Secondly, these protocols are inefficient in the percentage of input cells that differentiate into their relevant mature cell type, necessitating large numbers of hPS cells to generate cell types in the quantities

necessary for clinical applications. Thirdly, these methods are most often poorly

defined with xenogeneic animal products as crucial factors in the differentiation,

rendering these protocols unsuitable for human therapies. Furthermore, current

differentiation protocols are generally expensive in nature, making it significantly more

challenging to translate them to the scale necessary for clinical use.

One way to overcome these significant drawbacks is to develop fully-defined,

scalable culture systems for the expansion of multipotent intermediate progenitor

cells. Pluripotent stem cell differentiation protocols borrow strongly from cues learned

in developmental biology. Staying faithful to that approach of biomimicry, I focused

my efforts on recapitulating the well-established role that multipotent progenitor stem

cells have within the adult human (Li and Xie, 2005; Morrison and Spradling, 2008;

Scadden, 2006). While pluripotent embryonic stem cells have the ability to give rise

to all three embryonic germ layers—ectoderm, endoderm, and mesoderm (Chambers

and Smith, 2004; Thomson et al., 1998), multipotent progenitor stem cells are

progressively restricted in development, giving rise to a subset of cell types, or are

unipotent, giving rise to single lineage cells (Blanpain et al., 2004; Weissman, 2000;

Zuk et al., 2002). The embryo proper generates multipotent cells that are either germ

line stem cells for reproduction or somatic stem cells for organogenesis. These

intermediate progenitor populations allow blood, bone, gametes, epithelia, nervous

system, and muscle, among others, to be replenished by fresh cells throughout life,

comprising an essential component of tissue homeostasis. To sustain the function of

progenitor cells throughout the organism's life span, specific cues are required to

maintain the delicate balance between self-renewal and differentiation. The

underlying mechanisms controlling this delicate balance are fundamental to

understanding stem cell regulation, tumor formation, and the use of stem cells for

replacement therapies. Thusly, efforts have increasingly focused on identifying the signals that regulate stem cell function within their native tissues, known as the niche.

Importantly, progenitor stem cells can lie dormant over time until activated by specific life stages or due to injury. Knowing that progenitor cells can persist indefinitely while retaining their multipotency, it is theoretically possible to identify the culture conditions necessary to allow for progenitor maintenance and expansion. As such, *in vitro* expansion of intermediate progenitor populations of differentiating hPS cells followed by subsequent differentiation is a feasible approach for generating highly enriched and well-defined cell populations required for cell-based therapies and disease modeling. To that end, I took a systematic approach to define the necessary and sufficient culture conditions to promote expansion of progenitor cells while maintaining their multipotency.

Ecotermally- and endodermally-restricted progenitor populations from hPS cells

Previous studies have successfully expanded intermediate progenitor populations whose differentiation potential is restricted to a particular subset of cell types. For example, homogenous, expandable ectodermally-restricted progenitor populations have been generated from hPS cells (Chambers et al., 2009; Reubinoff et al., 2001; Shin et al., 2006). Ectodermal restriction has been achieved by prolonged exposure of hPS-derived cells to basic fibroblast growth factor and epidermal growth factor. Derivation of enriched neural progenitors was initiated on mouse embryonic fibroblasts (MEFs), ultimately allowing for the propagation of non-tumorigenic ectodermally-restricted progenitor cells over a 20-week period. These neural progenitors could give rise to mature neurons, astrocytes, and oligodendrocytes in vitro and participated in mammalian brain development in vivo.

Similarly, endodermally-restricted progenitor cells display extensive self-renewal in culture while also remaining non-tumorigenic (Cheng et al., 2012). These endoderm progenitors, as they are termed, have the ability to differentiate into endodermal lineages such as liver, pancreas, and intestine and fail to generate mesodermal or ectodermal derivatives in vitro or in vivo. The culture system for endoderm progenitors required undiluted Matrigel and a feeder layer of MEFs, which acted in concert with vascular endothelial growth factor, basic fibroblast growth factor, bone morphogenetic protein 4, and epidermal growth factor to promote indefinite expansion whilst maintaining multipotency. In a separate study, foregut stem cells were generated from hPS cells by using a specific cocktail of growth factors which included activin-A, basic fibroblast growth factor, bone morphogenetic protein 4, hepatocyte growth factor, and epidermal growth factor to maintain multipotency and a strong proliferative capacity (Hannan et al., 2013). While this investigation did not provide in vivo data to support their conclusions, they did show that their foregut stem cells could be induced to express markers indicative of the hepatic, pancreatic, or lung/thyroid lineages.

Although these studies show that the expansion of lineage-restricted progenitors is possible, the methods used are undefined and call for xenogeneic feeder layers to achieve progenitor expansion. These protocols may shed light on the developmental cues required for self-renewal of multipotent progenitors, but their clinical application is hampered by their undefined and poorly-scalable nature. In order to generate progenitors useful for cell replacement therapies, the specific cues that maintain the progenitor niche will need to be fully defined. This means that the signals provided by the xenogeneic factors and supporting cells will have to be recapitulated in defined, serum-free culture systems. One way to achieve this is

through optimizing the cell microenvironment without the use of animal products.
Before describing the experimental approach for optimization, let us first discuss the
elements of the microenvironment.

The cell microenvironment

The cell's microenvironment affects its intrinsic genetic programs, making it
critical to regulating self-renewal and differentiation of many progenitor populations
within the developing and fully mature adult organism. The microenvironment
includes cues from soluble growth factors and small molecules, extracellular matrix
interactions, cell-cell interactions, and mechanical forces (Chen et al., 1999;
Schofield, 1978). Firstly, soluble growth factors can exert long-range, potent effects
on stem cell behavior. Purified growth factors have been made commercially
available and, due to their solubility, can easily be added to cells' growth media to
exert mitogenic effects. Thusly, their relative ease of study have made growth factors
and their downstream signal transduction events well studied as determinants of stem
cell fate (Lowry and Richter, 2007; Molofsky et al., 2004; Rho et al., 2006). Secondly,
the extracellular matrix (ECM) is primarily defined as the adhesive substrate that
anchors cells within their microenvironment (Berrier and Yamada, 2007; Eshghi and
Schaffer, 2008; Humphries et al., 2006). The ECM in any given tissue is often
comprised of a mix of different proteins, most typically collagens, fibronectins,
vitronectin and laminins. The ECM can provide instructive cues for cells, by way of
the integrin family of cell surface adhesion receptors as well as by matrix elasticity
(Engler et al., 2006). In mammals, 24 heterodimeric integrin receptors consisting of
one of 18 α-subunits and one of 8 β-subunits have been identified. In addition to
mediating binding to specific ECMPs, integrin signaling serves as a link between the

extracellular and intracellular environments and in turn modulates various

downstream signaling pathways and components, such as MEK–ERK, PI3-kinase,

and SRC (Prowse et al., 2011). Moreover, many of these downstream pathways have

previously been implicated in regulating hESC self-renewal, proliferation, and

differentiation. Therefore, the study of ECMP-integrin signaling is important in

understanding the mechanisms that control hESC differentiation. Lastly, stem cells

are greatly influenced by the direct cell-cell signaling relationships that are

established with their neighbors. Through the interaction of cell-surface molecules,

these cell-cell contacts facilitate diffusion between cells and clustering of receptors,

which serves to polarize cells. Since screening various cell-cell interactions is

arduous and impractical, I focused my efforts on screening soluble growth factors and

extracellular matrix interactions.

Experimental Approach

There have been several recent findings that naturally-derived and synthetic

microenvironments can be engineered to gain control over stem cell fate (Ra'em and

Cohen, 2012). These studies commandeered microenvironmental cues from

development to cajole sensitive stem cells into committing to more mature specialized

tissues. To this end, I used a multifactorial high-throughput screening technology

(Brafman et al., 2012; Flaim et al., 2005) to study the effects of various bioactive

signals and consequently engineer *in vitro* microenvironments that allow for the

homogenous expansion of a hPS cell-derived progenitor population restricted to

either the endodermal or mesodermal lineage. In order to optimize the factors

necessary for progenitor expansion, I found it prudent to follow the basic principles of

high-throughput screening (Figure 1-1). Flow cytometric sorting was used to isolate a

homogenous starting population onto arrays containing the majority of possible microenvironments, after which I quantified proteins of interest to determine effects of each microenvironment. Beginning with a pure homogenous cell population is crucial to the validity of the results by limiting the experimental artifacts in the final output assay. Heterogeneity in the starting population adds a confounding variable that consequently makes the readout harder to interpret, since variations could be due to either the varying factors being tested or the varying starting populations. The arrayed cellular microenvironments onto which the pure cell populations are seeded should ideally contain all possible culture combinations. The nature of the screening platform is to present all unique combinatorials so that results are comprehensive as possible, taking care not to exclude conditions that may serve as potential valuable data, or hits. After seeding a homogenous starting population onto the comprehensive screening platform, the final assay provides a readout for measuring the effects of each screened condition, i.e. each microenvironment. This final assay should measure the protein of interest that provides the most sensitivity (least false negatives) and specificity (least false positives) to the experiment. After performing the high-throughput screens, I moved on to scale up the optimal hits from these screens into traditional cell culture formats in order to study the long-term effects of these culture conditions on progenitor expansion and maintenance.

In conclusion, I have set out to employ a high throughput screening platform known as arrayed cellular microenvironments in order to identify and optimize the necessary culture conditions for expansion and maintenance of a multipotent endodermally- or mesodermally-restricted progenitor population from hPS cells. To do so, I have screened the combinatorial effects of extracellular matrix proteins known to be crucially involved in embryogenesis as well as growth factors and small

molecules known to activate or antagonize the major signaling pathways for their ability to promote adhesion and maintenance of either endodermal or mesodermal markers. Previous studies have identified conditions that are sufficient for indefinite expansion of ectodermally- and endodermally-restricted progenitor populations from hPS cells. In these studies, multipotent progenitor populations were shown to possess strong proliferation capacity without tumorigenicity and were capable of subsequent differentiation into more mature linage-restricted derivatives. However, these culture methods are severely limited in their application to human therapeutics due to their dependence on poorly defined, xenogeneic factors. To amend these limitations, I am using only fully-defined, non-xenogeneic factors for optimizing culture conditions that foster expansion of endodermally- or mesodermally-restricted progenitor populations while maintaining their potential to differentiate into more specialized lineage-restricted tissues.
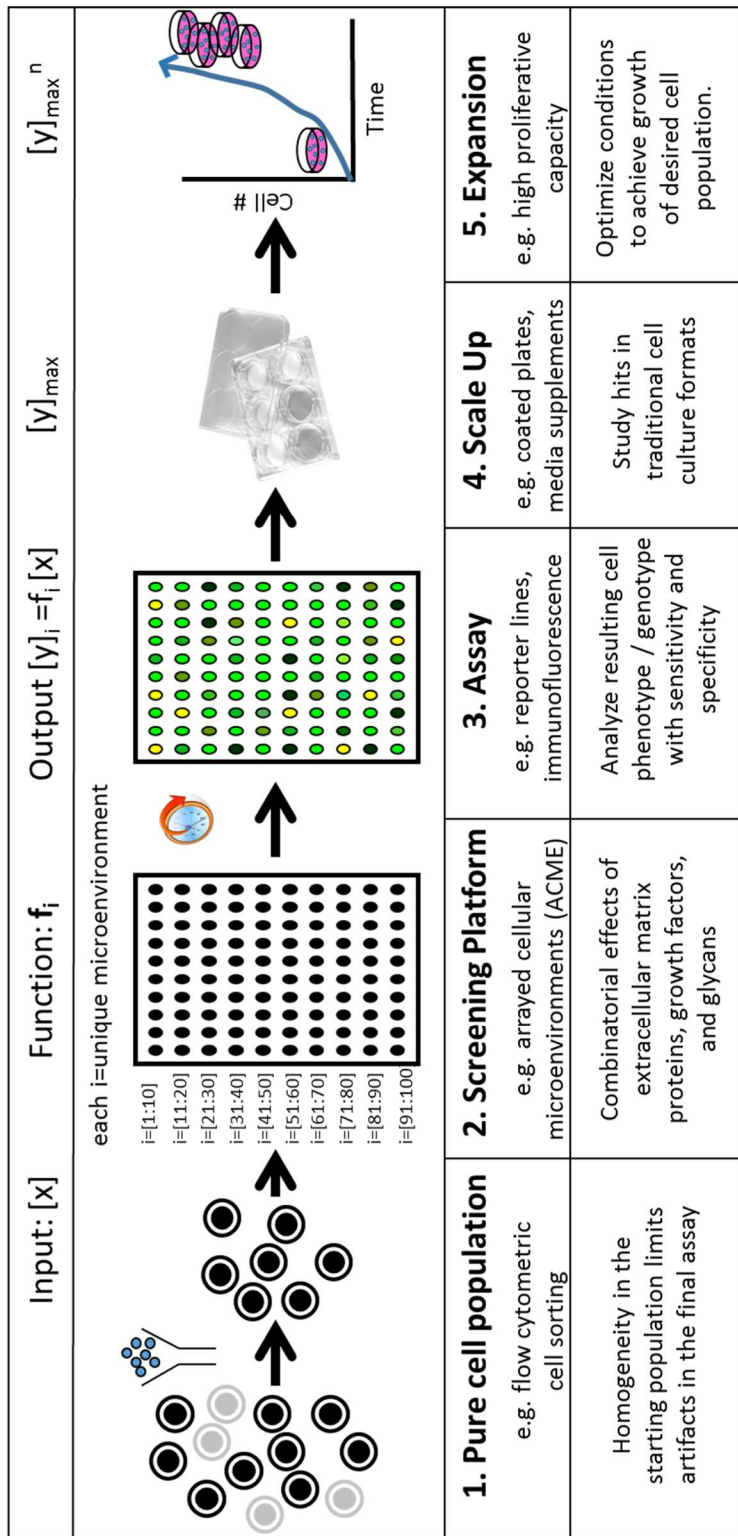
Figure 1-1. High-throughput screening flowchart. When performing high-throughput screens, it is important to begin with a pure population to limit confounding variables. The screening platform should be robust, including as many conditions as possible to increase comprehensiveness of the screen. The final readout should be sensitive to the results of interest so as to limit false positives and false negatives. Importantly, results from high-throughput screens should be scaled up to ensure the validity of results on a macroscopic scale. Finally, scaled up cultures should be tested for their ability to undergo expansion of the desired cell type.

Chapter 2. Endoderm Differentiation from Human Pluripotent Stem

Cells

Abstract

Human pluripotent stem cells (hPSCs) provide a virtually unlimited raw material to derive and engineer mature cell types with therapeutic value, including cell transplantation, disease modeling and drug screening. The first step to differentiate hPSCs into such cell types involves specification towards one of the three main embryonic cell populations, ecto-, endo- and mesoderm. Efficient induction into the correct lineage is critical to the success of subsequent differentiation steps and to the final yield of desired cells. Here we describe methods to generate definitive endoderm (DE), the progenitor cell population for such tissues as the thymus, liver, pancreas, stomach and intestine. In addition, we will provide methods to characterize and monitor the efficiency of DE differentiation. In addition, we will outline flow cytometry based methods to isolate and purify cells with DE properties. Such enrichment strategies are useful to eliminate undesired cell populations, especially undifferentiated hPSCs, which harbor the potential risk for seeding tumors upon transplantation. Furthermore, although these methods are described specifically for DE isolation, the basic methodologies for cell dissociation and analysis are applicable to many other hPSC derivative cell populations.

Introduction

In mammalian development, definitive endoderm gives rise to the epithelial lining of the respiratory and digestive tract as well as several major organs including the liver, lungs, intestines, pancreas, thymus and thyroid. The generation of these tissue types makes definitive endoderm distinct from extraembryonic tissues such as primitive endoderm, which includes visceral endoderm and parietal endoderm. During gastrulation, undifferentiated cells from specific regions of the epiblast ingress to the posterior structure known as the primitive streak where they undergo an

epithelial-to-mesenchymal transition, ultimately bringing about the mesodermal and endodermal tissues of the organism. It is this close relationship between mesoderm and endoderm development that supports the hypothesis that both lineages are inaugurated from a common bipotential precursor known as the mesendoderm, although the existence of a single embryonic cell with bipotential properties has yet to be substantiated in mammals. Nonetheless, the complex relationship between the two nascent germ layers is associated with the proximity in which endoderm and mesoderm spawn. Complexity within this signaling environment is in part attributed to the numerous growth factors produced by the primitive streak that likely act in various combinations to induce either endoderm or mesoderm (Beddington and Smith, 1993; Conlon et al., 1994; Faust and Magnuson, 1993; Tam and Behringer, 1997). The use of DE cells for the study and treatment of a variety of endoderm-associated diseases requires the development of scalable and robust protocols for the efficient generation of DE cells from hPSCs with minimal contamination of other germ layers. Here, we present an *in vitro* differentiation protocol based on the modulation of TGF-β and WNT signaling, as it occurs *in vivo*, that allows for the consistent and highly efficient generation of DE cells from hPSCs.

The earliest stages of DE commitment *in vivo* implicate an essential role for one such growth factor Nodal, a member of the TGF-β superfamily. However, applying this developmental knowledge to the generation of definitive endoderm *in vitro* is hampered by the inaccessibility of a source for highly active Nodal proteins. Fortuitously, activin, another member of the TGFβ superfamily which is readily sourced, binds to the same receptors as Nodal, excluding Nodal's coreceptor cripto, and is capable of triggering similar intracellular cascades. By that virtue, activin has been successfully used to activate the intracellular TGF-β pathways necessary for

endoderm commitment. Another transduction pathway known to be involved in formation of the primitive streak and subsequent definitive endoderm specification is that of the paramount canonical WNT family of proteins, which are highly conserved across species from fruit flies, where it was originally studied, all the way to humans. Genetic analyses in mice have shown that disruption of the WNT pathway prevents formation of the primitive streak and, subsequently, definitive endoderm (Haegel et al., 1995; Kelly et al., 2004; Liu et al., 1999). Since it is within reason that the signals directing endoderm differentiation in normal development could also instruct hPS cells to commit to an endodermal fate, previous work has mimicked these developmental cues to design cell culture techniques for deriving functional definitive endoderm cells from hPS cells (D'Amour et al., 2005; Hay et al., 2008; Kubo et al., 2004; Yasunaga et al., 2005). Triggering these two signaling pathways, TGF-β and WNT, at the proper time intervals has been shown to efficiently generate functional definitive endoderm in vitro. Here, we present a differentiation protocol (**Figure 1**) based on the modulation of TGF-β and WNT signaling that allows for the consistent and highly efficient generation of DE cells from hPS cells. Definitive endoderm can subsequently be differentiated into tissues of the anterior foregut, posterior foregut, and midgut/hindgut to obtain more specialized tissues, such as those of the liver and pancreas. These differentiation methods will serve as the building blocks to one day apply these cell types in functional regenerative medicine therapies, disease modeling, and drug discovery.
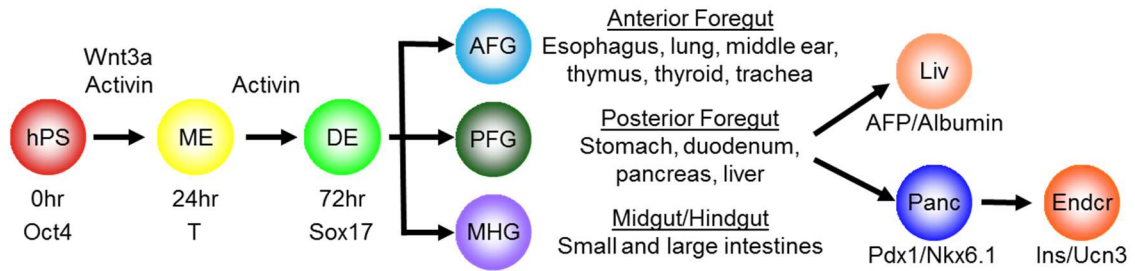
Figure 2-1. Differentiation schematic of definitive endoderm and derivative cell types. Timed exposure of hES cells to Wnt3a and Activin induces definitive endoderm formation in vitro. Definitive endoderm is subsequently capable of differentiating into tissues of the anterior foregut, posterior foregut, and midgut/hindgut. More mature cell types such as that of liver and pancreas can be further specified. ME=Mesendoderm, DE=Definitive Endoderm, AFG=Anterior Foregut, PFG=Posterior Foregut, MHG=Midgut/Hindgut, Liv=Liver, Panc=Pancreas, Endcr=Endocrine.

Materials

Equipment and Supplies

1. Biological safety cabinet

2. CO_2 incubator with humidity and gas controls to maintain a stable environment of 37°C, >95% humidity, and 5% CO_2

3. Water bath set at 37°C

4. Benchtop cell culture centrifuge

5. Pipet Controller

6. Serological pipettes (1, 5, 10, and 25 ml)

7. 10-, 20-, 200-, and 1,000 µl micropipette

8. 10-, 20-, 200-, and 1,000 µl micropipette tips

9. Tissue culture treated polystyrene dishes: 6-well, 12-well, and 24-well and 100 mm

10. 1.5 ml microcentrifuge tubes

11. Polystyrene conical tubes: 15- and 50- ml

12. Hemacytometer

13. Inverted light microscope with 4X, 10X, and 20X phase objectives

14. Bio-Rad Real-Time PCR System (or equivalent)

15. Falcon no. 2052 no. 2054 tubes

16. Becton Dickinson FACSCanto machine (or equivalent)

17. Becton Dickinson FACSAria machine (or equivalent)

Stock Solutions and Reagents

1. MEF-conditioned medium for maintenance of undifferentiated human ESCs. Make aliquots of 50 ml and store at 4°C.

2. RPMI (RPMI; Mediatech, cat.no. 15-040-CM)

3. Knockout™ DMEM (RPMI; Life Technologies, cat.no. 10829-018)

4. Fetal Bovine Serum (FBS; HyClone, cat.no. SH30070.01)

5. 100X MEM nono-essential amino acids solution (NEAA; Life Technologies; cat.no. 11140-050). Make aliquots of 5 ml and store at 4°C.

6. Penicillin-Sterptomycin (P/S) 5,000 U/ml (Life Technologies; cat.no. 15070-063). Make aliquots of 5 ml and store at -20°C.

7. GlutaMAX™ supplement (Life Technologies; cat.no. 35050-061). Make aliquots of 5 ml and store at -20°C.

8. Phosphate-Buffered Saline (PBS), ph 7.4 (Life Technologies, cat.no. 10010023)

9. StemPro® Accutase® cell dissociation reagent (Life Technologies, cat.no. A1110501). Make aliquots of 10 ml and store at -20°C.

10. Matrigel™, (BD Biosciences, cat.no. 354277)). Make aliquots of 250 μl and store at -20°C.

11. Trypan Blue Solution, 0.4% (Life Technologies, cat.no. 15250-061)

12. Rho-associated protein kinase inhibitor (ROCKi, Y-27632; EMD Millipore, cat.no. SCM075). Dissolve in DMSO at a concentration of 5mM. Make aliquots of 50 µl in 1.5 ml microcentrifuge tubes and store at -20°C. Protect from light. A final concentration of 10µM will be used for sorting live cells for continued culture by fluorescence-activated cell sorting (FACS).

13. Human recombinant bFGF (Life Technologies, cat.no. PHG6014). Reconstitute in sterile, distilled water at a concentration of 30 µg/ml. Make aliquots of 50 µl in 1.5 ml microcentrifuge tubes and store at -20°C. A final concentration of 30 ng/ml is used to culture and expand hPS cells.

14. Activin A (R&D Systems, cat.no. 338-AC-010)

15. CHIR99021 (Stemgent, cat.no. 04-0004)

16. Wnt3a (R&D Systems, cat.no. 1324-WN-002)

17. Fibronectin (FN) from human plasma, 1 mg/ml solution (Sigma, cat.no. F0895). Make aliquots of 1.0ml in 1.5ml microcentrifuge tubes and store at -20°C.

18. Vitronectin (VN) from human plasma, lyophilized (Sigma, cat.no. V8379). Make aliquots of 100µl in 1.5ml microcentrifuge tubes and store at -20°C.

19. Taqman Gene Expression Master Mix (Life Technologies, cat.no. 4369016)

20. CXCR4 Antibody (BD Biosciences, cat.no. 555976)

21. SOX17 Antibody (R&D Systems, cat.no. AF1924, 1:200 working concentration)

22. FOXA2 Antibody (R&D Systems, cat.no. AF2400, 1:200 working concentration)

23. Alexa Fluor 647 conjugated donkey anti-mouse IgG (Life Technologies, cat.no. A31571)

24. Alexa Fluor 647 conjugated donkey anti-goat IgG (Life Technologies, cat.no. A21447)

25. Alexa Fluor 647 conjugated donkey anti-rabbit IgG (Life Technologies, cat. no. A31573)

26. Alexa Fluor 488 conjugated donkey anti-mouse IgG (Life Technologies, cat. no. A21202)

27. Hoechst 33342 10mg/mL (Life Technologies, cat.no. H3570)

Derivation of Definitive Endoderm

The definitive endoderm derived from hPS cells is theoretically capable of becoming any of the endodermal derivatives, which include the epithelial lining of the respiratory and digestive tract as well as the liver, lungs, intestines, pancreas, thymus and thyroid. Therefore, directing hPS cells into definitive endoderm is a prerequisite for generating more mature endodermal tissues. The first such directed differentiation study was introduced by Kubo, which successfully differentiated mouse ES cells in embryoid bodies (EBs) into definitive endoderm with high doses of activin (Kubo et al., 2004). Kubo showed that EBs cultured in activin consisted of more than 50% forkhead box A2 (Foxa2)+ endoderm. Foxa2 is a pan-endoderm transcription factor that includes extra-embryonic visceral endoderm, is also expressed in axial mesoderm, and is therefore not specific to definitive endoderm (Ang et al., 1993; Sasaki and Hogan, 1993). Thereafter, Yasanuga employed reporter lines to induce mouse ES cells in monolayer to endoderm by way of high activin doses while simultaneously monitoring expression of Goosecoid (Gsc) and SRY-box 17 (Sox17) (Yasunaga et al., 2005). The use of the reporter lines allowed for distinction of definitive endoderm (Gsc+ Sox17+) from visceral endoderm (Gsc−Sox17+), so as to define culture conditions that permit for selective differentiation to either definitive or visceral endoderm.

Subsequently, D'Amour efficiently differentiated hES cells in monolayer into definitive endoderm using activin (D'Amour et al., 2005, 2006). In this protocol, initial mesendoderm differentiation of hES cells was induced using low concentrations of fetal bovine serum (FBS) supplemented with Wnt3a and activin, resulting in 80% definitive endoderm efficiency, as measure by co-expression of SOX17 and FOXA2. Specifically, hES cells were differentiated on Matrigel (BD Biosciences) beginning when the cultures reached 60%-80% confluency. Differentiation was carried out in RPMI (Mediatech) supplemented with Glutamax, penicillin/streptomycin and either 0% on the first day, then 0.2% (v/v) of defined FBS (HyClone) on days 2-3. On day 1, mesendoderm was induced using 25 ng/mL Wnt3a and 100 ng/mL activin. On days 2-3, 100 ng/mL activin was added to the cultures. At day 3, cells could be collected for analysis to assess efficiency of definitive endoderm differentiation. See protocols below for step-by-step instructions for hPS cell passaging and definitive endoderm differentiation.

Passaging of hPS cells

<u>Protocol</u>

Coating Plates with Matrigel Matrix

1. Thaw undiluted Matrigel™ on ice.

2. Make a 1:100 dilution of Matrigel™ in cold Knockout DMEM. The working solution of Matrigel™ should be maintained on ice and can be stored at 2 – 8 °C for up to 2 weeks.

3. Coat the desired number of plates with Matrigel (approximately 7 mL per 10 cm plate and 0.5 mL per well of a 24-well plate) and incubate for 1 - 2 hours at room temperature or at 37°C for 30 minutes.

4. Aspirate the Matrigel™ solution and wash once with sterile 1X PBS immediately prior to plating the cells.

5. Aliquot any remaining undiluted thawed Matrigel™ into pre-cooled tubes and store at ≤-20 °C.

Cell Dissociation

1. Warm the MEF-conditioned medium and Accutase ® solution in a 37°C water bath.

2. Aspirate MEF-conditioned medium from the growing hPS cells and gently wash with sterile 1X PBS. Add 5 mL of Accutase cell detachment solution to each 10 cm plate. Incubate at 37 °C for 3 - 5 minutes or until cells begin to slough off the plate. Gently tap the sides of the plate against a solid surface to ensure complete cell dissociation. If using cells from multiple plates, work in small batches (1 - 2 plates at once), so cells are not exposed to Accutase for an extended period of time.

3. Add 5 ml of MEF-conditioned medium to the plate. Using a 10 ml serological pipette, gently pipette over the plate until all the cells become detached.

4. Gently triturate the cell suspension until all noticeable cell clumps are broken up.

5. Transfer the cell suspension to a 15 mL centrifuge tube.

1. Take 10 µl of the cell suspension to perform a viable cell count using Trypan Blue and a hemocytometer.

6. Centrifuge the tube at 200 x g for 4 minutes.

Cell Plating

2. Resuspend the pellet in the appropriate amount of MEF-conditioned medium so that the final cell concentration is 1.5×10^5 cells/cm^2 of culture dish area.

3. Add 10 mM ROCKi and 30 ng/ml of bFGF to the cell suspension. ROCKi is only added during passaging to aid in hPS cell survival.

4. Plate the cells onto prepared Matrigel™ coated plates at a concentration of 1.5 x 10^5 cells/cm^2. Use 10 mL of MEF Conditioned Media per 10 cm plate and 0.6 mL/well of a 24-well plate.

5. Place the plate in the CO_2 incubator. Gently move the plate in several quick horizontal and vertical motions to disperse the cells evenly across the cell culture surface.

6. Grow overnight at 37 °C and 5% $C0_2$. The next day, each plate should contain tightly packed colonies of cells. Change the medium daily by aspirating the old medium and adding 10 ml of fresh MEF-conditioned medium supplemented with 30 ng/mL bFGF.

7. After 72 hours of growth, the cells should be 60-80% confluent and ready for endoderm induction.

Note: As an alternative to plating cells at a lower density and initiating differentiation 72 hours later as described above, cells can be plated at 1.1 x 10^6 cells/cm^2 and differentiated the following day. This method may introduce lower efficiency of differentiation.

Differentiation to definitive endoderm using growth factors

<u>Protocol</u>

Day 1 of Differentiation

1. Determine the required amount of Day 1 Differentiation Media. Larger volumes of media are required at day 1 to ensure plates do not become too acidic. Use 15 mL of media per 10 cm plate and 1.5 mL per well of a 24-well plate.

2. Prepare the required amount of Day 1 Differentiation Media: In RPMI, add 1x GlutaMAX and supplement with 25 ng/mL Wnt3a and 100 ng/mL Activin-A (25 ng/mL Wnt3a is sufficient for endoderm induction but we empirically determined that adding up to 80 ng/mL increases efficiency, albeit marginally).

3. Warm Day 1 Differentiation Media in a $37^{O}C$ water bath.

4. Aspirate the MEF-conditioned medium from each plate/well.

5. Gently wash each plate/well once with sterile 1X PBS. Use approximately 10 mL per 10 cm plate and 0.5 - 1.0 mL/well of a 24-well plate.

6. Add prepared Day 1 Differentiation Media to each plate and incubate overnight at 37 °C and 5% $C0_2$. Some cell death will occur in the first 24 hours.

Days 2 and 3 of Differentiation

1. Determine the required amount of Day 2 Differentiation Media. Use 10 mL of media per 10 cm plate and 1.0 mL per well of a 24-well plate.

2. Prepare the required amount of Day 2 Differentiation Media: In RPMI, add 1x GlutaMAX, 0.2% FBS, and supplement with 100 ng/mL Activin-A.

3. Warm Day 2 Differentiation Media in a $37^{O}C$ water bath.

4. Aspirate Day 1 Differentiation Media and replace it with Day 2 Differentiation Media.

5. Repeat steps 1 – 4 on Day 3 (Day 3 and Day 2 Differentiation Media are of the

    same composition, although media should be prepared fresh the day of feeding).

On Day 4 (at 72 hours of differentiation), the cells are ready for further differentiation
to downstream cell types or analysis.

Differentiation to definitive endoderm in defined conditions

The variability in endoderm differentiation across cell lines and from batch to
batch suggests that additional factors are required for efficient definitive endoderm
differentiation. We sought to investigate to what extent ECMPs affect the endodermal
differentiation of three hES cell lines, H9, HUES1, and HUES9 (Brafman et al., 2013).
To do so, we employed a cellular microarray screening platform previously developed
in our laboratory (Brafman et al., 2009a, 2009b, 2010, 2012). In this screening
platform, all possible combinations of seven ECMPs, collagen I (COL I), collagen III
(COL III), collagen IV (COL IV), collagen V (COL V), FN, laminin (LN) and VTN were
printed on microscope slides. For comparison we included Matrigel, the undefined
matrix that is used in the standard definitive endoderm differentiations. These arrays
were seeded with hES cells and the medium was supplemented with Wnt3a and
Activin A to promote endodermal differentiation. After three days of endoderm
induction on the arrays, cells were fixed, stained, and imaged for the definitive
endoderm marker SOX17. The results of these screens identified FN and VTN to be
the most effective universal promoters of DE differentiation across cell lines, which
was verified in scaled-up conventional cell culture formats, once again including
Matrigel as a control for reference.

<u>Protocol</u>

Coating Plates with FN-VTN Matrix

1. Determine the minimal volume of sterile 1X PBS needed to coat the desired
    number of plates, aliquot into a culture tube, and precool the PBS in its tube on
    ice for 30 min. This is important to avoid coating the culture tube with the defined
    matrix.

2. Dilute FN to 5 µg per cm^2 of culture dish surface in the precooled minimal PBS
    volume. Similarly, dilute VTN to 5 µg per cm^2 of culture dish surface in the same
    PBS. Once diluted, the solution should be used immediately for coating.

3. Coat the desired number of plates with FN-VTN PBS (approximately 7 mL per 10
    cm plate and 0.5 mL per well of a 24-well plate) and incubate for 1 - 2 hours at 37
    °C. Alternatively, plates can be coated overnight at 4 °C. Once coated, plates
    can be stored for 1-2 weeks at 4 °C, in which case the edges should be sealed
    with parafilm to avoid evaporation.

4. Remove the FN-VTN PBS solution by air drying prior to plating the cells. Excess
    volume can be aspirated, although this is not necessary.

*Proceed with Cell Dissociation, Cell Plating, and Days 1-3 of Differentiation as
described above*

Differentiation to definitive endoderm using small molecules

  Small molecules have been extensively studied for their ability to induce
endoderm formation from hPS cells (Borowiak et al., 2009; Chen et al., 2009; Hoveizi
et al., 2014; Takeuchi et al., 2014; Zhu et al., 2009). The use of small molecule
inhibitors can serve as a robust and scalable tool to efficiently and reproducibly direct

hPS cells toward a desired fate. To that end, recent reports have found that the

Wnt3a protein, which must be generated and purified, can instead be mimicked by

small molecule-mediated inhibition of glycogen synthase kinase 3 (GSK-3) (Bone et

al., 2011; Naujok et al., 2014). Bone successfully showed that activin in conjunction

with GSK-3 inhibition produced >60% CXCR4+ definitive endoderm cells and

exhibited SOX17 and FOXA2 protein expression by Western blot analysis. Further,

this study demonstrated the dose dependence of GSK-3 inhibition on the

differentiation potential of hPS cells, wherein low doses allowed for endodermal and

mesodermal fates while high doses restricted the differentiation to mesodermal

tissues. We have also observed GSK-3 inhibition in conjunction with activin to

promote definitive endoderm formation in a dose dependent manner (Figure 2-2A)

and actually found that certain doses produced greater efficiencies of CXCR4

expression as well as higher total cell numbers (Figure 2-2B). These studies

demonstrate the successful use of a small molecule-based mechanistic approach to

in vitro differentiation protocols such as that of endoderm derivation.
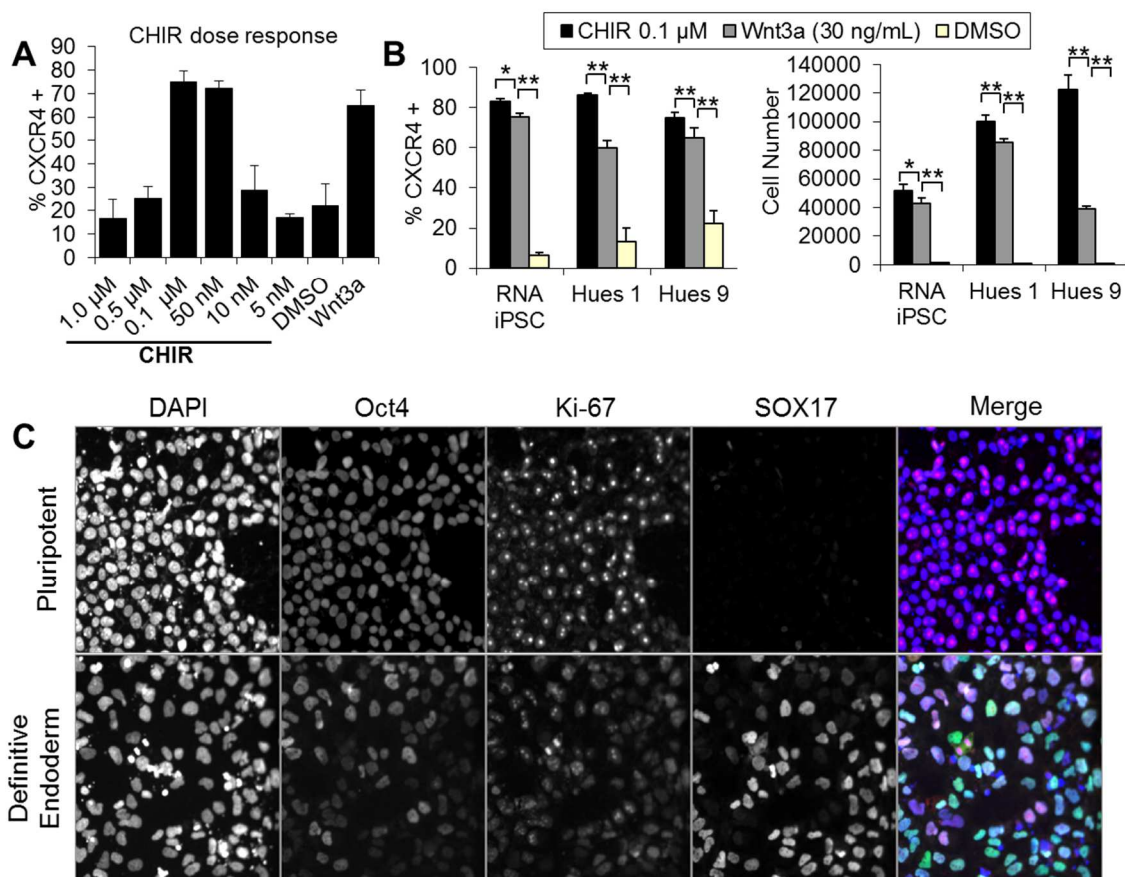
Figure 2-2. Differentiation to definitive endoderm using small molecules. A) A dose response of CHIR induction on CXCR4 expression by flow cytometry. This analysis was performed on Hues 9 hPS cells 72 hours after endoderm induction wherein CHIR was used place of Wnt3a. **B)** The optimal dose of CHIR, 0.1 μM, was tested across three different cell lines and assayed for CXCR4 expression and cell number by flow cytometry. Cell numbers indicated are for one well of a 24-well plate. Wnt3a at 25 ng/mL was used as a positive control and DMSO was used as a negative control. **C)** Immunofluorescence of pluripotent cells and 72 hour definitive endoderm cells from Hues 9. Samples were fixed, permeabilized, and stained for DAPI, OCT4, Ki-67, and SOX17.

<u>Protocol</u>

Perform Passaging of hPS cells, Cell Dissociation and Cell Plating as described

above

Day 1 of Differentiation

1. Determine the required amount of Day 1 Differentiation Media. Larger volumes of media are required at day 1 to ensure plates do not become too acidic. Use 15 mL of media per 10 cm plate and 1.5 mL per well of a 24-well plate.

2. Prepare the required amount of Day 1 Differentiation Media: In RPMI, add 1x GlutaMAX and supplement with 0.1 µM CHIR and 100 ng/mL Activin-A (0.1 µM CHIR was optimal for the cell lines we tested, but further optimization may be required for other cell lines).

3. Warm Day 1 Differentiation Media in a $37^{O}C$ water bath.

4. Aspirate the MEF-conditioned medium from each plate/well.

5. Gently wash each plate/well once with sterile 1X PBS. Use approximately 10 mL per 10 cm plate and 0.5 - 1.0 mL/well of a 24-well plate.

6. Add prepared Day 1 Differentiation Media to each plate and incubate overnight at 37 °C and 5% $C0_2$. Some cell death will occur in the first 24 hours.

Proceed with Days 2-3 of Differentiation as described above

Characterization of Definitive Endoderm

Population-Level Characterization

To characterize the generation of definitive endoderm, gene expression can be analyzed at the population level, which must be validated by single-cell analysis in order to determine the efficiency of definitive endoderm production. Since many genes expressed in definitive endoderm are also expressed in other embryonic tissues, definitive endoderm can only be accurately identified by measuring the gene expression of multiple markers of target and nontarget cell types.

qPCR

To test for the generation of definitive endoderm at the population level, real-time quantitative reverse transcription polymerase chain reaction (real-time qRT-PCR or qPCR) can be used to detect the expression levels of genes expressed in vertebrate definitive endoderm such as *SOX17*, *GSC* and *FOXA2*.   Since these genes are also expressed in extra-embryonic primitive, parietal, and/or visceral endoderm, it is necessary to simultaneously detect for the absence of markers specific to extra-embyronic endoderm such as *SOX7*, a gene marker that should not exist in definitive endoderm. Along similar lines, it is important to assess the purity of definitive endoderm by ensuring low gene expression levels for markers of mesoderm, such as *T*, *MESP1*, or *MEOX1*, and ectoderm, such as *SOX1*, *PAX6*, or *Nestin*. In order to extrapolate meaningful data from gene expression assays like qPCR, it is always helpful to include untreated controls, such as a pluripotent sample, to determine the relative expression for the genes of interest.

Equipment required: Bio-Rad Real-Time PCR System (or equivalent).

Protocol

1. Before running gene expression analysis, isolate total RNA from samples to use as a template for cDNA synthesis. Many kits are available but the gold standard for total RNA extraction is Trizol Reagent (Life Technologies #15596-026).

2. Perform reverse transcription to obtain cDNA from RNA samples (Life Technologies #4387406).

3. Evaluate the cDNA using a spectrophotometer to determine plasmid concentration and UV absorbance (A_{260}/A_{280}), which should be between 1.7 and 1.9 for pure DNA. It is recommended that you use 1 to 100 ng cDNA per 20-µL

amplification reaction and that the same amount of cDNA is used in each reaction.

Note: If you do not need to proceed immediately with PCR amplification, cDNA can be stored at -20 °C. Make smaller aliquots to avoid repeated freeze-thaw cycles.

4. Prepare reaction mix. Thaw reagents on ice, resuspend by gentle vortexing, and briefly centrifuge to bring liquid to the bottom of the tube.

5. Calculate the number of reactions. It is recommended that you perform four replicates per sample/gene and that endogenous controls are included. Optionally, a no template control for each gene expression assay can also be included.

6. For each sample, pipet the following into a nuclease-free 1.5 mL microcentrifuge tube, accounting for the total number of reactions run in quadruplicate: 10 µL 2x Taqman Gene Expression Master Mix (Life Technologies # 4369016), 4 µL cDNA template (1 to 100 ng), 6 µL RNAse-free water. Remember to include 20% excess to compensate for volume loss from pipetting.

7. Load the plate. Transfer 20 µL of PCR reaction into each well of a 48-, 96-, or 384-well plate.

8. Seal the plate with the appropriate cover. Centrifuge the plate briefly. Load the plate into the instrument.

9. Create the plate document for the run using the appropriate plate parameters and run the plate.

Single-Cell-Level Characterization

In order to characterize definitive endoderm cells at the single-cell level and quantify the percentage within a given mixed population, antibody detection can be

used. In this method, the cells are contacted with an antibody reagent specific to a particular receptor molecule on the surface of definitive endoderm cells or transcription factor within the nucleus that is not present in other cells of the mixed population. In this fashion, cells bound to that reagent can be quantified to determine the purity of the population.

Fluorescence-Activated Cell Sorting

Definitive endoderm cells can be effectively isolated from a mixed population of cells by FACS, affinity-based, or magnetic-based separation of cells tagged with antibodies for specific protein markers. FACS is a specialized form of flow cytometry in which cells are sorted one at a time by the light scatter of fluorescent labeled antibodies attached to the cell. In order to simultaneously enrich the population for only the live cells that bind to a specific definitive endoderm reagent, cells can be sorted into sterile containers ready for further analysis.

A cell-surface antibody marker specific to definitive endoderm is CXCR4, an alpha-chemokine receptor specific for stromal-derived-factor-1 (SDF-1) (Yasunaga et al., 2005). Until recently, SDF-1 and CXCR4 were believed to be a relatively monogamous ligand-receptor pair but a recent study demonstrates ubiquitin is also a natural ligand of CXCR4 (Saini et al., 2010). Nonetheless, CXCR4 is known to be a cell-surface ligand specific to definitive endoderm cells and not primitive/visceral endoderm (D'Amour et al., 2005). Permeabilization destroys the integrity of the cell membrane, making it undesirable in the instances where cells need to be kept alive. A cell-surface ligand like CXCR4 is beneficial when permeabilization of the cell membrane needs to be avoided, such as is the case when enriching, isolating, or substantially purifying definitive endoderm for further culture from a heterogeneous cell population.

Equipment required: Falcon no. 2052 no. 2054 tubes, Becton Dickinson FACSCanto machine (or equivalent), and Becton Dickinson FACSAria machine (or equivalent).

<u>Protocol</u>

1. For adherent cells create a single cell suspension by using trypsin/EDTA, TrypLE (Invitrogen), or other suitable dissociation agent.

2. Wash the cells with 2 mL cold PBS by centrifuging them at 200g for 4 minutes at 4°C.

3. Wash the cells again (optional)

4. Resuspend the cells in FACS buffer [PBS+1% bovine serum albumin (BSA)+0.1% NaN$_3$] and aliquot 1×10^5 - 100×10^5 cells per 100 µL (total volume once antibodies have been added) into Falcon no. 2052 or no. 2054 tubes on ice.

5. Add 20 µL of monoclonal antibody (1-10 µg/mL final concentration) or isotype control antibody.

6. Incubate the mixture for 30 minutes on ice.

7. Wash the cells again with 2 mL cold FACS buffer.

8. Resuspend the cells in 100 µL of secondary antibody (e.g. fluorophore-conjugated goat anti-mouse IgG). Skip to step 10 if directly conjugated monoclonal antibody is used.

9. Incubate the cells for 30 minutes on ice in the dark. Wash the cells again with FACS buffer.

10. Resuspend the cells in 100-500 µL cold FACS buffer and

    a. Analyze using a Becton Dickinson FACSCanto machine and FACSDiva software (BD Biosciences) or

b. Analyze live. Add propidium iodide (0.5 µg/mL final concentration). Live cells can be sorted by a Becton Dickinson FACSAria machine into tubes containing 100% serum supplemented with Y-27632 (Rock inhibitor). The ideal final concentration of cell should be $1x10^6$/mL.

Note: Using directly conjugated antibodies is faster and more reliable since it eliminates the need for a secondary antibody incubation.

Immunofluorescence

In other instances, it is desirable to study cells at the single-cell level without dissociating them, such as is the case with immunofluorescence. If this is the case, cell surface markers, cytoplasmic proteins, or transcription factors within the nucleus of cells can be targeted for analysis as they appear morphologically on the substrate upon which they were grown. Like flow cytometry, immunofluorescent labeling of cells and tissues enables the detection of specific factors using antibodies. Direct immunofluorescence uses a primary antibody directly conjugated to a fluorescent dye while indirect immunofluorescence uses a fluorochrome-tagged secondary antibody to detect the primary antibody. Cellular expression of a specific factor can then be studied in detail with a suitable microscope.

Immunolocalization of transcription factors *FOXA2* and *SOX17* are good measurements for definitive endoderm generation. It should be noted that *FOXA2* is also expressed in axial mesoderm, so it is the coexpression of the two transcription factors *FOXA2* and *SOX17* that is indicative of definitive endoderm differentiation. Co-staining for other genes which should be off, such as *POU5F1* (*OCT4*) *or T* (*Brachyury*), to corroborate the efficiency of differentiation is also useful in immunofluorescence assays (Figure 2-2C). Ki-67, a marker for proliferation, is useful to identify the cells that are actively cycling among the differentiated population. In

summary, using antibodies against both transcription factors *FOXA2* and *SOX17* is a reliable method to calculate the proportion of definitive endoderm cells within a mixed population.

> *Equipment required*: Inverted light microscope with 4X, 10X, and 20X phase objectives (or equivalent).

Protocol

1. For frozen tissue sections, thaw at room temperature. For adherent cells on coverslips, wash three times in PBS.

2. Fix the tissue/cells in 4% paraformaldehyde/PBS for 6-10 minutes and then wash in PBS three times for 5 min.

3. For tissue sections, clean the slide to remove water around the tissue. Use a water-resistant pen to encircle the tissue sections.

4. Incubate the tissue/cells in blocking solution (PBS+0.1% Triton X-100+2% normal blocking serum) for 1 hr at room temperature.

5. Incubate the tissue/cells with the primary antibody diluted in blocking solution for 1 hr at room temperature or overnight at 4 °C. Be sure to include a negative control sample incubating in blocking solution without primary antibody.

6. Wash the slide in PBS three times for 10 minutes at room temperature.

7. Incubate the tissue/cells with secondary antibody conjugated to a fluorophore diluted in blocking solution at for 45 minutes at room temperature. Be sure to protect samples from light.

8. Incubate the tissue/cells with 4',6-diamidino-2-phenylindole (DAPI) (5 µM) diluted in PBS for 10 minutes at room temperature to counterstain nuclei.

9. Wash the slide in PBS three times for 10 minutes at room temperature. Be sure to protect samples from light.

10. Mount the slide/coverslip using antifade mounting medium (e.g. Vectashield, Vector Laboratories) and observe the cells using a fluorescence microscope.

Note: For double immunofluorescence staining, use two antibodies raised in different species in step 5 and two secondary antibodies conjugated with different dyes in step 7. The blocking solution should contain the sera from both of the animals in which the secondary antibodies were raised.

Table 2-1. Primers needed for definitive endoderm characterization.

Reagent	Type	Vendor	Catalog #	Concentration Used
18s	Primer	Life Technologies	Hs99999901_s1	1 µL/sample
POU5F1	Primer	Life Technologies	Hs04260367_gH	1 µL/sample
NANOG	Primer	Life Technologies	Hs04399610_g1	1 µL/sample
SOX2	Primer	Life Technologies	Hs01053049_s1	1 µL/sample
FOXA2	Primer	Life Technologies	Hs00232764_m1	1 µL/sample
SOX1	Primer	Life Technologies	Hs01057642_s1	1 µL/sample
MESP1	Primer	Life Technologies	Hs01001283_g1	1 µL/sample
MIXL1	Primer	Life Technologies	Hs00430824_g1	1 µL/sample
SOX17	Primer	Life Technologies	Hs00751752_s1	1 µL/sample
NESTIN	Primer	Life Technologies	Hs04187831_g1	1 µL/sample
T	Primer	Life Technologies	Hs00610080_m1	1 µL/sample

Chapter 2, in part, is a reprint of the material as it appears in "Endoderm Differentiation from Human Pluripotent Stem Cells; Working with Stem Cells - Quick and easy methodologies and applications." Brafman, Dave; Kumar, Nathan; Willert, Karl, Springer Publishing, 2015. I am the primary author and researcher.

Chapter 3. Defined Culture Conditions Enhance Maintenance of

Endoderm Derived from Human Embryonic Stem Cells

Introduction

The development of universal protocols to differentiate any hPS cell line into a homogenous population of a specific cell type has been rendered difficult by the inherent variability that exists between lines. Epigenetic memory, inconsistent reprogramming, and genetic background are likely to be the main causes of this variability, which poses a major hurdle for the development of personalized medicines and for modeling diseases with a low-penetrance phenotype. As an alternative, expansion of intermediate stages of differentiation could address this issue, especially if these cell types can be isolated from a heterogeneous population. For example, neural stem cells can be expanded from human pluripotent stem cell lines differentiated toward neuroectoderm and then subsequently differentiated into a variety of neurons, thereby bypassing the need to continuously culture pluripotent cells (Falk et al., 2012).   However, neural stem cells are by no means a uniform cell population which can be attributed to the complexity of anterior-posterior and dorsal-ventral neuronal cell types.

Along the same vein, endoderm differentiation is hindered by the complex combination of inductive signals controlling the patterning of this germ layer, making it difficult to reproduce in vitro (Sneddon et al., 2012). Even though the inductive signals are difficult to mimic, endoderm formation has been well studied in developmental biology. During embryogenesis, the inner cell mass gives rise to an epithelial population known as the epiblast. As the embryo undergoes gastrulation, these cells migrate with the primitive streak, forming early mesoderm and definitive endoderm (DE) (Lawson and Schoenwolf, 2003; Tam et al., 1997). Broadly speaking, nascent DE organizes to form the primitive gut tube, which ultimately gets refined into three distinct domains: the foregut, midgut, and hindgut (Viotti et al., 2014; Zorn and Wells, 2009). The foregut ultimately gives rise to the esophagus, trachea, lungs, thyroid, parathyroid, thymus,

stomach, liver, and pancreas, while the midgut and hindgut become the colon and small intestine. Current endodermal differentiation strategies involve guiding hESCs through sequential, staged protocols that mimic early embryonic signaling events known to control primitive streak formation and gastrulation. In this manner, hepatic (Basma et al., 2009; Gouon-Evans et al., 2006), intestinal (Spence et al., 2011), and pancreatic cells (D'Amour et al., 2006) can be generated from ESCs and iPSCs. While these studies exemplify the potential of PSC-derived endodermal tissues for cell transplantation therapies, these protocols are often variable and inefficient. This variability is in part due to the pluripotent nature of hPSCs resulting in generation of various cells types from multiple germ layers in the majority of differentiation protocols. Since most differentiation schemes are subject to this variability, it is challenging to generate homogenous monolineage cultures of a desired cell type from hPSCs (Murry and Keller, 2008). Additionally, undifferentiated ESCs and iPSCs are tumorigenic and therefore must be completely excluded from their derivative mature tissues to be useful for transplantation therapies (Hentze et al., 2009).

As a potential solution to these obstacles, we used high-throughput screens to optimize the microenvironment necessary for DE formation and maintenance. While many studies have focused on the roles of signaling molecules in the complex differentiation towards DE, relatively little is known about the role of extracellular matrix proteins (ECMPs) and their role in controlling hESC fate. The majority of hESC differentiation protocols utilize xenogeneic matrices, such as Matrigel (BD Biosciences, San Jose, CA, USA), which is a protein mixture produced by EHS mouse sarcoma cells. While such protein extracts provide extracellular components necessary to support cell adhesion, they fail to mimic the specialized microenvironments to which cells are

exposed *in vivo*. In addition, these commercial matrices are generally not fully defined, contain animal products and are highly variable from batch-to-batch.

In this study, we employed a high-throughput combinatorial ECMP array platform to identify fibronectin (FN) and vitronectin (VTN) as components that improve differentiation of hESCs to DE as well as maintenance of DE thereafter. Having established that FN and VTN were critical ECMP components to promote DE differentiation, I also set out to generate a self-renewing DE progenitor line from both human ESCs and iPSCs. An endoderm progenitor line would provide a powerful tool to study how different gut tissues are specified from a common multipotent endodermal progenitor and to optimize monolineage differentiation. Moreover, creation of endoderm progenitor cells from ESCs/iPSCs may represents a strategy to optimize the production of pure, non-tumorigenic cells for tissue replacement therapies.

Materials and Methods

Quantitative RT-PCR

RNA was isolated using RNeasy Plus Micro Kit (Qiagen) and reverse-transcribed with random primers and qScript cDNA Supermix (Quanta). Before reverse transcription, 5 µg of RNA was digested by RNase-free DNase I (Ambion) to remove genomic DNA. Quantitative PCR was carried out using a Real-Time PCR System (Bio-Rad) and Taqman qPCR Mix with a 10-min gradient to 95 °C followed by 40 cycles at 95 °C for 15 s and 60 °C for 1 min. Taqman gene expression assay primers (Life Technologies; Supplementary Table 1) were used. Gene expression was normalized to 18S rRNA levels. Delta C_t values were calculated as $C_t^{target} - C_t^{18s}$. All experiments were performed with three technical replicates. Relative fold changes in gene expression were calculated using the $2^{-\Delta\Delta C_t}$ method (VanGuilder et al., 2008).

Flow cytometry

Cells were dissociated with Accutase (Life Technologies) at 37 °C for 4 min and triturated using fine-tipped pipettes. For intracellular antibody staining, cells were fixed for 15 min with Cytofix (BD Biosciences), washed twice with flow cytometry buffer (PBS, 1 mM EDTA, and 0.5% FBS), permeabilized with Cytoperm (BD Bioceiences) for 30 minutes on ice, and washed twice with flow cytometry buffer, and resuspended at a maximum concentration of 5×10^6 cells per 100 ul. Cells were incubated with primary antibodies on ice for 1 hour (hr), washed twice with flow cytometry buffer and, if necessary, incubated with secondary antibodies on ice for 1 hr and then washed three times. Antibodies and concentrations used are listed in Supplementary Table 1. After passing through a 40 µm cell strainer, cells were resuspended in flow cytometry buffer at a final density of 2×10^6 cells ml^{-1}. Propidium iodide (Sigma) was added at a final concentration of 50 mg ml^{-1} to exclude dead cells. Cells were analyzed on the FACS Fortessa (Becton Dickinson). For each sample, at least three independent experiments were performed. Results were analyzed using FlowJo software.

Immunocytochemistry

Monolayer cultures were gently washed with PBS prior to fixation. Cultures were fixed for 10 min at 4 °C with fresh paraformaldehyde (4% (w/v) in PBS). For sectioning aggregates of cells in suspension, samples were fixed with 4% paraformaldehyde, embedded in optimal cutting temperature (OCT) compound (Tissue Tek) and cryosectioned at 10-µm thickness before staining, Cells were blocked and permeabilized with 2% (w/v) BSA, 0.2% ((v/v) in PBS) Triton X for 30 min at RT. Cells were then washed twice with PBS. Primary antibodies were incubated overnight at 4 °C and washed twice with PBS. Secondary antibodies were incubated for 1 hr at 37 °C.

Antibodies used are listed in Supplementary Table 1. Prior to imaging, samples were stained with DAPI for 10 minutes, washed and mounted in Vectashield (Vector Laboratories), covered with coverslips, and sealed with nail polish. Images were taken using an Olympus FluoView1000 multi-photon confocal microscope. All immunofluorescence analyses were repeated a minimum of three times and representative images are shown.

Human pluripotent stem cell (hPSC) culture

Human ES cell lines H9 and Hues9 were obtained from WiCell and Harvard University, respectively. All experiments described in this study were approved by a Stem Cell Research Oversight Committee (Protocol #100210ZX, PI Willert). The human induced pluripotent stem cell line BJ RiPS (Warren et al., 2010) were provided under a Material Transfer Agreement from Dr. D. Rossi (Childrens Hospital Boston, MA). The following medium were used: BJ RiPS and Hues 9 ES (DMEM/F12 mixed, 20% (v/v) Knockout Serum Replacement, 1% (v/v) penicillin-streptomycin, 1% (v/v) nonessential amino acids, 2 mM L-glutamate, 0.1 mM b-mercaptoethanol and 10 ng/mL FGF2 (Peprotech); H9 ES (DMEM/F12 supplemented with L-Ascorbic Acid, Selenium, Transferrin, $NaHCO_3$, Insulin, TGFβ1, and FGF2 as described previously (Chen et al., 2011). Fresh media was added daily to all cells. Every five days, colonies were enzymatically passaged with Accutase and transferred to a Matrigel-coated. All media components are from Life Technologies unless indicated otherwise. For all experiments, hPSCs were used between passages 20 and 50 in this study.

Human ES cell endoderm differentiation

ES cells were passaged onto Matrigel-coated plates and differentiated as described previously (D'Amour et al., 2005). Initiated on days 4–6 after passage (depending on culture density), sequential, daily media changes were made for the entire differentiation protocol. After a brief wash in PBS (with Mg/Ca), the cells were cultured in RPMI (without FBS), activin A (100 ng/ml) and Wnt3a (25 ng/ml) for the first day. The next day the medium was changed to RPMI with 0.2% vol/vol FBS and activin A (100 ng/ml), and the cells are cultured for 2 additional days. Definitive endoderm was obtained at day 3.

Array fabrication and characterization

Arrayed cellular microenvironment (ACME) slides were fabricated as previously described (Brafman et al., 2012). Briefly, glass slides were cleaned, silanized, and then functionalized with a polyacrylamide gel layer. For ECMP arrays, stock solutions of ECMPs were suspended at 250 µg/ml in ECMP printing buffer (100 mM acetate, 5 mM EDTA, 20% (v/v) glycerol and 0.25% (v/v) Triton X-100, pH 5.0). ECMP solutions were mixed in all possible 128 combinations in a 384-well plate. For GF and SM arrays, stock solutions were suspended at 1 mg/ml in soluble factor printing buffer (100 mM acetate, 5 mM EDTA, 19% glycerol (v/v) and 0.25% (v/v)Triton X-100,10 mM trehalose dehydrate (Sigma), 1% poly(ethylene glycol), pH 5.). GF solutions were then mixed into 519 combinations representing all single, pairwise, and non-redundant three-way combinations possible in a 384-well plate. The ECMPs, GFs, and SMs used are listed in Table 2-1. The hit ECMP condition from the primary screen was used as a substrate to print the GFs and SMs in the secondary screen. Twenty individual spots of each protein/growth factor/small molecule mixture, clustered into groups of five and printed in

different quadrants of the slide, were deposited with a 450 μm pitch on the acrylamide

gel pad using a SpotBot Personal Microarray Printer (ArrayIt) equipped with Stealth SMP

4.0 split pins. The pins were cleaned by sonication in 5% Micro Cleaning

Solution (ArrayIt) and dH_2O immediately before use. Between each sample in the source

plate, the pins were dipped in a 50% DMSO and water solution, washed for 25 seconds

with dH_2O and dried.

Endoderm induction on ACME slides

Before their use, slides were soaked in PBS while being exposed to UVC

germicidal radiation in a sterile flow hood for 10 min. Before seeding onto the ACME

slides, hESCs were cultured for two passages on Matrigel (BD) with MEF-conditioned

media supplemented with 30 ng/ml bFGF to remove residual feeder cells. HESCs were

then Accutase-passaged onto the ACME slides (5.0 × 105 cells per slide) and allowed to

settle on the spots for 18 h. Array slides were then gently washed twice with RPMI (Life

Technologies) to remove cell debris and residual hESC media. The medium was then

changed to RPMI supplemented with 1% (v/v) Gluta-MAX and 100 ng/ml recombinant

human Activin A (R&D Systems, Minneapolis, MN, USA). Cells were cultured for 3 days,

with FBS concentrations at 0% for the first day and 0.2% for the second and third days.

Cultures were supplemented with 30 ng/ml purified mouse Wnt3a for the first day.

Endoderm induction on defined ECMPs

H9, HUES9 and HUES1 were cultured on Matrigel (BD) with MEF-conditioned

media supplemented with 30 ng/ml bFGF for 2 passages to remove residual MEFs. The

human ECMP-coated plates were prepared by coating tissue culture plates in the ECMP

(diluted in 10 mM acetic acid) overnight, followed by air drying. 10 μg of total protein was

plated per cm^2 of culture dish surface. Human ECMP-coated plates were used immediately after air drying. HESCs were passaged at a density of 2.5 × 10^5 cells/ml onto human ECMP or Matrigel-coated plates in order to achieve confluency the following day. HESCs were then gently washed twice with RPMI (Life Technologies) to remove cell debris and residual hESC media. The medium was then changed to RPMI supplemented with 1% (v/v) Gluta-MAX and 100 ng/ml recombinant human Activin A (R&D Systems). Cells were cultured for 3 days, with FBS concentrations at 0% for the first day and 0.2% for the second and third days. Cultures were supplemented with 30 ng/ml purified mouse Wnt3a for the first day.

Endoderm expansion in suspension

ES cells were passaged onto Matrigel-coated plates and differentiated as described previously (D'Amour et al., 2005). Flow cytometric sorting was used to isolate the CXCR4+ population for expansion. Immediately after sorting, 2.5 x 10^6 CXCR4+ cells were seeded with Y-27632 into each well of a low-binding 6-well plate and placed on a 95 rpm incubator shaker overnight in 4 mL of endoderm expansion media (RPMI+10% KSR+1x GlutaMAX+1x Non-essential Amino Acids+0.1 mM 2-Mercaptoethanol) with hit growth factors WNT (50 ng/mL) + FGF (20 ng/mL). Half the media was replaced with fresh media daily.

Slide imaging, quantification, and analysis

Slides were fixed with 4% PFA for 10 minutes at room temperature and washed with PBS. Slides were imaged using the CellInsight™ CX5 High Content Screening (HCS) Platform (ThermoFisher). The system was programmed to visit each spot on the array, perform autofocus, and acquire DAPI and FITC (GFP). Cell counts and stain

intensities were measured using Thermo ScientificTM HCS StudioTM 2.0 Software using

the built-in object identification and cell intensity algorithms.

Generation of Probability Density Functions

Single-cell analysis was performed using the CellInsight™ CX5 High Content

Screening (HCS) Platform (ThermoFisher). The system was programmed to define the

borders of each cell as measured by DAPI staining. Each cell's surface area was

calculated and the system was instructed to output the average stain intensity per cell by

dividing total stain intensity by surface area. The average stain intensities per cell were

exported to a spreadsheet software, which was used to generate histograms of the

distributions. Data bin intervals were made small enough so that there were at least 10

bins for each microenvironment in order to provide a resolved distribution curve. The

resultant histograms were then divided by the total number of cells for that

microenvironment so that the area under each curve was equal to one. In this way, one

could measure the probability (on the y-axis) that a cell would express a given stain

intensity (on the x-axis) in that particular microenvironment if the experiment were to be

repeated.

Statistical analyses

All averaged data are expressed ± standard error of the mean of three

independent biological replicates unless otherwise stated. For comparisons of discrete

data sets, unpaired Student's t-tests were performed to calculate *p*-values between

experimental conditions and controls and a *P*-value <0.05 was considered statistically

significant. For each ACME experiment, the ratio (R_i) of the $\log_2$ of the T-GFP signal and

the DNA signal was calculated for each spot. From this a differentiation *z*-score was

calculated for each spot $Z_{DIF}=(R_i−\mu_{DIF})/\sigma_{DIF}$, where R_i was the ratio for the spot, μ_{DIF} was

the average of the ratios for all spots on each array, and σ_{DIF} was the S.D. of the ratios

for all spots on each array. Differentiation *z*-scores from replicate spots (*n*=5 per

condition) were averaged for each ECMP condition on the array. The replicate

average *z*-scores were displayed in a heat map with rows corresponding to individual

conditions and columns representing independent array experiments (n=5 for each

replicate). For each array experiment, all columns were mean-centered and normalized

to one unit S.D. The rows were clustered using Pearson correlations as a metric of

similarity. All clustering was performed using Gene Cluster. The results were displayed

using a color code with red and green representing an increase and decrease,

respectively, relative to the global mean. All heat maps were created using Tree View.

Results

Endoderm Progenitors do not Form with Known Culture Conditions

      Initially, I set out to optimize the conditions for generating stable, self-renewing

DE progenitors. In order to generate these endoderm progenitors in vitro, I first tested

the capacity of SOX17+CXCR4+ endoderm cells generated from hPSCs to retain their

endoderm expression without the factors described for EPs. Endoderm was formed

from hPSCs with Wnt and Activin induction (D'Amour et al., 2005; Kroon et al., 2008;

Schulz et al., 2012) (Figure 3-1A), and a heterogeneous population of endoderm cells

was treated with Accutase, replated onto Matrigel-coated plates and supplemented with

10% KSR (Life Technologies, Carlsbad). This induction protocol consistently produced

endoderm across cell lines as measured by SOX17 and FOXA2 albeit with varying

efficiencies (Jiang et al., 2013). Initially, 65% of the differentiated cell population

expressed SOX17+CXCR4+. After five additional days in these conditions, the

heterogeneous population of endoderm cells retained only 3% SOX17+CXCR4+ cells

(Figure 3-1B, C), indicating the transient expression of these endodermal marker

proteins in these generic culture conditions. This temporal decline of SOX17 and

CXCR4 can be used as a template upon which to improve with high throughput

screening.
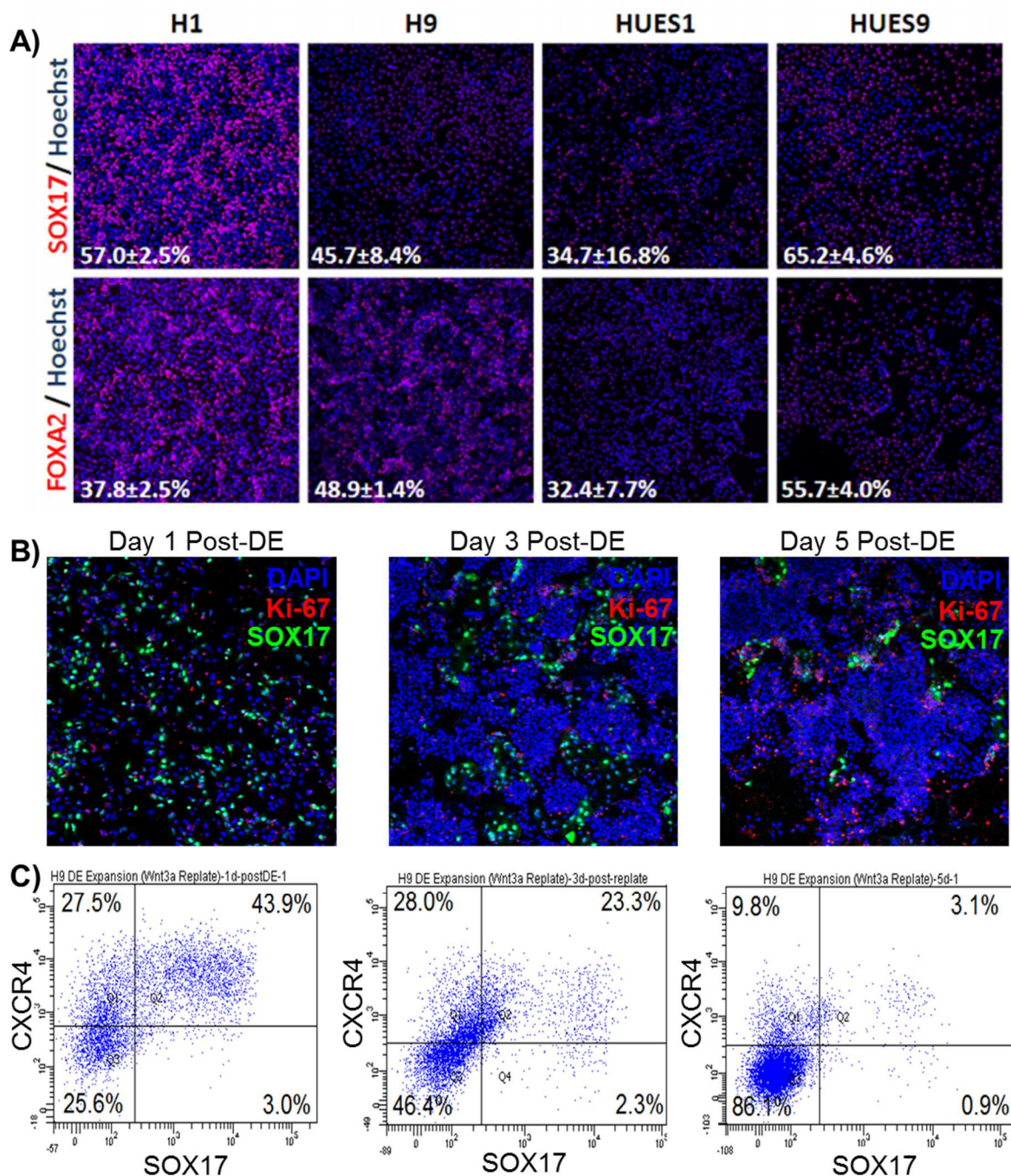
Figure 3-1. Current definitive endoderm (DE) differentiation protocols are neither efficient nor robust. A) Adapted from Brafman et al. 2013. A previously published DE protocol (Kroon 2008) applied to several hESC lines (H1, H9, HUES1, HUES9) results in poor DE induction (n=3 biologically independent experiments; (mean± S.D.). B) H9 DE cells lose SOX17 and CXCR4 expression when replated onto Matrigel in RPMI 10% KSR. This provides temporal information on maintenance of these proteins, which can be used as a template to improve upon using high-throughput screening of culture conditions.

Before moving on to employing high throughput screens via arrayed cellular microenvironments, I first tested the capacity of published protocols to generate endoderm progenitors. One such protocol, published by Cheng et al. (Cheng et al., 2012), involved the use of undiluted Matrigel, a feeder layer of Swiss-Webster MEFs, and a specific cocktail of growth factors, resulting in the generation of indefinitely self-renewing, non-tumorigenic, multipotent endoderm progenitors (EPs). Xenogeneic factors such as these make this protocol undefined and non-scalable, which is precisely what we are trying to move away from. Nonetheless, I attempted to recreate these conditions in our lab to see if I could generate an expanded endoderm progenitor line to use for our high-throughput screens. Using the H9 SOX17-GFP line (Figure 3-2A), it was possible to observe the real-time expression of SOX17, which was robustly upregulated 24 hours after sorting (Figure 3-2A). Figure 3-2B shows the sorting strategy that I utilized, taking only the highest SOX17+CXCR4+ expressers and replating them into the published endoderm progenitor conditions. However, after less than two weeks in culture, far shorter than the timeframe used in the published endoderm progenitor paper, the expression of endoderm markers FOXA2 and SOX17 was limited to a small subset of cells (Figure 3-2C). Further, the cell population never grew as robustly as the growth curves published. I attempted to generate endoderm progenitors in more than three separate trials and even went so far as to use a frozen vial of endoderm progenitors provided by Cheng et al. Cheng et al. also generously sent us their Matrigel reagent to mitigate possible batch-to-batch variations. Amidst all these efforts, I was not successful in recreating the indefinitely self-renewing endoderm progenitor population discussed in the published paper. At this point, we realized our best approach to defining endoderm expansion conditions was by using an early (day

3) transient endoderm population derived from hPS cells to screen with extracellular

matrix proteins and growth factors/small molecules.
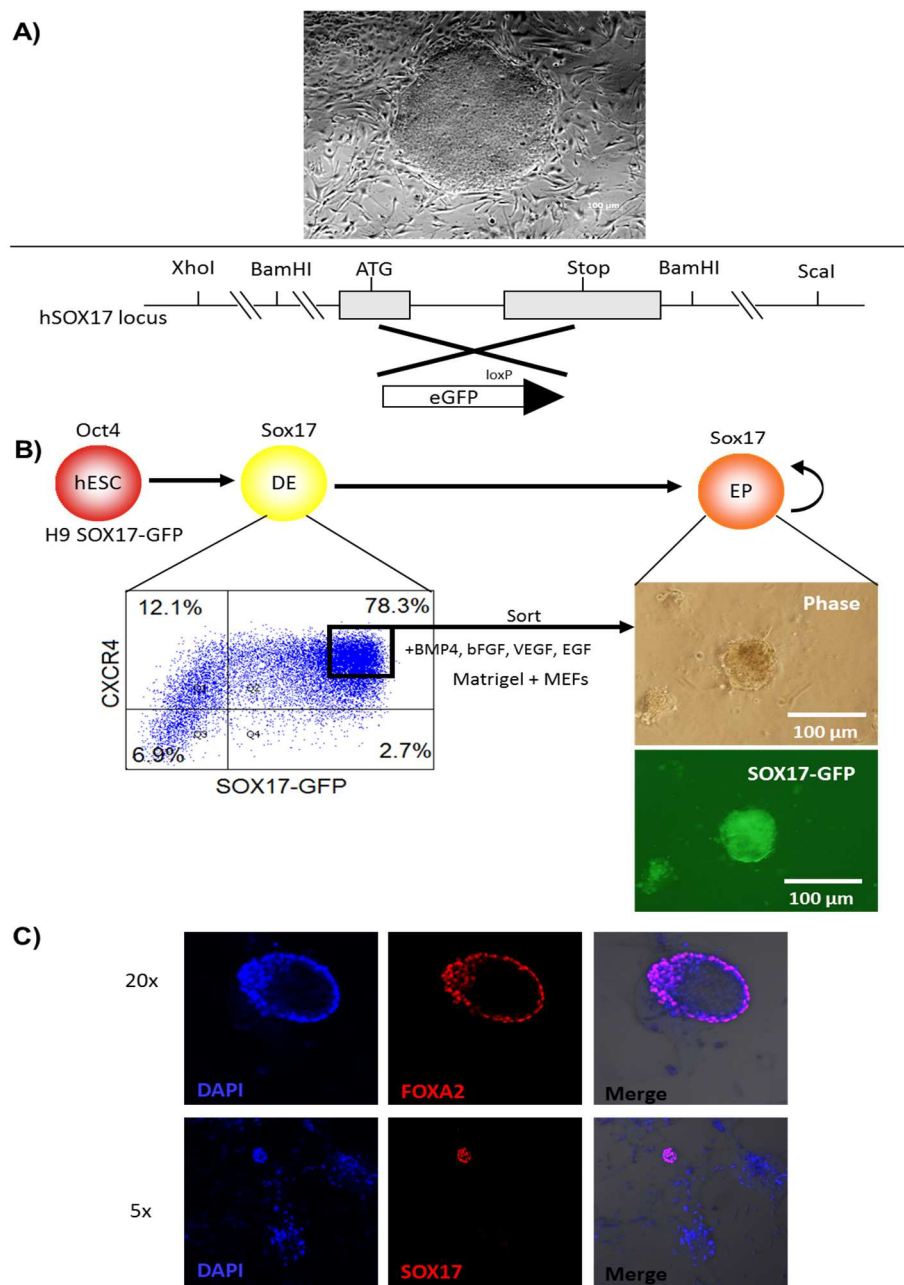
Figure 3-2. Deriving endoderm progenitors using published protocols with undefined culture conditions. A) Targeting of *eGFP* reporter into the human *SOX17* locus adapted from Kita-Matsuo et al., 2009. Representative image of H9 SOX17-GFP cells in culture atop MEF cells as well as a schematic representation of human *SOX17* targeting strategy. B) Sorting strategy for generating endoderm progenitors. The initial sort selected only CXCR4+SOX17+ cells to be cultured in undiluted Matrigel with Swiss-Webster MEFs and a specific cocktail of growth factors. C) Immunofluorescence of endoderm progenitors 10 days after sorting. Cell growth was not observed to be as robust as published and FOXA2/SOX17 expression was limited to a fraction of cells.

Specific Extracellular Matrix Proteins Promote the Differentiation of Endoderm Cells

The screen described in this section was performed with others in the laboratory as described in Brafman et al (Brafman et al., 2013). In order to screen optimal conditions for transient DE expansion, we first wanted to generate DE cells under fully-defined conditions. Although certain hES cell lines, such as CyT49, efficiently differentiate into DE, other cell lines yield variable amounts of DE cells, ranging from 32–65% (Figure 3-1a), suggesting that additional factors are required for DE differentiation. We sought to investigate to what extent ECMPs affect the endodermal differentiation of three hES cell lines, H9, HUES1, and HUES9 (Brafman et al., 2013). To do so, we utilized a cellular microarray screening platform previously developed in our laboratory (Brafman et al., 2009a, 2009b, 2010, 2012). In this screening platform, all possible combinations of seven ECMPs, collagen I (COL I), collagen III (COL III), collagen IV (COL IV), collagen V (COL V), FN, laminin (LN) and VTN were printed on microscope slides as described (see Materials and Methods). For comparison we included Matrigel (BD Biosciences), which is typically used in differentiation protocols of adherent hES cell cultures. These arrays were seeded with hES cells and the medium was supplemented with Wnt3a and Activin A to promote endodermal differentiation. After three days of endoderm induction on the arrays, cells were fixed, stained, and imaged for the DE marker SOX17 and DNA (Hoechst Stain 33342) (See Figure 1B in Brafman et al., 2013, attached in Appendix; Figure A3-8A).

Hierarchical clustering of data sets divided the results of the screen into eight clusters (See Figure 1C in Brafman et al., 2013, attached in Appendix; Figure A3-8B), depicting ECMP combinations that either promoted high SOX17 expression in all three hES cell lines tested (Cluster I), two out of three hES cell lines tested (clusters II, III, and

IV), one out of the three hES cell lines tested (cluster V, VI, VII), or in none of the hES cell lines tested (cluster VIII). To identify the ECMPs that most efficiently fostered DE formation, we performed a full factorial analysis,(Abdi and Williams 2010) which revealed FN and VTN as the most common DE-promoting ECMPs (See Figure 1D in Brafman et al., 2013, attached in Appendix; Figure A3-8C). Other ECMPs had either no effect on DE differentiation, such as LN, or negative effects, such as COL V.

FN and VTN Promote Endodermal Differentiation in Traditional Cell Culture Formats

The scaled-up verification of the screen described in this section was performed with others in the laboratory as described in Brafman et al (Brafman et al., 2013). Arrayed cellular microenvironment screens identified FN and VTN to be the most effective universal promoters of DE differentiation across cell lines. To verify that FN and VTN facilitated DE differentiation of hES cells we tested their effects in conventional cell culture formats, including Matrigel as a control. HUES9 hES cells were allowed to adhere on either Matrigel or the combination of FN and VTN (FN+VTN) and subsequently differentiated to DE. Immunofluorescent (IF) staining demonstrated that FN+VTN fostered a statistically significant increase in the percentage of cells expressing the DE marker SOX17 (See Figure 2A in Brafman et al., 2013, attached in Appendix; Figure A3-9A). Furthermore, differentiation on FN+VTN also increased the total number of SOX17+ cells, as well as the overall cell number (See Figure 2B in Brafman et al., 2013, attached in Appendix; Figure A3-9B). Flow cytometry revealed that culture on FN+VTN increased the percentage of cells expressing the DE marker CXCR4 (See Figure 2C in Brafman et al., 2013, attached in Appendix; Figure A3-9C). Finally, quantitative PCR (qPCR; See Figure 2D in Brafman et al., 2013, attached in Appendix;

Figure A3-9D) of DE markers *SOX17*, *FOXA2*, and *CXCR4* showed that FN+VTN increased the efficiency of DE differentiation on a transcript level relative to Matrigel.

Specific Extracellular Matrix Proteins Augment the Maintenance of SOX17 in Endoderm Cells

After determining the optimal ECMPs for the derivation of DE from hPS cells, I moved on to defining the optimal culture conditions for facilitating DE maintenance and self-renewal. In order to determine the optimal culture conditions for expanding definitive endoderm cells, I employed iterative high throughput screens using arrayed cellular microenvironments. In the primary screen, I tested the effects of all possible combinations of ECMPs on adhesion and maintenance of definitive endoderm cells. To do so, I printed all possible combinations of ECMPs in replicates of five atop microscope slides, sorted by flow cytometry to seed the slides with a pure SOX17+ definitive endoderm population, and fixed 72 hours later to assay for cell number and SOX17-GFP. Representative clusters from the resulting heatmap show the effects of various protein combinations on endoderm adhesion and maintenance (Figure 3-3A). Of these clusters, the one of most interest contained ECMPs that promoted both adhesion and SOX17 maintenance. Within this particular cluster, hits Fibronectin-Vitronectin (FN + VTN) and Collagen III-Collagen V-Vitronectin (C3 C5 VTN) were selected for further investigation based on their ability to support adhesion and maintain SOX17 to a greater extent than other conditions. Representative images of these hits on the arrayed cellular microenvironment screen are shown in comparison to Matrigel (Figure 3-3B). Differences in spot size are due to viscosity differences between Matrigel and soluble defined proteins. To provide more resolution on the quantification of SOX17, a probability density function uses single-cell analysis to display the distribution of SOX17

expression within each condition (Figure 3-3C, see Materials and Methods for generation of probability density functions). In defined hit conditions, a significant portion of cells are shifted towards the high end of SOX17 expression as compared to Matrigel. Before moving forward with additional iterations of screens, I validated the results of the primary screen in scaled-up traditional cell culture formats by coating dishes with either FN + VTN, C3 C5 VTN, or Matrigel and seeding SOX17+ cells before analyzing 72 hours later for cell number and %SOX17-GFP+ (Figure 3-3D). It was reassuring to observe similar trends in endoderm expansion on both a micro- and macro- level for the given ECMPs. Hit condition FN + VTN fostered a significantly higher number of cells and a significantly higher percentage of positive SOX17 cells as compared to Matrigel.
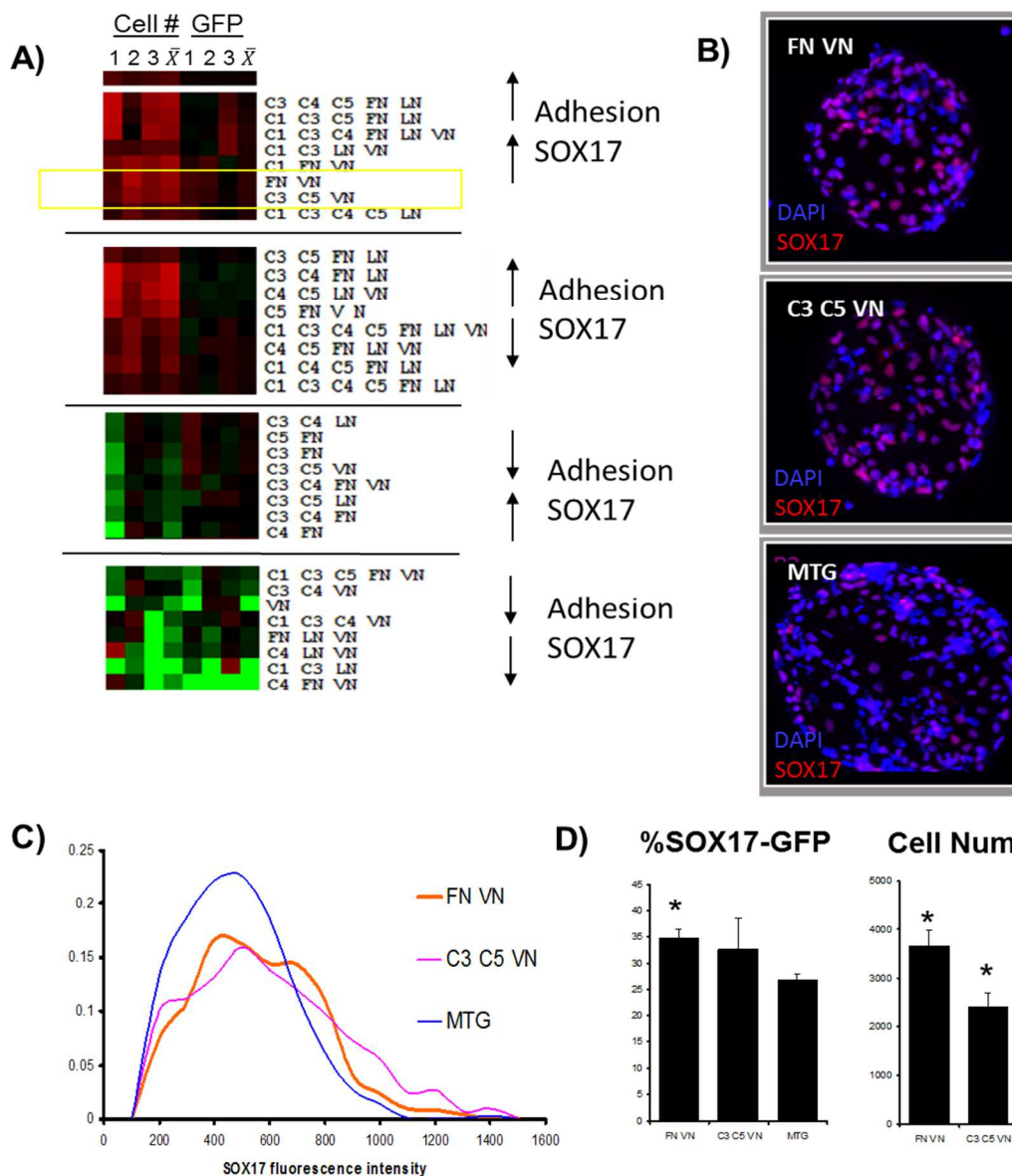
Figure 3-3. Primary extracellular matrix protein screen for maintenance and expansion of definitive endoderm cells. A) Heatmap of various extracellular matrix protein combinations shown in representative clusters based on number of cells and SOX17-GFP maintenance. A pure population of definitive endoderm cells were plated onto arrayed cellular microenvironments, cultured for 72 hours, then fixed and assayed for cell number and SOX17-GFP maintenance. The data could be segmented into four representative clusters. B) Representative images of the hits FN + VTN and C3 C5 VTN and control MTG on the arrayed cellular microenvironments. C) Single-cell FACS-like analysis to show distribution of SOX17 fluorescence for hits FN + VTN and C3 C5 VTN and control MTG on the arrayed cellular microenvironments. D) Scale up validation in traditional cell culture formats. Coated culture dishes validated the results found in the primary screen based on cell number and SOX17-GFP maintenance. Abbreviations: VN=VTN=Vitronectin.

Specific Growth Factors and Small Molecules Augment the Maintenance of SOX17

in Endoderm Cells

After performing the primary screen, top hit FN + VTN was used as a substrate

for the next iteration of high throughput screening. Since there are many more cell types

in organisms than there are signaling factors, biology encodes information not just

through the presence or absence of signals, but also through their combinations, level,

and timing. In the secondary screen, I set out to determine the optimal combination of

growth factors (GF) and small molecules (SM) for adhesion and maintenance of

definitive endoderm cells as marked by SOX17-GFP. To do so, I fabricated arrayed

cellular microenvironments, this time with FN + VTN as a substrate. Atop FN + VTN on

microscope slides, I printed all possible combinations of GFs and SMs in replicates of

five, sorted by flow cytometry to seed the slides with a pure SOX17+ definitive endoderm

population, and fixed 72 hours later to assay for cell number and SOX17-GFP.

Conditions with contradicting combinations were omitted, such as an agonist and

antagonist to the same pathway (e.g. Wnt3a+DKK1). Assaying for cell number did not

yield significant differences between conditions, most likely due to the fact that FN +

VTN was a known favorable substrate and fostered initial attraction and adhesion

regardless of the GFs and SMs printed. SOX17 maintenance, however, was variable

across conditions, as shown by plotting %SOX17-GFP+ across the various GF and SM

combinations (Figure 3-4A). A line of best fit was calculated for the resulting distribution

curve, with an R^2-value of 0.9614. Those conditions with the highest %SOX17-GFP+

were selected for further analysis. Single-cell analysis of these top conditions produces

probability density functions that indicate the distribution of SOX17 expression for a

given combination of GFs and SMs (Figure 3-4B). Probability density functions are

shown against the No GF condition for reference. The augmented shift in SOX17

maintenance is quantified by calculating the area under the curve that falls above our pluripotent control, which emitted a basal background level on the GFP channel.   The indicated percentage represents the portion of cells that expressed SOX17-GFP above that of the pluripotent sample.

To indicate the appearance of these spots during the screen, representative images of these hits on the arrays are shown (Figure 3-4C). Taking into account the entirety of the secondary screen, I performed a principal component analysis (Abdi and Williams, 2010), which revealed those GFs and/or SMs that either augmented (positive value) or diminished (negative value) SOX17 maintenance when included in a microenvironment (Figure 3-4D).   By observation, I noticed those GFs/SMs that augmented SOX17 maintenance were mostly Wnt agonists or members of the FGF superfamily.
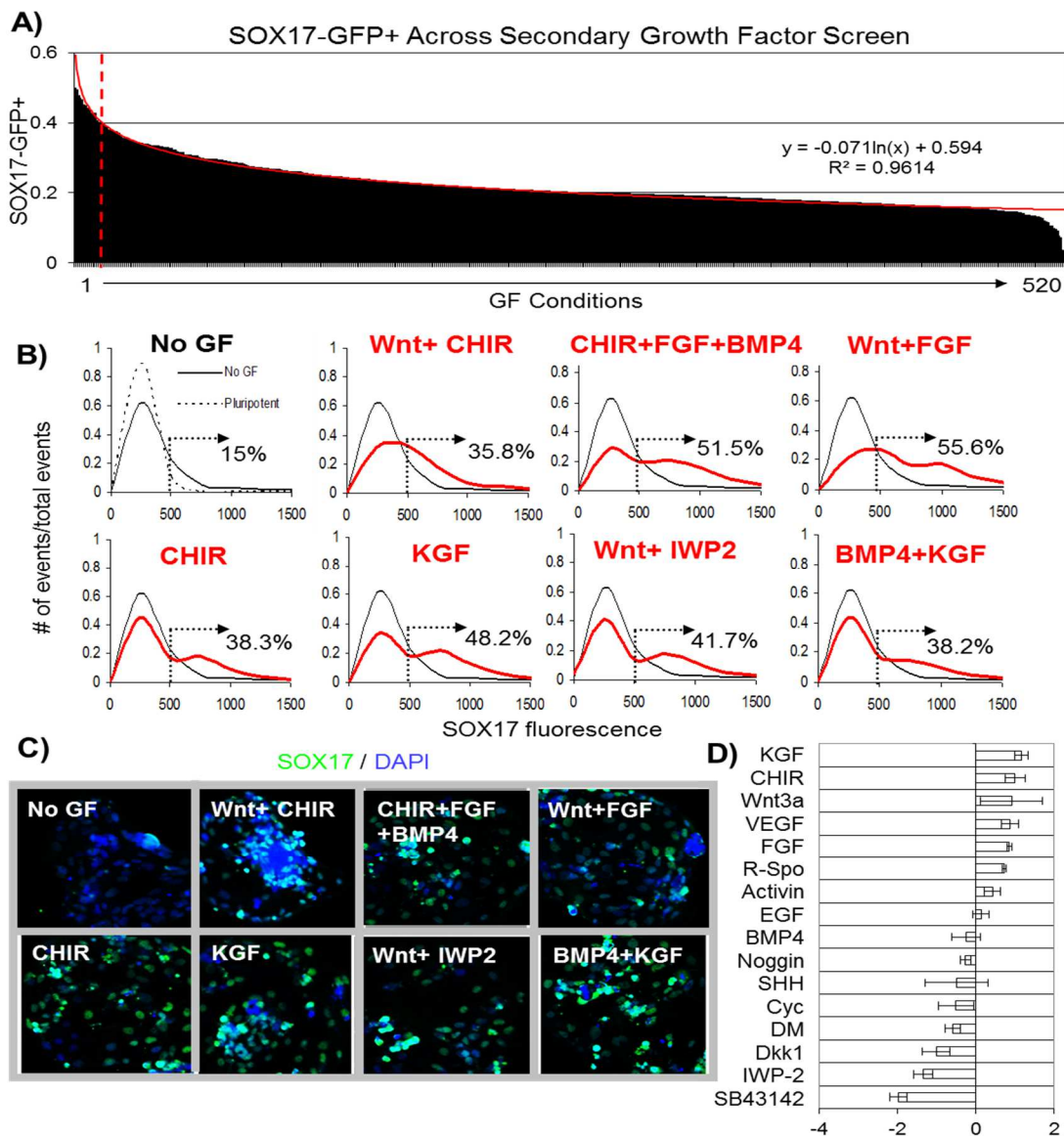
Figure 3-4. Secondary growth factor screen for maintenance and expansion of definitive endoderm cells. A) Proportion of cells that are SOX17-GFP+ across growth factor conditions ordered from highest to lowest. A pure population of definitive endoderm cells were plated onto arrayed cellular microenvironments containing all single, pairwise and three-way combinations of selected growth factors, cultured for 72 hours, then fixed and assayed for cell number and SOX17-GFP maintenance. A line of best fit is shown to quantify the distribution. The dotted red line indicates the cutoff for growth factor conditions that were further analyzed. B) Single-cell FACS-like analysis shows the SOX17 fluorescence probability density functions of hit growth factor conditions and the No GF control on the arrayed cellular microenvironments. C) Representative images of hit growth factor conditions and No GF control on the arrayed cellular microenvironments. D) Principal component analysis of the secondary growth factor screen.

In order to validate and further narrow down our hits to a specific combination, I scaled up the results from the secondary screen into traditional cell culture formats to isolate top performing conditions. To be as comprehensive as possible, I included both individual hits from the principal component analysis and specific combinatorial hits from the arrayed cellular microenvironment screen as well as any remaining pairwise combinations of those hits. In addition, the growth factor cocktail known to promote the self-renewal of posterior foregut cells was included (PFSC) (Hannan et al., 2013). Traditional cell culture dishes were coated with FN + VTN and a pure population of SOX17+ endoderm cells was cultured for 3 days in the presence of these GF/SM combinations, at which point conditions were analyzed for %SOX17-GFP+ and %SOX17-GFP+Ki-67+ as well as cell number (Figure 3-5A, B). Ki-67 is a marker of cell proliferation; since our goal is to generate an expandable definitive endoderm progenitor, it is of value to know which culture conditions fosters the most proliferation of SOX17+ cells. Those conditions that outperformed included CHR+FGF and WNT+FGF. Next, I performed a dose response with WNT, RSP and CHR in the presence of FGF (Figure 3-5C). These conditions significantly maintained SOX17-GFP as compared to the Matrigel No GF control and the optimal dosage proved to be WNT at 50 ng/mL in conjunction with FGF. In summary, the secondary GF/SM screen produced various hits which were scaled up and tested in traditional culture formats. The final optimal growth conditions for endoderm cells was FN + VTN supplemented with WNT and FGF.
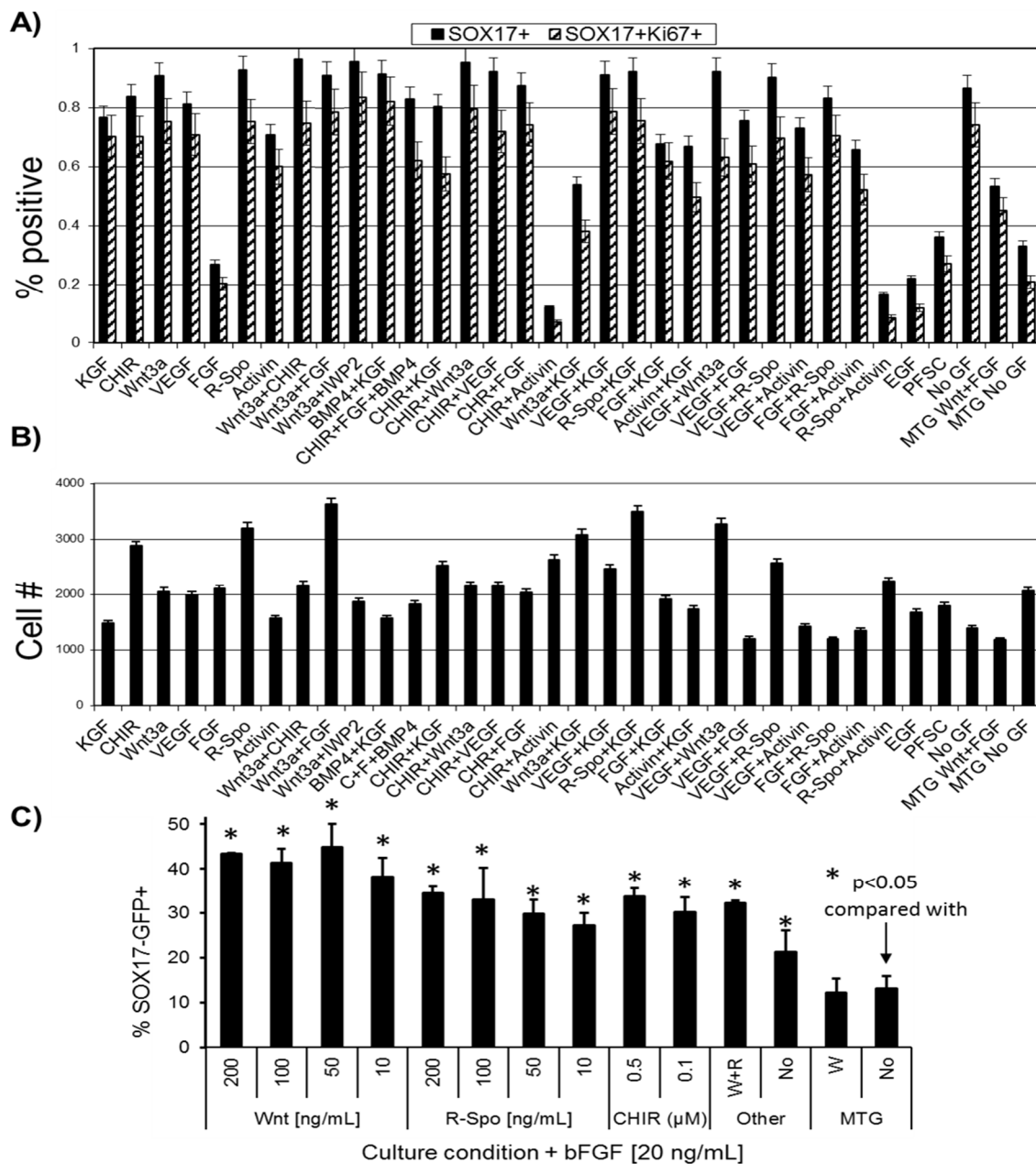
Figure 3-5. Scale up validation of secondary growth factor screen. A) Specific hits from the secondary growth factor screen and single growth factor hits from the principal component analysis were further investigated by scaling up into traditional cell culture dishes coated with FN + VTN. Flow cytometric analysis shows the percentage of cells in each condition that are SOX17+ or SOX17+GFP+. Most high performing conditions include a Wnt protein agonist and a member of the FGF superfamily. B) Cell number was also quantified for all scaled-up conditions. C) Wnt agonists supplemented with bFGF at 20 ng/mL were tested in scaled up culture dishes coated with FN + VTN to determine the most effective Wnt agonist for SOX17 maintenance. Abbreviations: PFSC=posterior foregut stem cell growth factors.

Definitive Endoderm Cells Fail to Passage in Monolayer Culture with Hit Conditions

Once I settled on a combination of defined ECMPs and GFs that maintained SOX17-GFP, I attempted to translate this to culturing endoderm cells across multiple passages. Initially, I used our knowledge from the high throughput screens to grow endoderm cells in monolayer conditions coated with hit ECMPs, FN + VTN, and supplemented with hit GFs, WNT and FGF. I hoped to observe maintenance of SOX17-GFP for not only a few days but for a few passages. Instead, I noticed that while DE cells favorably adhered to the defined substrate, they were certainly not proliferative enough to grow into another passage. Several seeding densities were tested to ensure that this was not a cell density-dependent issue. Even when cells were seeded densely to endure adequate cell number for another passage, there was an issue with DE cells grown in defined conditions being enzymatically dissociated and replated. Various dissociation reagents, including Accutase, EDTA, and Trypsin, and even mechanical scraping did not allow DE cells to grow after passaging. I speculate that the inability of DE cells to grow past passage one was likely due to the integrin expression of these cells being modified after initial DE induction and subsequent growth on FN + VTN with WNT and FGF. After much trial and error, it became apparent that DE cells at passage one were not identical to DE cells at passage zero, rendering the hit conditions not suitable for consistent serial passaging.

ACME screens identified hit ECMPs and GFs that allowed for one passage of monolayer growth of DE cells but further passaging proved to be an insurmountable challenge. Taking a step back, our initial research goal was to expand a DE population so I decided to work around this passaging issue by broadening my approach. I already knew that removing the growth factors was not favorable for the maintenance of SOX17-

GFP. Instead of monolayer culture, I considered trying to grow DE cells in suspension, as has been successfully done previously in various other models of expansion protocols(Cormier et al., 2006; Kallos and Behie, 1999; Krawetz et al., 2009; Lorences and Fry, 1991; Zandstra et al., 1994; Zweigerdt et al., 2011). It seemed that the FN + VTN substrate was sufficient for transient maintenance of SOX17-GFP but was not allowing for perpetual expansion of this DE population. I next posited that removing the FN + VTN substrate and expanding these cells in suspension culture formats would allow the cells to form their own ECM architecture and would potentially facilitate successful passaging of DE cells.

Definitive Endoderm Cells Exhibit Modest Growth in Suspension Culture with Hit Growth Factors

Adherent culture of SOX17+ definitive endoderm cells in hit conditions showed early signs of promise, allowing for strong adhesion and the relative increase in SOX17 maintenance compared to Matrigel and other defined matrices. However, the apparent inability to passage the endoderm population led us to a dead end with that approach. Other studies have reported success with growing stem cell populations in suspension without losing the characteristics of that stem cell (Olmer et al., 2012; Steiner et al., 2010; Wang et al., 2013; Zandstra et al., 1994; Zweigerdt et al., 2011). Since we initially set out to expand an endoderm progenitor population and adherent culture conditions were insufficient, it seemed logical to employ suspension cultures, where cells are allowed to aggregate without the use of defined matrices or microcarriers. Sorting the definitive endoderm cells in order to purify a homogenous SOX17+ population repeatedly resulted in contamination issues, even with stringent sterility measures and the use of antibiotics, so I decided to try aggregation of the heterogenous DE population,

which included cells that were still undifferentiated. I was hopeful when I noticed the

heterogenous definitive endoderm cells were rather effective at forming aggregates in

the presence of CHR+FGF and even effectively reaggregated after single-cell passaging

into passage two (Figure 3-6A). Flow cytometric analysis was performed for TRA-1-81

and SOX17-GFP at each passage to determine what population of cells was persisting

in these suspension conditions. As expected, the population at DE showed a mixed

group of three distinct populations, with no TRA-1-81+SOX17+ double-positive cells. At

passage one, the SOX17-GFP population was diminishing while the TRA-1-81+

population was increasing. At passage two, both markers receded and most cells

became double negative (Figure 3-6B). Although the growth of this heterogenous

population seemed to be moving away from DE, I did finally notice a significant growth

curve within the population, increasing up to 8-fold in conditions supplemented with both

WNT and FGF (Figure 3-6C). These growth factors, when used individually instead of

together, fostered less proliferation while culture conditions supplemented with no

growth factors grew the slowest and were least prone to reaggregation after single-cell

passaging.
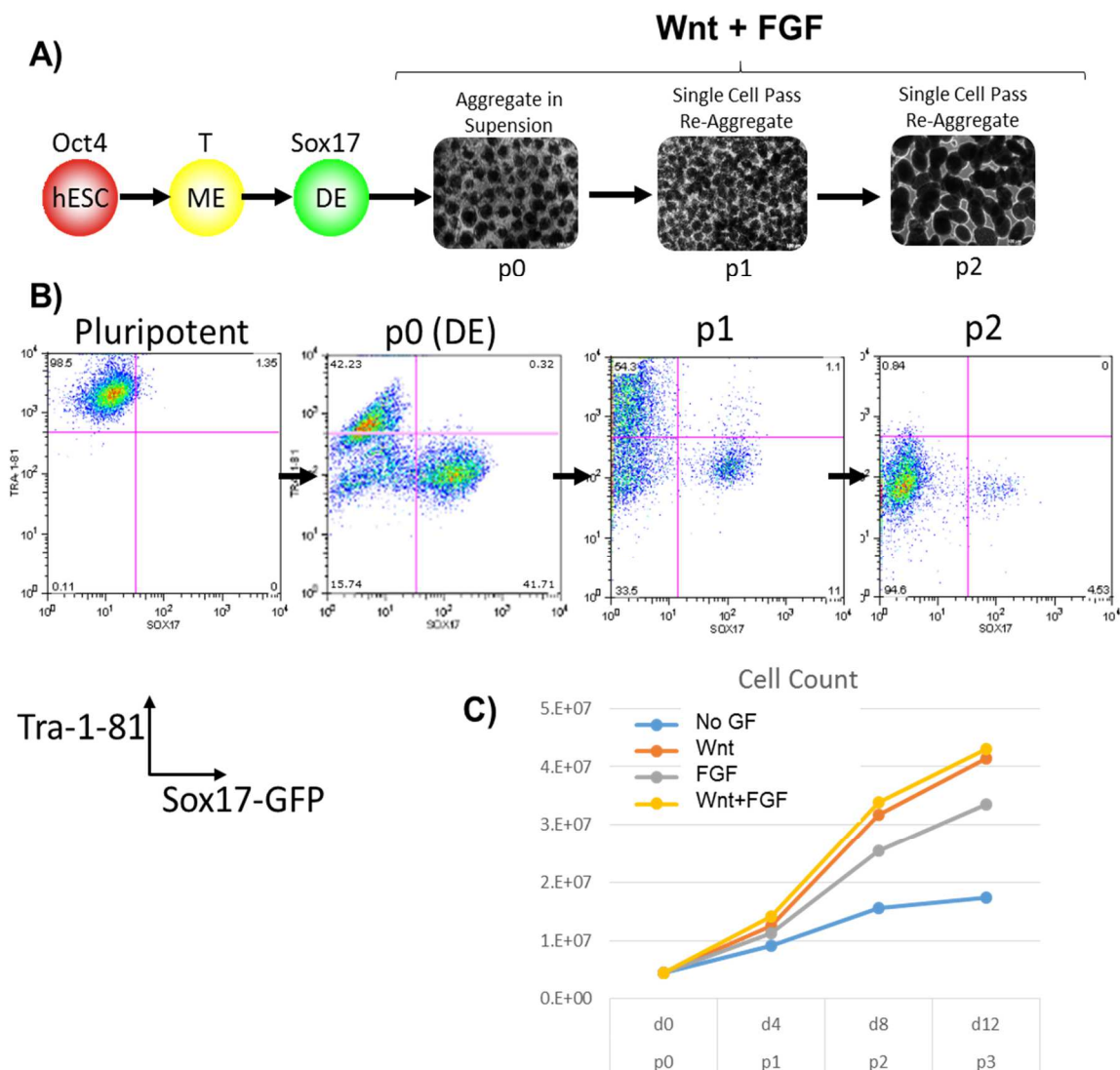
Figure 3-6. Expansion of definitive endoderm cells in optimal culture conditions.
A) Schematic showing the experimental approach to generating endoderm progenitors from hESCs. DE cells failed to self-renew on FN + VTN substrates, so DE expansion was attempted in suspension with hit growth factors. At each passage, cells were dissociated to single cell and reaggregated. B) Flow cytometric analysis of expanded DE cells showing that by passage 2, there are virtually no pluripotent TRA-1-81+ cells but also very few SOX17+ cells. C) Growth curve of expanded DE cells. Growth reached a stopping point after passage 2.

In addition to flow cytometric analysis, I observed gene expression over these passages by quantitative PCR, looking closely at endoderm markers *CXCR4, SOX17, FOXA2* and pluripotent markers *OCT4* and *NANOG*. Included in the analysis were conditions that included only FGF or only WNT and a No GF condition. Pluripotent ES and differentiated DE were used as controls (Figure 3-7). I noticed that cells that grew into passages one through three with WNT and FGF supplementation were significantly upregulated for DE markers as compared to ES and that pluripotent markers were significantly downregulated. Expression of DE markers was less than half that of the DE control by passage three, but the significance value is still strong compared to the ES control. Conditions containing FGF only seemed to lose expression of DE markers and upregulate *NANOG* over the course of three passages, suggesting that the pluripotent population outcompeted the DE cells relatively quickly. By transcriptional analysis, the results would support the notion that I was indeed expanding an endoderm progenitor of sorts. However, studying this population further is severely hindered by the fact that I cannot indefinitely passage these cells. After single-cell dissociating them twice in order to reaggregate for further expansion, this population no longer exhibits proliferative properties necessary for passaging. This may be a result of definitive endoderm senescence or that the growth factors WNT and FGF are not sufficient to induce proliferation of the endoderm population. It is interestingly of note that although indefinite expansion was not possible, these endoderm populations can be expanded ~8-fold and retain gene expression indicative of definitive endoderm over the course of two weeks (passaging twice).
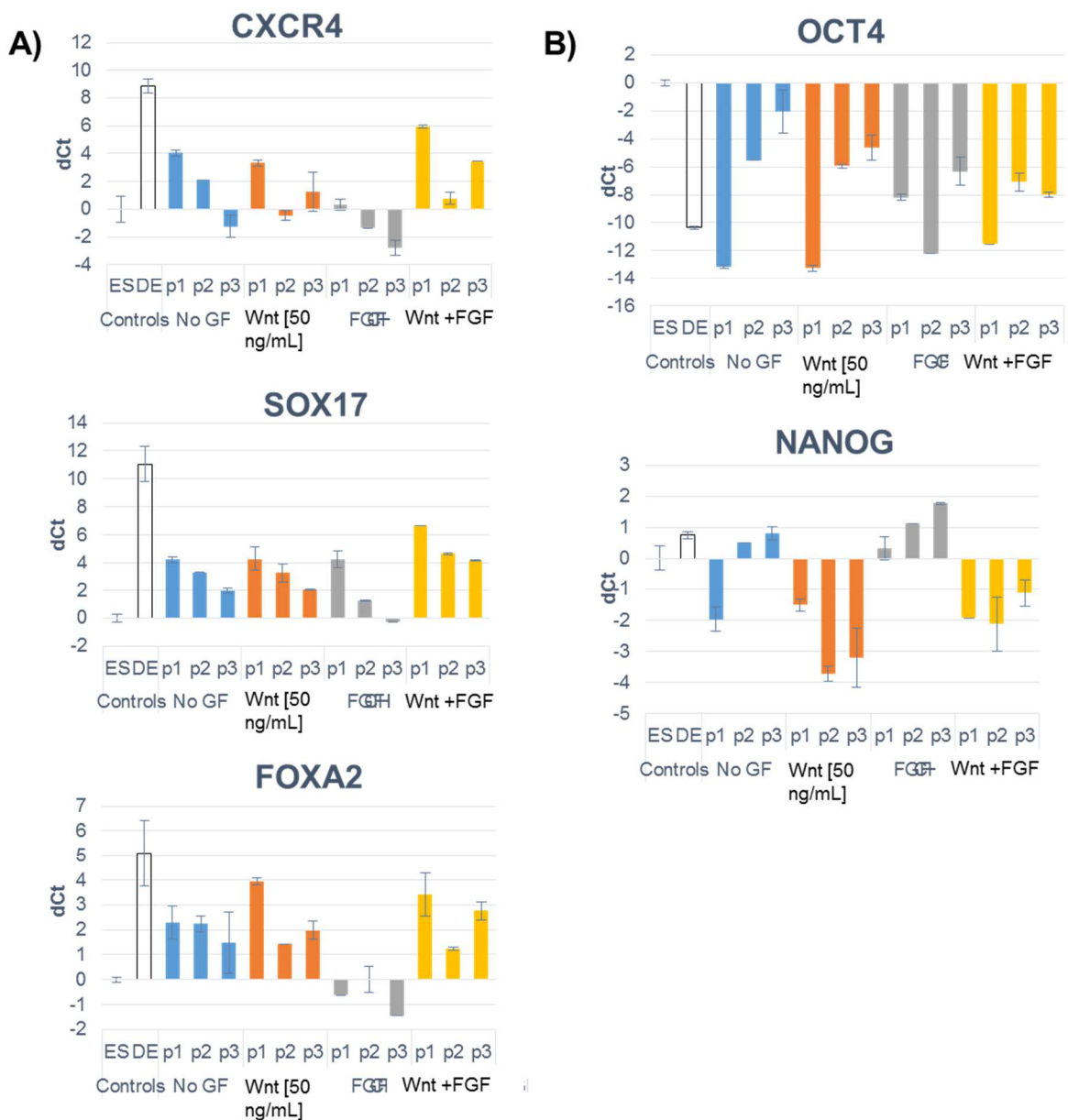
Figure 3-7. Gene expression analysis of definitive endoderm cells expanded in suspension culture conditions. A) Quantitative PCR analysis of endoderm markers in expanded DE cells. Included in the analysis are samples from passages 1-3 in culture conditions containing No GF (blue bars), Wnt only (orange bars), FGF only (gray bars), or both Wnt and FGF (yellow bars) B) Quantitative PCR analysis of pluripotent markers in expanded DE cells.

Discussion

The extracellular matrix is critical for hES cell maintenance (Braam et al., 2008; Brafman et al., 2009a), and here we show that the ECMP components also greatly influence hES cell differentiation to DE. By systematically screening ECMP combinations for their ability to promote either differentiation or maintenance of DE, we identified two ECMPs, FN, and VTN, which make differentiation to DE and maintenance of DE significantly more efficient, thereby overcoming the use of poorly defined and xenogeneic factors, such as Matrigel.

While others previously have explored the role of physical properties within the microenvironment, such as three-dimensional culture (Chen et al., 2007) and substrate rigidity, (Engler et al., 2006) we focused our study on the ECM's role in differentiation and maintenance of DE. We found that the composition of the ECM potently influenced the ability of hES cells to express markers associated with endoderm, both in the derivation and maintenance of DE. Our results suggest that appropriately defining the ECMP substrate in addition to the soluble signaling molecule environment is critical for optimizing the differentiation of hES cells. Since the ECMP affects the ability of growth factors such as Wnt3a and Activin to influence hES cells, this dependence on the ECM is widely applicable to differentiation into any lineage, not just DE.

Consistent with our findings that FN and VTN optimized differentiation towards DE, I found through systematic high-throughput screening that this defined substrate also optimized maintenance of SOX17 in our transient DE population. It should be stressed that in our experiments only the initial matrix compositions are specified. Cells exposed to these ECMPs begin to remodel their supporting matrix and eventually secrete their own ECMPs, serving to autologously modify their microenvironment. Even so, the observed cellular responses are a direct response to the initial composition of

the ECM. Although culturing transient DE cells on FN + VTN supplemented with hit growth factors WNT + FGF did not generate an indefinitely self-renewing endoderm population, it did serve to identify some components of the fully-defined culture system that will be necessary to do so.

Derivation of endoderm-specific stem cells with the ability to self-renew would serve as a source for disease modeling, developmental studies, and cell-based therapies. Our inspiration was to realize this potential but our results represent only a starting point to that end, describing a stepwise method to differentiate hPSCs into a population of endoderm-like stem cells with limited self-renewal capacity. Our study provides a defined serum- and feeder-free culture system allowing the isolation and limited expansion of endoderm-like stem cells. Similarly, a recent study has shown that multipotent, self-renewing DE cells could be expanded in vitro (Cheng et al., 2012; Sneddon et al., 2012), however, these cells express a broad diversity of markers that render their developmental identity difficult to establish. Furthermore, these studies relied on xenogeneic feeders, Matrigel, 3D culture conditions, or serum, any of which is not scalable or useful for clinical applications.

To conclude, expansion of a multipotent endoderm progenitor population would be advantageous for clinical applications. Self-renewing, multipotent, non-tumorigenic stem cells could provide a beneficial source for generating large numbers of differentiated cells suitable for cellular therapy, since they would eliminate the risk of teratomas associated with pluripotent stem cells. Indeed, our culture system is compatible with large-scale production of endodermal-like cells that could significantly simplify the generation of mature, therapeutic cells. However, the limited self-renewal capacity of our endoderm-like progenitors make our culture system only a starting point and will require additional factors to derive a functionally multipotent progenitor

population. Furthermore, derivation of endoderm progenitors would allow for

systematic differentiation of numerous hPSC lines without the need to establish

individual protocols. Thusly, self-renewing multipotent progenitors would not only

provide a compelling in vitro model of developmental biology but also serve to advance

the field of personalized medicine. Further research is critical to realizing this goal and

it is our hope that this work will be a useful starting point to that end.

Table 3-1. **ECMPs, GFs, SMs used for high-throughput screens.**

Product	Vendor	Catalog #	Concentration Used
Collagen I	Sigma-Aldrich	C7774	250 µg/mL
Collagen III	Sigma-Aldrich	C4407	250 µg/mL
Collagen IV	Sigma-Aldrich	C7521	250 µg/mL
Collagen V	Sigma-Aldrich	C3657	250 µg/mL
Fibronectin	Sigma-Aldrich	F2518	250 µg/mL
Laminin	Sigma-Aldrich	L6274	250 µg/mL
Vitronectin	Sigma-Aldrich	V8379	250 µg/mL
Wnt3a	In House		100 ng/mL
R-Spondin	In House		100 ng/mL
CHIR98014	Selleck Chemicals	S2745	50 ng/mL
Dkk-1	R&D Systems	5439-DK-010	50 ng/mL
IWP-2	Tocris	3533	50 ng/mL
FGF	Life Technologies	13256-029	40 ng/mL
KGF	Life Technologies	PHG0094	50 ng/mL
VEGF	R&D Systems	293-VE-010	50 ng/mL
EGF	R&D Systems	236-EG-01M	50 ng/mL
SHH	R&D Systems	464-SH-025	50 ng/mL
Cyclopamine	Tocris	1523	50 ng/mL
BMP4	R&D Systems	314-BP-010	50 ng/mL
Activin	R&D Systems	338-AC-010	50 ng/mL
Dorsomorphin	Sigma-Aldrich	P5499-5MG	50 ng/mL
SB 431542	Tocris	1614	50 ng/mL
Noggin	R&D Systems	6057-NG-025	50 ng/mL

Table 3-2. **Primer sequences used for gene expression analysis**.

Gene	ABI Assay
18s	Hs99999901_s1
OCT4	Hs04260367_gH
NANOG	Hs04399610_g1
SOX2	Hs01053049_s1
FOXA2	Hs00232764_m1
SOX1	Hs01057642_s1
MESP1	Hs01001283_g1
MIXL1	Hs00430824_g1
LHX1	Hs00232144_m1
SOX17	Hs00751752_s1

Table 3-3. **Antibodies used for immunofluorescence**.

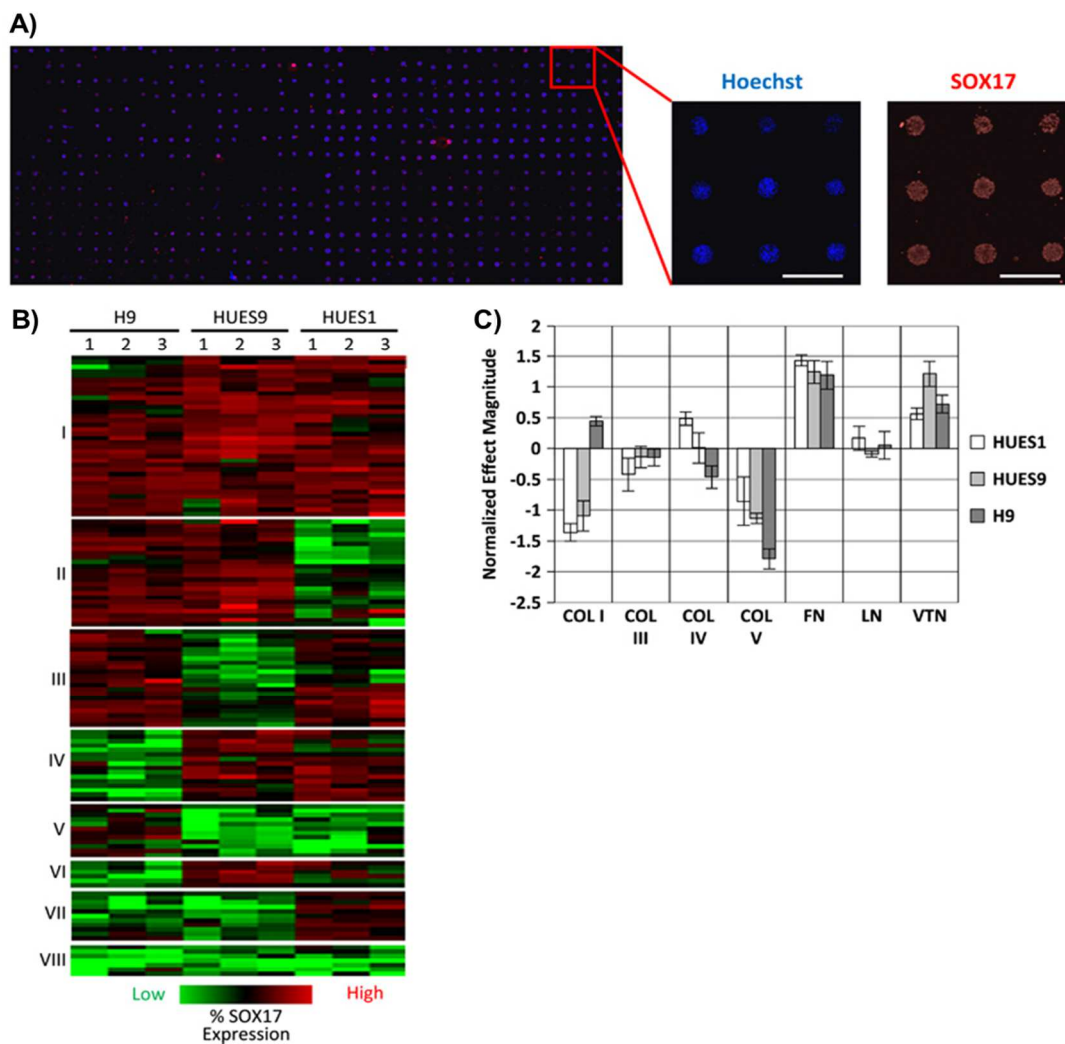| Antibody	Vendor	Catalog #	Concentration Used
Rabbit anti-NANOG	Santa Cruz	SC-33759	1:50
Rabbit anti-OCT4	Santa Cruz	SC-9081	1:50
Mouse anti-MIXL1	R&D Systems	MAB2610	1:200
Goat anti-SOX17	R&D Systems	AF1924	1:200
Goat anti-FOXA2	R&D Systems	AF2400	1:200
Rabbit anti-Ki-67	Abcam	ab15580	1:200
Alexa-647 Mouse IgG2a Isotype Control	BD	558053	20 μl per test
PE Mouse IgG1 Isotype Control	BioLegend	400113	5 ul per test
PE Mouse IgG2a Isotype Control	BD	561552	5 ul per test
Alexa 647 Donkey Anti-Goat	Life Technologies	A-21447	1:200
Alexa 647 Donkey Anti-Rabbit	Life Technologies	A-31573	1:200
Alexa 647 Donkey Anti-Mouse	Life Technologies	A-31571	1:200
Alexa 546 Donkey Anti-Rabbit	Life Technologies	A-10040	1:200
Alexa 546 Donkey Anti-Mouse	Life Technologies	A-10036	1:200
Alexa 488 Streptavidin Conjugate	Life Technologies	S-11223	1:200
Alexa 488 Donkey Anti-Rabbit	Life Technologies	A-21206	1:200
Alexa 488 Donkey Anti-Mouse	Life Technologies	A-21202	1:200

Figure A3-8. Adapted from Brafman et al. 2013**. High-throughput ECMP screen reveals the influence of ECMPs in DE differentiation.** (A) hESCs (H9, HUES1, HUES9) were cultured on ECMP arrays using previously published DE differentiation conditions.[8] On day 3, arrays were fixed and stained with Hoechst and an antibody to SOX17, a marker for DE (scale bar=450 μm). (B) Heat map representing the cell number normalized SOX17 expression of each ECMP combination (rows) for each independent array experiment. Three independent array experiments were performed with each hESC line. Columns were mean normalized and scaled to one unit S.D. Hierarchical clustering of ECMP conditions was performed using Pearson correlation coefficient as a similarity metric. Clustering segregated ECMP combinations into eight groups based on the normalized SOX17 expression induced in each hESC line. (C) Magnitude of the main effects from a full factorial analysis of the ECMP array data reveals that specific ECMP components, FN and VTN, have largest positive effects on DE differentiation efficiency (*n*=3 independent array experiments; error bars, S.E.M.)
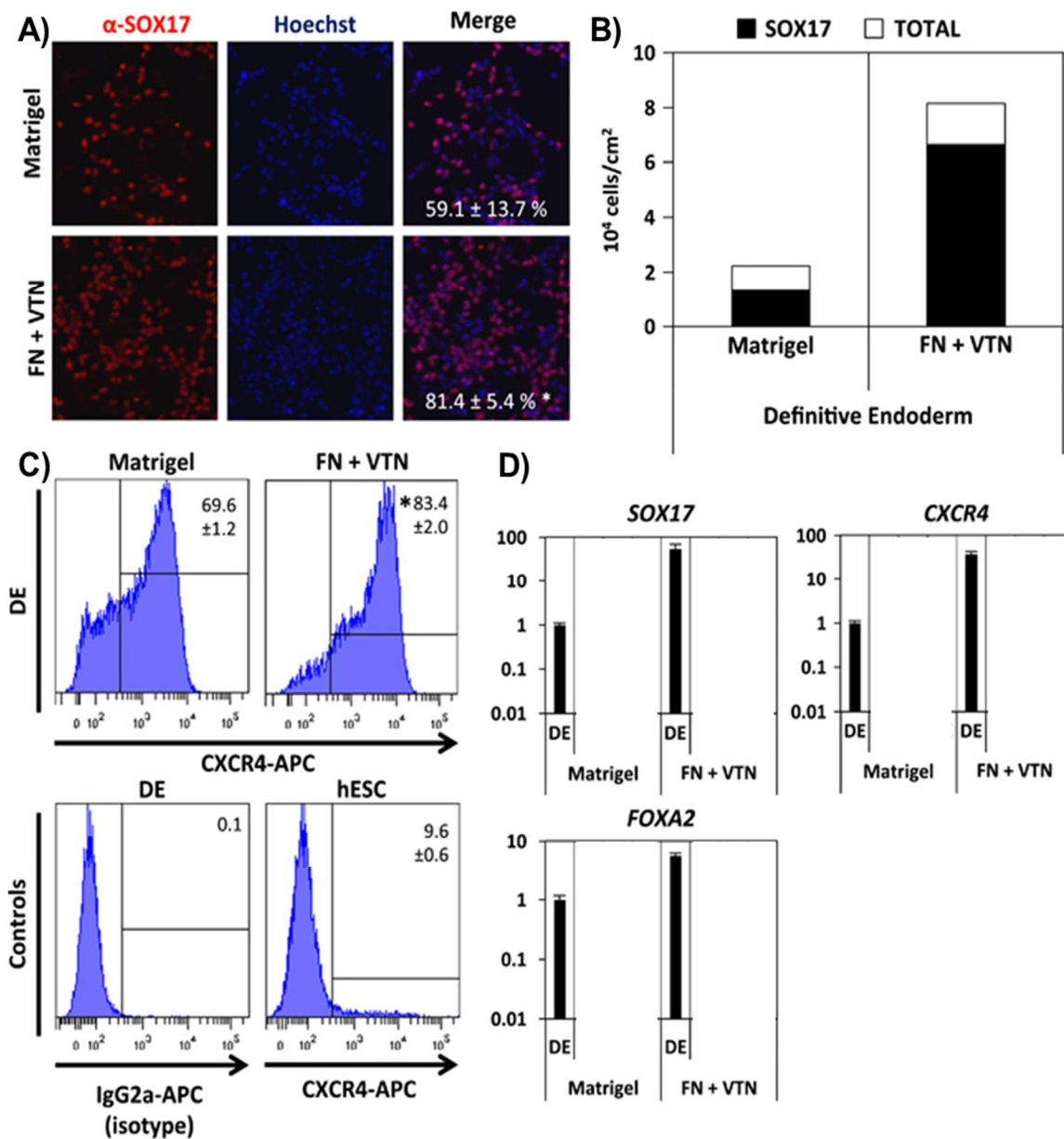
Figure A3-9. Adapted from Brafman et al. 2013. **ECMPs improve efficiency of hESC differentiation to DE, PGT, PF endoderm, and PE.** HESCs were cultured on MGEL and FN and VTN (FN+VTN) using previously published protocols.[2, 8, 9] (a) Representative images of *α*SOX17 immunofluorescence of HUES9 hESCs differentiated to DE on MGEL and FN+VTN (mean±S.E.M.). (b) Quantification of HUES9 hESCs stained by SOX17 cells out of total cell number (*n*=3; mean±S.E.M.). (c) Flow cytometric analysis of CXCR4 expression of HUES9 hESCs differentiated to DE on MGEL and FN and VTN (FN+VTN). (d) Gene expression analysis for markers of DE (SOX17, FOXA2, CXCR4)

Chapter 4. Generation of an expandable intermediate mesoderm

restricted progenitor cell line from human pluripotent stem cell

Abstract

The field of tissue engineering entered a new era with the development of human pluripotent stem (hPS) cells, which are capable of unlimited expansion whilst retaining the potential to differentiate into all mature cell populations and tissues. However, in their undifferentiated state, these cells harbor significant risks, such as the ability to form tumors upon transplantation. One way to mitigate this risk is to develop expandable progenitor cell populations with restricted differentiation potential. In this study, we used a cellular microarray technology to identify a fully defined and optimized culture condition that supports the derivation and propagation of a cell population with mesodermal properties. This cell population, which we refer to as mesodermal progenitor (MP) cells, is capable of virtually unlimited expansion, lacks tumor formation potential, and, upon appropriate stimulation, readily acquires properties of the renal lineage. When cocultured with E12.5 kidney cells, MP-derived MM cells integrate into renal organoids and surround epithelial cap mesenchyme and collecting duct structures *in vitro*. Interestingly, MP cells fail to differentiate into other mesodermally-derived tissues, such as blood and heart muscle, suggesting that these cells are restricted to an intermediate mesodermal fate. Taken together, we have developed under fully defined conditions an expandable progenitor population that can be used as a non-tumorigenic source of intermediate mesodermal-derived tissues for regenerative medicine approaches.

Introduction

Human pluripotent stem cells (hPS cells; including human embryonic stem [hES] cells and human induced pluripotent stem [hiPS] cells) have the potential to generate the various cell types of the adult body. Therefore, hPS cells provide a potentially unlimited source of mature cell types that can be used for disease modeling, drug discovery, and regenerative medicine purposes. Current methods for generating these therapeutically relevant cell types follow a linear approach in which hPS cells are differentiated in small, discrete steps that mimic the sequence of events occurring during development. The initial stage in these protocols typically involve specification of hPS cells into one of the three embryonic germ layers—ectoderm, endoderm, or mesoderm. As such, several protocols have been developed for the generation of mesodermally-derived tissues including muscle, blood, and urogenital cells (Kee and Reijo Pera, 2008; Lian et al., 2012; Ng et al., 2008; Taguchi et al., 2014a, 2014b). While these studies have demonstrated the potential of hPS cell-derived mesodermal tissues for cell replacement therapies, these protocols result in the generation of heterogeneous cell populations, some with tumor forming potential, which limits their clinical application. Additionally, because of the inefficiency of these established protocols, large numbers of input cells are necessary to generate cell types in the quantities necessary for clinical applications.

Expansion of intermediate progenitor populations of differentiating hPS cells followed by subsequent differentiation is an alternative approach for generating highly enriched and well-defined cell populations required for cell-based therapies and disease modeling. For example, homogenous, expandable ectodermally- and endodermally-restricted progenitor populations have been generated from hPS cells (Chambers et al., 2009; Cheng et al., 2012; Reubinoff et al., 2001; Shin et al., 2006). However, similar

methods to generate cell types restricted to the mesodermal lineage have yet be developed.

The cell microenvironment plays a critical role for regulating the self-renewal and differentiation of many progenitor cell populations that exist within the developing and fully mature adult organism (Jones and Wagers, 2008; Moore and Lemischka, 2006). To that end, I used a multifactorial high-throughput screening technology (Brafman et al., 2012; Flaim et al., 2005) to engineer *in vitro* microenvironments that allow for the homogenous expansion of a hPS cell-derived mesodermally restricted progenitor population, which I refer to as mesoderm progenitors (MPs). The optimized microenvironments allow for the long-term expansion of MPs that lack tumor forming potential and display a genetic signature similar to that of mesoderm. Upon modulation of their culture conditions, MPs readily generate urogenital cell types. Interestingly, MP cells fail to differentiate into other mesodermal lineages, such as blood and cardiac muscle. Therefore, MP cells provide a useful tool to not only study the mechanisms that regulate human mesoderm development but also a homogenous, non-tumorigenic cell source for regenerative medicine purposes.

Materials and Methods

Human pluripotent stem cell (hPSC) culture

Human ES cell lines H9 and Hues9 were obtained from WiCell and Harvard University, respectively. All experiments described in this study were approved by a Stem Cell Research Oversight Committee (Protocol #100210ZX, PI Willert). The human induced pluripotent stem cell line BJ RiPS (Warren et al., 2010) were provided under a Material Transfer Agreement from Dr. D. Rossi (Childrens Hospital Boston, MA). The following media were used: BJ RiPS and Hues 9 ES (DMEM/F12 mixed, 20% (v/v)

Knockout Serum Replacement, 1% (v/v) penicillin-streptomycin, 1% (v/v) nonessential amino acids, 2 mM L-glutamate, 0.1 mM β-mercaptoethanol and 10 ng/mL FGF2 (Peprotech); H9 ES (DMEM/F12 supplemented with L-Ascorbic Acid, Selenium, Transferrin, $NaHCO_3$, Insulin, TGFβ1, and FGF2 as described previously (Chen et al., 2011). Fresh media was added daily to all cells. Every five days, colonies were enzymatically passaged with Accutase and transferred to a Matrigel-coated culture dish. All media components are from Life Technologies unless indicated otherwise. For all experiments, hPSCs were used between passages 20 and 50 in this study.

Array fabrication and characterization

Arrayed cellular microenvironment (ACME) slides were fabricated as previously described (Brafman et al., 2012). Briefly, glass slides were cleaned, silanized, and then functionalized with a polyacrylamide gel layer. For ECMP arrays, stock solutions of ECMPs were suspended at 250 μg/ml in ECMP printing buffer (100 mM acetate, 5 mM EDTA, 20% (v/v) glycerol and 0.25% (v/v) Triton X-100, pH 5.0). ECMP solutions were mixed in all possible 128 combinations in a 384-well plate. For GF and SM arrays, stock solutions were suspended at 1 mg/ml in soluble factor printing buffer (100 mM acetate, 5 mM EDTA, 19% glycerol (v/v) and 0.25% (v/v)Triton X-100,10 mM trehalose dehydrate (Sigma), 1% poly(ethylene glycol), pH 5.). GF solutions were then mixed into 400 combinations representing all single, pairwise, and non-redundant three-way combinations possible in a 384-well plate. The following ECMPs, GFs, and SMs (Product/Vendor/Catalog #/Concentration) were used: Collagen I/Sigma-Aldrich/C7774/250 μg/mL, Collagen III/Sigma-Aldrich/C4407/250 μg/mL, Collagen IV/Sigma-Aldrich/C7521/250 μg/mL, Collagen V/Sigma-Aldrich/C3657/250 μg/mL, Fibronectin/Sigma-Aldrich/F2518/250 μg/mL, Laminin/Sigma-Aldrich/L6274/250 μg/mL,

Vitronectin/Sigma-Aldrich/V8379/250 µg/mL, Wnt3a/   In House/100 ng/mL, R-Spondin/In House/100 ng/mL, CHIR98014/Selleck Chemicals/S2745/50 ng/mL, Dkk-1/R&D Systems/5439-DK-010/50 ng/mL, IWP-2/Tocris/3533/50 ng/mL, FGF/Life Technologies/13256-029/40 ng/mL, KGF/Life Technologies/PHG0094/50 ng/mL, VEGF/R&D Systems/293-VE-010/50 ng/mL, EGF/R&D Systems/236-EG-01M/50 ng/mL, SHH/R&D Systems/464-SH-025/50 ng/mL, Cyclopamine/Tocris/1523/50 ng/mL, BMP4/R&D Systems/314-BP-010/50 ng/mL, Activin/R&D Systems/338-AC-010/50 ng/mL, Dorsomorphin/Sigma-Aldrich/P5499-5MG/50 ng/mL, SB 431542/Tocris/1614/50 ng/mL, Noggin/R&D Systems/6057-NG-025/50 ng/mL. The hit ECMP condition from the primary screen was used as a substrate to print the GFs and SMs in the second screen. Twenty individual spots of each protein/growth factor/small molecule mixture, clustered into groups of five and printed in different quadrants of the slide, were deposited with a 450 µm pitch on the acrylamide gel pad using a SpotBot Personal Microarray Printer (ArrayIt) equipped with Stealth SMP 4.0 split pins. The pins were cleaned by sonication in 5% Micro Cleaning Solution (ArrayIt) and dH_2O immediately before use. Between each sample in the source plate, the pins were dipped in a 50% DMSO and water solution, washed for 25 seconds with dH_2O and dried.

Slide imaging, quantification, and analysis

Slides were fixed with 4% PFA for 10 minutes at room temperature and washed with PBS. Slides were imaged using the CellInsight™ CX5 High Content Screening (HCS) Platform (ThermoFisher). The system was programmed to visit each spot on the array, perform autofocus, and acquire DAPI and FITC (GFP). Cell counts and stain intensities were measured using Thermo Scientific™ HCS Studio™ 2.0 Software using the built-in object identification and cell intensity algorithms.

MP cell derivation and culture

Undifferentiated hPSCs were re-plated on Matrigel at a density of 3×10^3 cells/cm^2 and cultured in ES cell culture medium for four days. To direct cells to the mesoderm lineage, the media was switched to serum free differentiation media (consisting of RPMI 1640, 1x B27 minus Insulin, and 1% (v/v) penicillin-streptomycin). Cells were treated with 10 µM CHIR-98014 (CHR, Tocris) for the first 24 hours and then allowed to recover for an additional 24 hours without CHR. Tissue culture plates were incubated with ECMP coating buffer (PBS with 15 ng/ml Collagen I [C1], 15 ng/ml Collagen III [C3], 15 ng/ml Collagen IV [C4], 50 ng/ml Fibronectin [FN], 15 ng/ml Vitronectin [VN]) overnight at 37° with volume sufficient to coat the surface area of the well. Mesoderm (48 hours) cells were single-cell passaged with Accutase and replated onto C1 C3 C4 FN VN-coated plates at a density of 3.5×10^3 cells/cm^2 in serum free differentiation media supplemented with 1 µM CHR and 20 ng/ml FGF. Media was also supplemented with 10 mM Y27632 (Wako) for improve passaging efficiency. Optimal CHR concentration varied with cell line; Hues 9 MP cells propagated in colonies most efficiently at 0.25 µM while BJ RiPS cells did so at 0.05 µM. Manual picking of colonies in passage 1 improved MP expansion. Differentiated cells around colonies were scraped away before passaging. Half the media was changed the day after passaging and then full media changes were made every other day thereafter. For routine passaging, MP cell cultures reaching 85% confluency were dissociated using a 0.5 mM EDTA (in Ca^{2+}/Mg^{2+}-free PBS, pH 8.0) at room temperature (RT) for 5 min. MP cells were removed from the plate via gentle washing with the EDTA solution. Using this method, MP cells were routinely passaged every 5-8 days.

Differentiation of hES cells to endoderm (EN), ectoderm (EC) and mesoderm (ME)

Endoderm Differentiation: Human ES cells were differentiated to endoderm as previously described (D'Amour et al., 2005). Initiated on days 4–6 after passage (depending on culture density), sequential, daily media changes were made for the entire differentiation protocol. After a brief wash in PBS (with Mg/Ca), cells were cultured in RPMI (without FBS), Activin A (100 ng/ml) and Wnt3a (25 ng/ml)(generated in house as described (Willert, 2008) for the first day. The next day the medium was changed to RPMI with 0.2% vol/vol FBS and Activin A (100 ng/ml), and the cells are cultured for 2 additional days. Definitive endoderm was collected at day 3 for analysis.

Ectoderm Differentiation: Human ES cells were differentiated to ectoderm by modifying an established neural rosette protocol (Wilson and Stice, 2006). Two days before passaging hES cells, medium was changed to N2 medium (DMEM/F12 with 1x N2). One day before passaging, medium was changed to N2 medium supplemented with 1uM of Dorsomorphin (Calbiochem, cat# 171261). The day of passaging, EBs were initiated by detaching cells with Accutase and gentle cell scraping. 2e6 H9 cells were used to seed one well of a 6-well low binding plate and placed on a rotating platform (95 rpm) in a 37°C incubator. Two days later, medium was changed to N2 medium with 1uM Dorsomorphin and media changes were made as needed until 8 days after EB formation, at which point EBs were replated onto Matrigel-coated plates using NBF media (DMEM/F12 with 0.5x N2, 0.5x B-27, 20ng/mL of FGF and 1% P/S) to form rosettes. Four to six days after plating onto Matrigel, cells were collected for analysis.

Mesoderm differentiation: Human ES cells were differentiation to mesoderm as previously described (Lian et al., 2013). Once hES cells were 50-60% confluent, medium was changed to serum free differentiation medium (RPMI supplemented with 1x (v/v) B27 (without insulin)) with 10 µM CHIR-98014. After 24 hrs, the medium was changed

to serum free differentiation medium without CHIR-98014. Cells were collected at 48

hours for analysis

Human ES and MP cell differentiation

Hematopoietic differentiation: Human ES and MP cells were differentiated to the

hematopoietic lineage as previously described(Ng et al., 2008). ES cells were

differentiated towards hematopoietic precursors first by ME induction with 25

ng/ml human BMP4 for 4 days. MP cells were treated as d4 ME, bypassing BMP4

treatment. After mesoderm induction, cells were treated with 20 ng/ml FGF and 50

ng/ml human VEGF (Humanzyme) for 4 days and then with 50 ng/ml Flt-3L (R&D

Systems) and 150 ng/ml IL-6 (R&D Systems) for 4 days.

Cardiomyocyte differentiation: Human ES and MP cells were differentiated to the

cardiac lineage as previously described (Lian et al., 2012). Human ES cells were

induced to mesoderm with 10 µM CHIR 98014 for 24 hrs, then incubated for 48 hrs in

serum free differentiation media. MP cells were treated as d3 cultures, bypassing this

initial treatment. Cells were then treated with IWP-2 for 4 days, incubated for an

additional 2 days in serum free differentiation media, then supplemented with insulin at

day 9.

Germ line differentiation: Human ES and MP cells were differentiated to primordial

germ cells as previously described (Kee and Reijo Pera, 2008). When cells were 40%-

50% confluent, hES and MP cells were differentiated in hES differentiation media

(Knockout DMEM [Invitrogen catalog # 10829-018], 20% (v/v) FBS, 2 mM L-glutamine,

1% (v/v) nonessential amino acids, 90 µM β-mercaptoethanol and 1% (v/v)

penicillin/streptomycin supplemented with 50 ng/mL BMP (bone morphogenetic protein)

4, BMP7, and BMP8b). Half the media was replaced with fresh differentiation media on day 3 and cells were collected for analysis at day 7.

Kidney differentiation: Human ES and MP cells were differentiated to the kidney lineage as previously described (Taguchi et al., 2014a). In serum free differentiation media (SFDM; DMEM/F12 supplemented with 2% (v/v) B27 (without retinoic acid), 2 mM L-glutamine, 1% (v/v) ITS, 1% (v/v) nonessential amino acids, 90 µM β-mercaptoethanol and 1% (v/v) penicillin/streptomycin), hES and MP cells were aggregated at 10,000 cells per well in U-bottom 96-well low-cell-binding plates to form EBs. EBs were formed in the presence of 10 mM Y27632 (Wako) and 0.5 ng/ml human BMP4 (Stemgent). After 24 hrs, the SFDM was supplemented with 1 ng/ml human Activin A and 20 ng/ml human FGF2. After 48 hours, the SFDM was supplemented with 0.5 ng/ml BMP4 and 10 µM CHIR. MP cells were treated as d3 cultures, bypassing this initial treatment. Subsequently, half of the culture medium volume was refreshed with new SFDM every other day. On day 9, the medium was changed to SFDM supplemented with 1 ng/ml human Activin A, 0.5 ng/ml BMP4, 3 µM CHIR, and 0.1 µM retinoic acid. On day 11, the medium was changed to SFDM containing 1 µM CHIR and 5 ng/ml FGF9. All data shown are representative examples of at least three independent experiments.

Quantitative RT-PCR

RNA was isolated using RNeasy Plus Micro Kit (Qiagen) and reverse-transcribed with random primers and qScript cDNA Supermix (Quanta). Before reverse transcription, 5 µg of RNA was digested by RNase-free DNase I (Ambion) to remove genomic DNA. Quantitative PCR was carried out using a Real-Time PCR System (Bio-Rad) and Taqman qPCR Mix with a 10-min gradient to 95 °C followed by 40 cycles at 95 °C for 15

s and 60 °C for 1 min. The following Taqman (Life Technologies) gene expression assay

primers (Gene/ABI Assay #) were used: 18s/Hs99999901_s1, OCT4/Hs04260367_gH,

NANOG/Hs04399610_g1, SOX2/Hs01053049_s1, FOXA2/Hs00232764_m1,

SOX1/Hs01057642_s1, MESP1/Hs01001283_g1, MIXL1/Hs00430824_g1,

LHX1/Hs00232144_m1, PDGFRA/Hs00998018_m1, PAX1/Hs01071293_g1,

TBX6/Hs00365539_m1, TCF15/Hs00231821_m1, MEOX1/Hs00244943_m1,

NKX2.5/Hs00231763_m1, ISL1/Hs00158126_m1, LMO2/Hs00153473_m1,

KDR/Hs00911700_m1, PAX2/Hs01057416_m1, EYA1/Hs00166804_m1,

SALL1/Hs01548765_m1, OSR1/Hs01586544_m1, LHX1/Hs00232144_m1,

WT1/Hs01103751_m1, CITED2/Hs01897804_s1, PECAM1/Hs00169777_m1,

HOXC9/Hs00396786_m1, ITGA8/Hs00233321_m1, PBX1/Hs00231228_m1,

HOXA10/Hs00172012_m1, HOXA11/Hs00194149_m1, GDNF/Hs01931883_s1,

FOXD1/Hs00270117_s1, SIX2/Hs00232731_m1, CDX2/Hs01078080_m1,

FGF5/Hs03676587_s1. Gene expression was normalized to 18S rRNA levels. Delta C_t

values were calculated as $C_t^{target} - C_t^{18s}$. All experiments were performed with three

technical replicates. Relative fold changes in gene expression were calculated using the

$2^{-\Delta\Delta C_t}$ method (VanGuilder et al., 2008).

Flow cytometry

Cells were dissociated with Accutase (Life Technologies) at 37°C for 4 min and

triturated using fine-tipped pipettes. For intracellular antibody staining, cells were fixed

for 15 min with Cytofix (BD Biosciences), washed twice with flow cytometry buffer (PBS,

1 mM EDTA, and 0.5% FBS), permeabilized with Cytoperm (BD Biosciences) for 30 min

on ice, and washed twice with flow cytometry buffer, and resuspended at a maximum

concentration of 5×10^6 cells per 100 µl. Cells were incubated with primary antibodies on ice for 1 hour, washed twice with flow cytometry buffer. If necessary, cells were incubated with secondary antibodies on ice for 1 hour and then washed three times. The following antibodies were used (Antibody/Vendor/Catalog #/Concentration): Rabbit anti-NANOG/Santa Cruz/SC-33759/1:50, Rabbit anti-OCT4/Santa Cruz/SC-9081/1:50, Mouse anti-MIXL1/R&D Systems/MAB2610/1:200, Mouse anti-PAX2/Creative Diagnostics/DMABT-H14539/1:200, Rabbit anti-SIX2/Abcam/ab68908/1:200, Rabbit anti-WT1/Santa Cruz/sc-192/1:200, Rabbit anti-SALL1/Abcam/ab31526/1:200, Mouse anti-E Cadherin/Abcam/ab1416/1:200, Mouse anti-Human Nuclear Antigen/Abcam/ab191181/1:250, Biotinylated Dolichos Biflorus Agglutinin (DBA)/Vector Laboratories/B-1035/1:200, Rabbit anti-Ki67/Abcam/ab15580/1:250, APC anti-human CD56 (NCAM)/BioLegend/318309/5 ul per test, PE anti-human CD326 (EpCAM)/BioLegend/324205/5 ul per test, Alexa-647 Mouse IgG2a Isotype Control/BD/558053/20 µl per test, PE Mouse IgG1 Isotype Control/BioLegend/400113/5 ul per test, PE Mouse IgG2a Isotype Control/BD/561552/5 ul per test, Alexa 647 Donkey Anti-Goat/Life Technologies/A-21447/1:200, Alexa 647 Donkey Anti-Rabbit/Life Technologies/A-31573/1:200, Alexa 647 Donkey Anti-Mouse/Life Technologies/A-31571/1:200, Alexa 546 Donkey Anti-Rabbit/Life Technologies/A-10040/1:200, Alexa 546 Donkey Anti-Mouse/Life Technologies/A-10036/1:200, Alexa 488 Streptavidin Conjugate/Life Technologies/S-11223/1:200, Alexa 488 Donkey Anti-Rabbit/Life Technologies/A-21206/1:200, Alexa 488 Donkey Anti-Mouse/Life Technologies/A-21202/1:200. After passing through a 40 µm cell strainer, cells were resuspended in flow cytometry buffer at a final density of 2×10^6 cells ml^{-1}. Propidium iodide (Sigma) was added at a final concentration of 50 mg ml^{-1} to exclude dead cells. Cells were analyzed

on the FACS Fortessa (Becton Dickinson). For each sample, at least three independent experiments were performed. Results were analyzed using FlowJo software.

Immunocytochemistry

Monolayer cultures were gently washed with PBS prior to fixation. Cultures were fixed for 10 min at 4 °C with fresh paraformaldehyde (4% (w/v) in PBS). For sectioning aggregates of cells in suspension, samples were fixed with 4% paraformaldehyde, embedded in optimal cutting temperature (OCT) compound (Tissue Tek) and cryosectioned at 10-µm thickness before staining, Cells were blocked and permeabilized with 2% (w/v) BSA, 0.2% ((v/v) in PBS) Triton X for 30 min at RT. Cells were then washed twice with PBS. Primary antibodies were incubated overnight at 4°C and washed twice with PBS. Secondary antibodies were incubated for 1 hour at 37°C. Antibodies used are as listed (see Flow Cytometry section above). Prior to imaging, samples were stained with DAPI for 10 minutes, washed and mounted in Vectashield (Vector Laboratories), covered with coverslips, and sealed with nail polish. Images were taken using an Olympus FluoView1000 multi-photon confocal microscope. All immunofluorescence analyses were repeated a minimum of three times and representative images are shown.

High throughput RNA sequencing (RNA-seq)

Isolated cells were isolated, depleted of genomic DNA and rRNA and fragmented to ~200 bp by RNase III. After ligating the Adaptor Mix, fragmented RNA was converted to the first strand cDNA by ArrayScript Reverse Transcriptase (Ambion), size selected (100-200bp) by gel electrophoresis, and amplified by PCR using adaptor-specific primers. Deep sequencing was performed on an Illumina Genome Analyzer II. Analysis of genome-wide expression data was performed as previously described (Trapnell et al.,

2012, 2013). Briefly, raw reads were aligned to the reference human genome (hg19) using TopHat. Cufflinks was used to assemble individual transcripts from the mapped reads. Cuffmerge was used to merge the assembled transcripts from the two biologically independent samples. Cuffdiff was used to calculate gene expression levels and test for the statistical significance of differences in gene expression. Reads per kilobase per million mapped reads (RPKM) were calculated for each gene and used as an estimate of expression levels. The full RNA-seq data set for the MP cells is provided in Table 4-2.

Re-aggregation assay

The re-aggregation assay was performed as previously described (Davies et al., 2012, 2014; Unbekandt and Davies, 2010). To prepare the kidney tissue for recombination, embryonic kidneys from 12.5–13.5-dpc (days post coitum) mice were isolated and dissected free of surrounding tissues as previously described (Gallegos et al., 2012; Martovetsky et al., 2013). Briefly, embryonic kidneys were digested with trypsin at 37°C for 10 min and dissociated by manually pipetting. After the cells had been filtered through a 100 µm cell strainer, 4–10×10^5 embryonic kidney cells were recombined with 4% (by number) of hESC-derived cells and then centrifuged at 400g for 2 min to form a pellet. The pellet was allowed to aggregate by culturing in DMEM supplemented with 10% FBS overnight in a sterile PCR tube. The following day, the aggregate was transferred to the top of a Transwell polycarbonate filter (0.4 µm pore size). The filter was placed with the well of a 12-well dish to which DMEM supplemented with 10% FBS was added to bottom of the well. The aggregate was then cultured for 4 days at the air-fluid interface before fixation and analysis.

Spinal cord co-culture assay

hES or MP-derived MM cells were cultured with mouse embryonic spinal cord taken from E11.5 or E12.5 embryos at the air-fluid interface on a polycarbonate filter (0.8 mm; Whatman) fed with DMEM containing 10% fetal calf serum, as described previously (Gallegos et al., 2012; Kispert et al., 1998; Martovetsky et al., 2013; Osafune et al., 2006).

Teratoma/Transplantation Assay

For the subcutaneous injection, 0.5×10^6 H9 hES or MP cells were dissociated, mixed with 250 μL Matrigel, and transplanted subcutaneously into the thigh and shoulder of nude mice. Teratoma formation was monitored over a period of 4–12 weeks. All animal work was approved by the institutional IACUC committee (Protocol Number S06321, PI Willert).

Chromosome Counting

Chromosome numbers were quantified as previously described (Ross et al., 2014) . Briefly, cells were cultured to 80% confluence and then for an additional 16-20 hours in media containing 100 μM Nocodazole (Sigma-Aldrich). Cells were then enzymatically dissociated to single cells, pelleted by centrifugation at 200xg for 5 minutes, washed once with 1X PBS and pelleted again by centrifugation at 200xg for 5 minutes. Cell pellets were re-suspended in 5 ml 0.57% (w/v) potassium chloride, incubated at room temperature for 25 minutes and pelleted by centrifugation at 200xg for 5 minutes. Cells were resuspended in pre-chilled fixative (3:1 [v/v] methanol:acetic acid), incubated at room temperature for 5 minutes, and pelleted by centrifugation at 200xg for 5 minutes. This fixation step was repeated. Cell pellets were re suspended in an appropriate

amount of pre-chilled fixative. A single drop of the cell suspension was dropped using a

micropipettor from a height of 25 cm onto a glass microscope slide that was pre-chilled

in 100% ethanol (Sigma-Aldrich) at 4ºC and wiped dry. After fixative evaporated from the

slide 4-5 drops of ProLong Gold Antifade Reagent with DAPI (Life Technologies) was

added along one edge and a cover slip was mounted onto the slide. Images were

acquired using a Zeiss Axio Imager A1 fluorescence microscope. Chromosome counting

was done on using ImageJ software.

Statistical analyses

All averaged data are expressed ± standard error of the mean of three

independent biological replicates unless otherwise stated. For comparisons of discrete

data sets, unpaired Student's t-tests were performed to calculate *p*-values between

experimental conditions and controls and a *P*-value <0.05 was considered statistically

significant. For each ACME experiment, the ratio (R_i) of the $\log_2$ of the T-GFP signal and

the DNA signal was calculated for each spot. From this a differentiation *z*-score was

calculated for each spot $Z_{DIF}=(R_i-\mu_{DIF})/\sigma_{DIF}$, where R_i was the ratio for the spot, μ_{DIF} was

the average of the ratios for all spots on each array, and σ_{DIF} was the S.D. of the ratios

for all spots on each array. Differentiation *z*-scores from replicate spots (*n*=5 per

condition) were averaged for each ECMP condition on the array. The replicate

average *z*-scores were displayed in a heat map with rows corresponding to individual

conditions and columns representing independent array experiments (n=5 for each

replicate). For each array experiment, all columns were mean-centered and normalized

to one unit S.D. The rows were clustered using Pearson correlations as a metric of

similarity. All clustering was performed using Gene Cluster. The results were displayed

using a color code with red and green representing an increase and decrease,

respectively, relative to the global mean. All heat maps were created using Tree View. Global main effects principal component analysis was performed as previously described (Abdi and Williams, 2010).

Results

ACME screen to identify culture conditions of MP cells

Using a high-throughput screening platform previously developed in our laboratory referred to as arrayed cellular microenvironments (Brafman et al., 2012) (ACME) I sought to identify culture conditions to derive, maintain and expand a cell population with mesodermal properties from human pluripotent stem cells (hPS cells, including human embryonic and human induced pluripotent stem [hES and iPS] cells). To readily observe and detect acquisition of a mesodermal phenotype, I utilized the hES cell line H9/WA09 harboring the gene encoding green fluorescent protein (GFP) under the control of the *Brachyury* (*T*) promoter (referred to as H9-T-GFP (Kita-Matsuo et al., 2009)). *Brachyury*, which is expressed early in embryonic development in the primitive streak, is transiently expressed as hPS cells exit the pluripotent state and differentiate into mesodermal (ME) lineages (Rivera-Pérez and Magnuson, 2005) .

To induce mesodermal differentiation, I treated H9-T-GFP cells with the GSK3 inhibitor CHIR98014 (CHR) for 2 days, at which point cells uniformly expressed GFP (Figure 4-1A) and were seeded onto ACME slides printed with combinations of bioactive molecules. I performed two sequential screens to identify conditions that maintain GFP expression over a 3-day period: a first screen to identify an optimal substrate composed of extracellular matrix proteins (ECMPs), and a second screen to identify growth factors (GF) and small molecules (SM) (Figure 4-1A). The second screen was performed using the optimal substrate

composition identified in the first screen. GFP expression for each condition was evaluated and quantified using a high content imaging system and software.

In the first screen, all possible 128 combinations of 7 purified ECMPs (Collagen 1, 3, 4, 5 [C1 C3 C4 C5], Fibronectin [FN], Laminin [LN], Vitronectin [VN]), were tested for their ability to support cell adhesion and maintain GFP expression. Hit conditions were defined as those ECMP combinations that supported cell adherence, as well as GFP expression. The distribution of total cell number and GFP signal intensity across conditions was summarized in a normalized, clustered heat map (Figure 1B). Interestingly, several defined ECMP combinations increased cell adhesion relative to Matrigel, a commercially available extracellular matrix that is commonly used for growth of hPS cells and their derivatives. Further, several ECMP combinations maintained expression of GFP to a greater extent than Matrigel. A matrix composed of C1 C3 C4 FN and VN maximally supported adherence and GFP expression (Figure 4-1B and C).

For the second GF and SM screen, I used the optimal matrix composition (C1 C3 C4 FN VN) as a substrate to deposit combinations of up to three GF and SM, which are known to exert potent effects during early developmental processes. Certain factor combinations increased, while others decreased, adherence and GFP expression (Figure 4-1D). Conditions with positive effects in this assay contained a Wnt agonist (either Wnt3a [WNT] or CHR) and a member of the FGF superfamily (Figure 4-1D and E). Consistent with this observation, a global main effects principal component analysis of all GF and SM revealed that CHR, WNT, Rspondin (RSP) and FGF exerted the most potent effects on GFP expression (Figure 4-2B). To a lesser extent, the FGF family members VEGF (VGF) and KGF, also positively influenced GFP expression, whereas Wnt antagonists (DKK1 and IWP2) negatively influenced GFP expression.

Figure 4-1. Arrayed cellular microenvironment (ACME) screen identified conditions that maintain expression of the mesodermal reporter T-GFP. A. Schematic of the ACME experimental design. Human ES cells carrying a GFP reporter under control of the BRY/T promoter were treated with CHIR98014 (CHR). GFP positive (T-GFP) cells were seeded onto ACME slides printed with combinations of extracellular matrix proteins (ECMP), growth factors (GF) and small molecules (SM). A primary screen contained all possible combinations of ECMP Collagen I (C1), Collagen III (C3), Collagen IV (C4), Collagen V C5), Fibronectin (FN), Laminin (LN), and Vitronectin (VN). A second GF and SM screen contained all possible single, pairwise, and three-way combinations of Wnt3a (WNT), CHIR98014 (CHR), Rspondin (RSP), Dkk-1 (DKK), IWP-2 (IWP), FGF-2 (FGF), FGF-7 (KGF), VEGF (VGF), EGF (EGF), SHH (SHH), Activin (ACT), Cyclopamine (CYC), Dorsomorphin (DSM), BMP4 (BMP), SB4-31542 (SB4), and Noggin (NOG). The second screen was performed on the optimal ECMP combination identified in the primary screen. 72 hours after seeding, GFP expression and DAPI staining were captured and analyzed using a high content imaging microscope. **B.** Results of the primary ECMP screen. A heat map of average T-GFP intensity was generated showing the distribution across the data set. Representative clusters are magnified. The position of the Matrigel condition in the cluster is also indicated for reference. Rows represent different ECMP combinations. Columns 1-3 represent biological replicates for cell number (Cell #) or T-GFP (GFP). Columns marked $\bar{X}$ represent the average of the 3 biological replicates. **C.** Representative images of ECMP conditions in the array format. Matrigel is shown in comparison to the hit condition C1 C3 C4 FN VN. Scalebar = 50 μm. **D.** Results of the second GF and SM screen. A heat map of average T-GFP intensity was generated showing the distribution across the data set. Representative clusters are magnified. The position of the condition lacking growth factors (No Factor) is also indicated for reference. Rows represent different GF and SM combinations. Columns 1-3 represent biological replicates for cell number (Cell #) or T-GFP (GFP). Columns marked $\bar{X}$ represent the average of the 3 biological replicates. **E.** Representative images of GF and SM conditions in the array format. No GF or SM is shown in comparison to the hit condition CHR+FGF. Scalebar = 50 μm. Figure 1—figure supplement 1 provides a global main effects principal component analysis for all GF and SM used in this second screen.
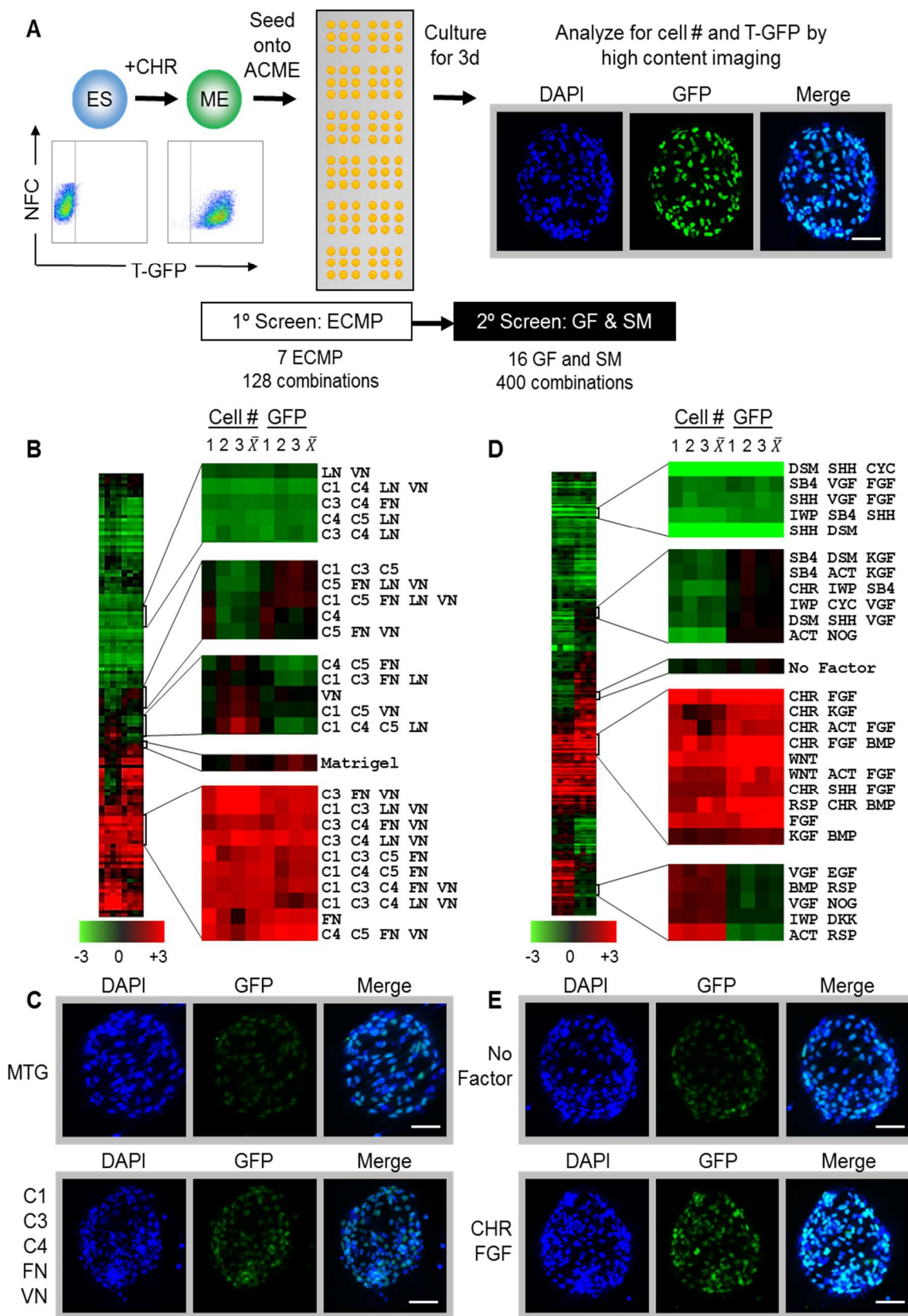
I confirmed these ECMP and GF/SM hit conditions by scaling up into traditional cell culture formats. Compared to Matrigel and a sub-optimal matrix (C1 C4 C5 LN), the ECMP hit condition significantly increased the percentage of GFP positive cells (Figure 4-2A). I also plated cells in traditional cell culture format on the optimized matrix in the presence of individual soluble factors as well as the top 27 combinatorial hits from the GF-SM screen. (Figure 4-2C). This analysis confirmed that the combination of CHR and FGF most potently supported maintenance of GFP expression and cell growth. Since bioactive molecules like CHR (or Wnt) and FGF often exhibit distinct effects at varying concentrations, I performed a dose response analysis to identify optimal CHR and FGF concentrations. The optimal CHR dose was 1.0 μM while the dose of FGF was less dynamic, with its effects saturating at 20 ng/ml FGF (Figure 4-2D).

Figure 4-2. Validation of high-throughput arrayed cellular microenvironment (ACME) screens. Scale up analysis of hits from the ACME screens. Human ES cells carrying a GFP reporter under control of the BRY/T promoter were treated with CHIR98014 (CHR) for 24 hours. After 48 hours, GFP positive (T-GFP) cells were cultured in multi-well plates for 72 hours to validate conditions from the ACME screens. **A.** Compared to Matrigel and a sub-optimal matrix (C1 C4 C5 LN), the hit condition (C1 C3 C4 FN VN) significantly increased the percentage of GFP positive cells. Statistical comparisons are made to the Matrigel condition. n.s. = not statistically significant. **p<0.005. **B.** Global main effects principal component analysis of GF and SM ACME screen demonstrates that WNT and FGF agonists exert positive effects on T-GFP expression. **C.** GFP+ cells were cultured in multi-well plates coated with the optimal matrix (C1 C3 C4 FN VN) and various growth factor/small molecule (GF/SM) combinations. Statistical comparisons are made to the conditions containing no GF/SM. *p<0.05 **p<0.005. **D.** GFP+ cells were cultured in multi-well plates coated with the optimal matrix (C1 C3 C4 FN VN) and various concentrations of CHR and FGF2 (FGF).

Expansion of a mesodermal cell population in defined conditions

The previous analysis was performed 3 days after plating cells in the optimized culture condition. I also examined to what extent this optimized culture condition could support long term growth and expansion of cells with mesodermal properties (Figure 4-3A). In addition, to test whether these culture conditions exhibited similar effects on other hPS cell lines, I included two additional cell lines, BJ-RiPS and HUES9 cells (Figure 4-4). When seeded at a density of 10^4 cells/cm^2, cells formed and grew in tight clusters (Figure 4-3B). Cells with these morphological properties were expanded by serial passaging with approximate doubling rates of 60.2±4.2 hours (H9 = 55.4 hrs, Figure 4-3C; Hues9 = 61.8 hrs, RiPS = 63.4 hrs, Figure 4-4A) and expressed the proliferative marker Ki-67 (Figure 4-4B). Cell counts taken at each passage revealed that 1 x 10^4 cells could theoretically be expanded to approximately 1 x 10^{12} cells over 10 passages (Figure 4-3C and Figure 4-4A). These cells maintained 46 chromosomes (Figure 4-3D), indicating that cultured cells did not acquire genomic changes that afforded a growth advantage. Reverse transcription quantitative PCR (qPCR) showed that expression of genes associated with pluripotency (*OCT4*, *NANOG*, *SOX2*) was rapidly lost during expansion (Figure 4-3E; Figure 4-4C). This loss of pluripotency-associated properties was further confirmed by immunofluorescence (IF) staining (OCT4 and NANOG, Figure 4-4D) and flow cytometry (TRA-1-81 and SSEA4, Figure 4-4E). In contrast, genes associated with the mesodermal (ME) lineage (*MESP1*, *MIXL1*, *LHX1*) were upregulated and maintained over ten passages (Figure 4-3F; Figure 4-4F). IF staining confirmed the presence of MIXL1 protein in these expanded cell cultures (Figure 4-3G). Using flow cytometry, I furthermore showed that the expanded cells shared a cell surface signature of CD56+ CD326- (Figure 4-3H; Figure 4-4G), previously defined for a multipotent mesoderm-committed cell population (Evseenko et al., 2010). In addition, expression of

the endodermal (EN) marker *FOXA2* and the ectodermal (EC) marker *SOX1* was

significantly reduced in these cells (Figure 4-3I, J; Figure 4-4H, I). Given this distinct

mesodermal-like expression profile, we preliminarily referred to these cells as

mesodermal progenitor (MP) cells.

The apparent indefinite expansion of MP cells (greater than 20 passages at the

time of this submission) raised the possibility that these cells, like undifferentiated hPS

cells, harbored tumorigenic potential. Importantly, unlike hPS cells, MP cells did not

produce tumors when injected into immune compromised mice (Figure 4-3K). Among

the 12 MP cell injections, only one site maintained a small lump (~1 millimeter in

diameter), which did not grow in size over 12 weeks. In contrast, all 6 hPS cell injections

produced readily visible teratomas (greater than 10 millimeters in diameter). Taken

together, I have generated a non-tumorigenic progenitor population capable of nearly

indefinite expansion with a mesodermal phenotype.

Figure 4-3. Characterization of mesodermal progenitor population derived from H9.
A. Schematic showing derivation of mesoderm progenitor (MP) cells. Human ES cells were differentiated into mesoderm (ME) with CHIR98014 (CHR) and then replated onto the defined substrate C1 C3 C4 FN VN and cultured with CHR and FGF2 (FGF) for up to 20 passages (p0 to p20). **B.** Representative images of MP cells derived from the hES cell line H9/WA09 at passage 1 and 10 in C1 C3 C4 FN VN with CHR and FGF. Scale bar = 50 µm. **C.** Growth rate of MP cells derived from H9 T-GFP. Cell counts were taken at each passage. **D.** Chromosome counts of MP cells. Chromosome numbers were obtained for p15 MP cells. No metaphase spreads exceeded 46 chromosomes. Note that this method to quantify chromosome numbers is only reliable in determining the maximum number of chromosomes; metaphase spreads with less than 46 chromosomes are due to loss of chromosomes during the preparation of the samples. **E.** Quantitative PCR analysis for expression of pluripotency markers *OCT4*, *NANOG*, and *SOX2*. Expression of these markers in MP cells at passages 1, 5 and 10 is lower than in undifferentiated cells (ES). Cells differentiated into mesoderm (ME), endoderm (EN) and ectoderm (EC) served as controls. All statistical comparisons are made to the ES sample. $*p < 0.05$ $**p < 0.005$. **F.** Quantitative PCR analysis for expression of mesodermal markers *MESP1*, *MIXL1*, and *LHX1*. Expression of these markers in MP cells at passages 1, 5 and 10 is comparable to that observed in ME and higher than in ES, EN and EC. All statistical comparisons are made to the ME sample. $*p < 0.05$ $**p < 0.005$. **G.** MIXL1 immunofluorescence in MP cells. MP cells at passage 15 were fixed and stained with MIXL1-specific antibody. Number indicates percentage of MIXL1 expressing cells in the MP cell population. Standard deviation represents the variation between the fields of view used for counting (n=20). Scale bar = 50 µm. **H.** Flow cytometry analysis for CD56 (NCAM) and CD326 (ECAM). Pluripotent cells (ES, CD326+CD56-) are differentiated to ME cells (CD326-CD56+). MP cells at p10 exhibit a similar cell surface expression of these 2 markers as ME. **I.** Quantitative PCR analysis for expression of the endodermal marker *FOXA2*. Expression of *FOXA2* is only detected in cells differentiated towards EN. All statistical comparisons are made to the ES sample. **J.** Quantitative PCR analysis for expression of the ectodermal marker *SOX1*. Expression of *SOX1* is only detected in cells differentiated towards ectoderm (EC). All statistical comparisons are made to the ES sample. **K.** MP cells are non-tumorigenic. Nude mice were injected with H9-derived MP cells or H9 ES cells. Injected ES cells generated tumors while injected MP cells did not form any growth in 11/12 injections. Figure 3—figure supplements 1 through 9 provide a similar analysis for 2 additional hPS cell lines (BJ RiPS and HUES9).
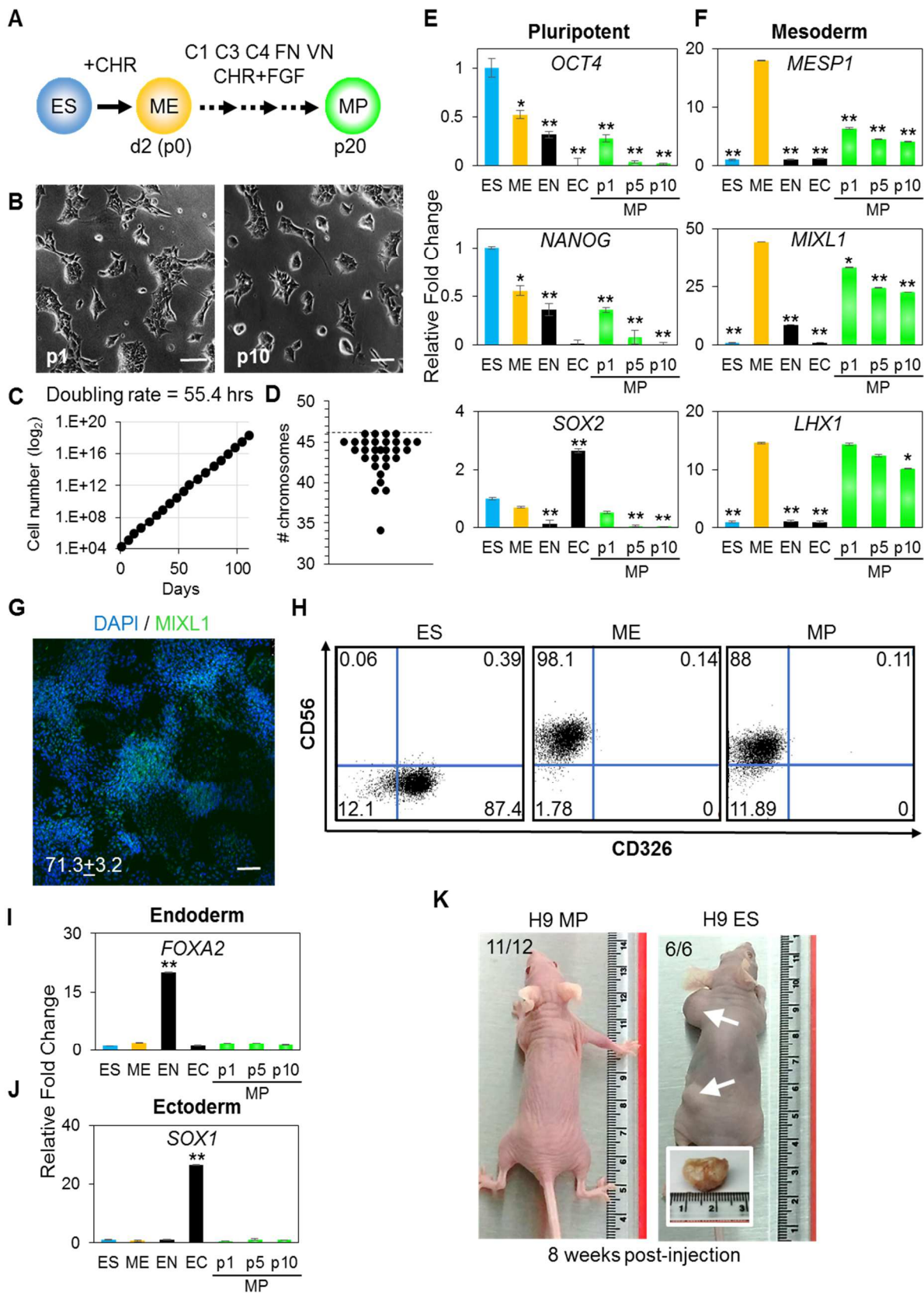
A

ES — +CHR → ME d2 (p0) ⇢ C1 C3 C4 FN VN CHR+FGF ⇢ MP p20

B p1, p10

C Doubling rate = 55.4 hrs

D # chromosomes

E Pluripotent — OCT4, NANOG, SOX2

F Mesoderm — MESP1, MIXL1, LHX1

G DAPI / MIXL1 — 71.3+3.2

H CD56 / CD326 — ES, ME, MP

I Endoderm — FOXA2

J Ectoderm — SOX1

K H9 MP (11/12), H9 ES (6/6) — 8 weeks post-injection

Figure 4-4. Characterization of mesodermal progenitor population derived from Hues 9 and BJ RiPS. A. Growth rate of MP cells derived from Hues 9 or BJ RiPS. Cell counts were taken at each passage. **B.** Flow cytometry analysis of Ki-67 in human ES, ME, and MP. MP cells were analyzed at passage 10. **C.** QPCR analysis for expression of pluripotency markers *OCT4*, *NANOG*, and *SOX2*. Expression of these markers in MP cells at passage 10 is lower than in undifferentiated cells (Pluri). Cells differentiated into mesoderm (ME), endoderm (EN) and ectoderm (EC) served as controls. All statistical comparisons are made to the ES sample. **D.** Immunofluorescence of Hues 9 ES and MP cells demonstrate that MP cells do not express OCT4 and NANOG proteins. Scale bar = 100 µm. **E.** Flow cytometry analysis of Hues 9 ES and MP (p10) cells for Tra-1-81 and SSEA4. MP cells do not express pluripotent cell surface markers. **F.** QPCR analysis of MP cells derived from Hues 9 and BJ RiPS for expression of mesodermal markers *MESP1*, *MIXL1*, and *LHX1*. Expression of these markers in MP cells at passages 1, 5 and 10 is comparable to that observed in ME and higher than in ES, EN and EC. All statistical comparisons are made to the ME sample. **G.** Flow cytometry analysis for CD56 (NCAM1) and CD326 (EPCAM) in undifferentiated RiPS cells as well as ME and MP (p10) cells derived from RiPS cells. MP cells exhibit a similar cell surface expression of these two markers as ME. **H.** QPCR analysis of MP cells derived from Hues 9 and BJ RiPS. Low expression of *FOXA2* demonstrates that MP cells are not committed to the endodermal lineages. All statistical comparisons are made to the pluripotent (ES or hPS) sample. **I.** QPCR analysis of MP cells derived from Hues 9 and BJ RiPS. Low expression of *SOX1* demonstrates that MP cells are not committed to the ectodermal lineages. All statistical comparisons are made to the pluripotent (ES or hPS) sample. *p<0.05 **p<0.005.
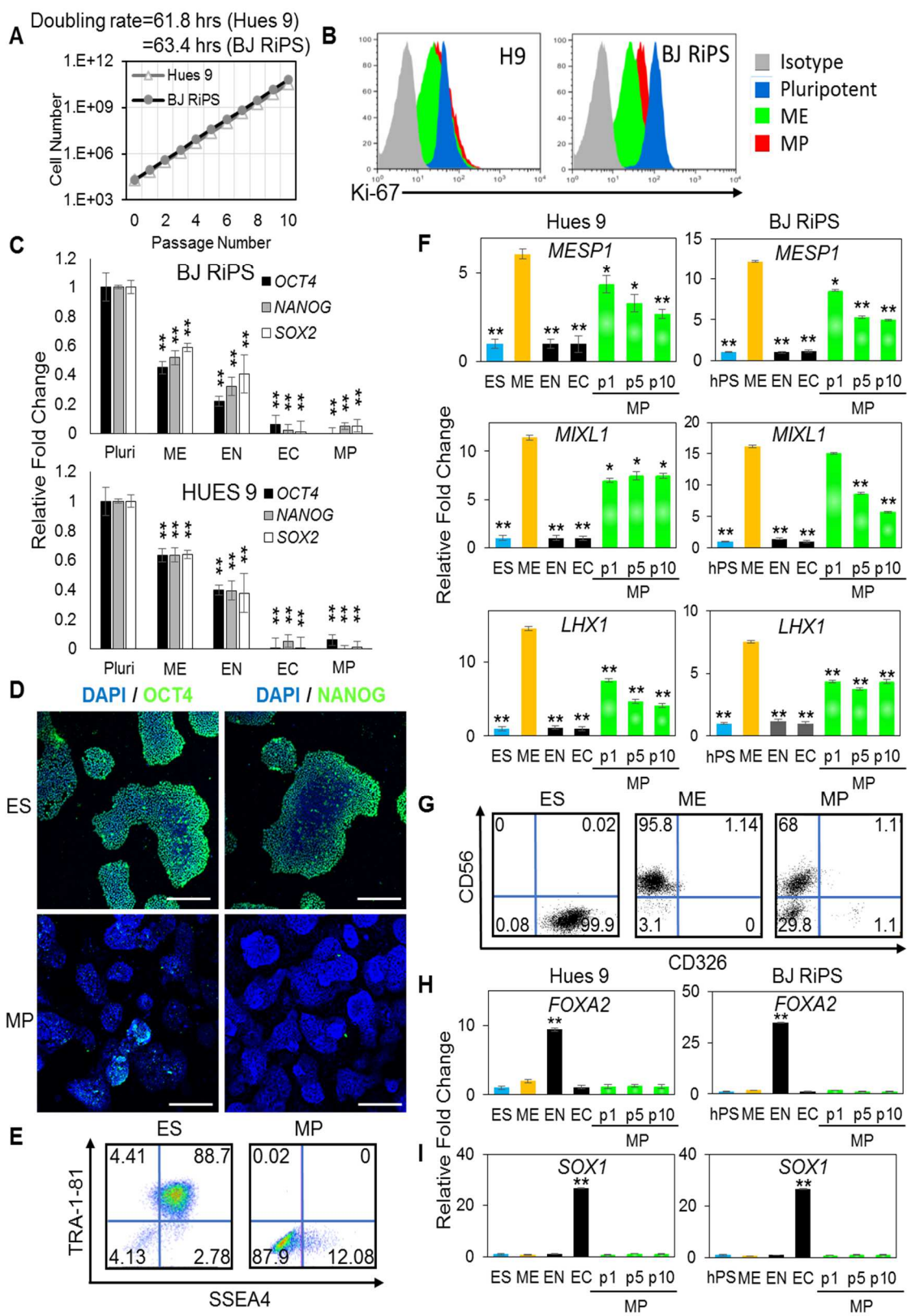
Optimized culture conditions are necessary to generate and maintain MP cells

From the ACME screens, I identified a defined matrix (C1 C3 C4 FN VN) and combination of soluble factors (CHR + FGF) that allow for the derivation and expansion of MP cells. I wanted to explore to what extent these defined conditions were critical for the derivation and expansion of MP cells. To this end, I first compared the effectiveness of the defined matrix relative to Matrigel and of CHR+FGF relative to no factors in deriving MP cells (Figure 4-5A), as assayed by qPCR of mesodermal markers. Importantly, cells cultured in the absence of CHR and/or FGF failed to passage beyond one passage, indicating that these soluble factors are essential to the expansion of MP cells. Furthermore, although Matrigel with CHR and FGF yielded cells expressing the mesodermal markers *MESP1*, *MIXL1*, and *LHX1*, our optimized matrix significantly increased their expression (Figure 4-5B). By passage 3, cells cultured in our optimized conditions expressed 1.5 to 2 fold greater levels of *MESP1*, *MIXL1*, and *LHX1* compared to cells cultured on Matrigel (Figure 4-5B).

Next, I compared the effectiveness of the defined matrix relative to Matrigel and of CHR+FGF relative to no factors in maintaining MP cells (Figure 4-5C). For this analysis, MP cultures were grown in the optimized conditions (C1 C3 C4 FN VN and CHR + FGF) through passage 6, at which point cultures were either passaged onto Matrigel or the defined matrix in the presence or absence of the soluble factors CHR and FGF. Again, the optimized culture condition outperformed all other conditions, as assayed at passage 9 for the maintenance of mesodermal marker expressions (Figure 4-5D). MP cultures without CHR and FGF failed to expand beyond the first passage. Taken together, these results indicate that the defined substrate C1 C3 C4 FN VN as well as CHR and FGF are required for optimal MP cell generation and maintenance.

Figure 4-5. Optimized culture conditions are required to generate and maintain MP cells. A. Human ES cells were treated with CHIR98014 (CHR) for 24 hours. After 48 hours, cells were cultured on either Matrigel or the optimal matrix (C1 C3 C4 FN VN) in the absence (no factor) or in the presence of the optimal growth factor and small molecule (GF/SM) combination (CHR + FGF). Only cells cultured with CHR + FGF could be serially passaged. **B.** QPCR analysis for mesodermal markers *MESP1*, *MIXL1*, and *LHX1*. Conditions containing no factor did not grow beyond passage 1, while the CHIR+FGF samples represent expression at passage 3. Statistical comparisons are made to C1 C3 C4 FN VN with CHR+FGF condition. *$p < 0.05$ **$p < 0.005$ **C.** MP cells were expanded to p6 on the optimal ECMP (C1 C3 C4 FN VN) and GF/SM combination (CHR +FGF). MP cells were then then either transitioned to Matrigel or maintained on C1 C3 C4 FN VN in the absence or presence of CHR+FGF. **D.** QPCR analysis for mesodermal markers *MESP1*, *MIXL1*, and *LHX1*. Conditions containing no factor did not grow past p7, while the CHR+FGF sample represents expression at p9. All statistical comparisons are made to the C1 C3 C4 FN VN with CHR+FGF condition. *$p < 0.05$ **$p < 0.005$
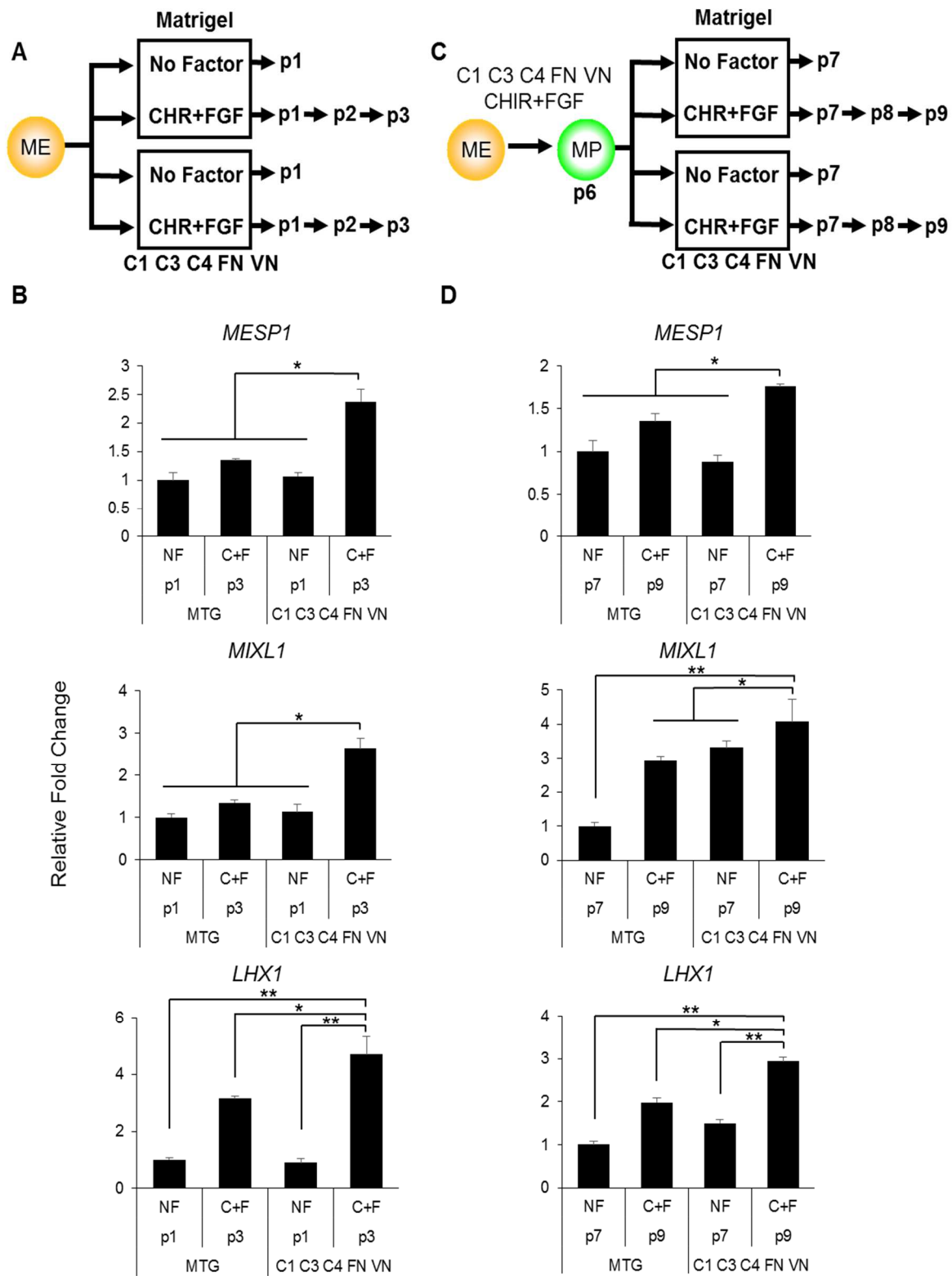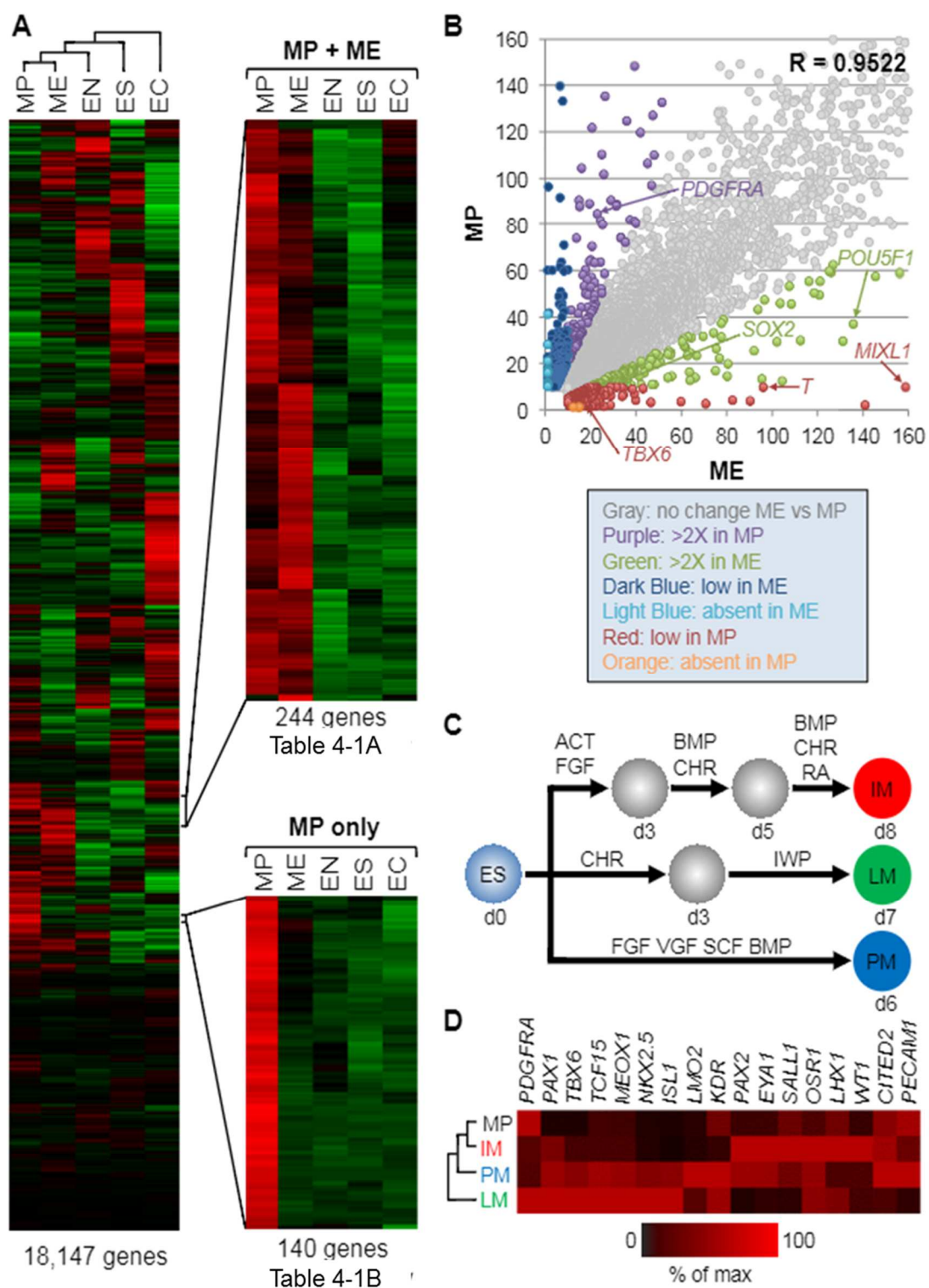
Global gene expression demonstrates an intermediate mesodermal (IM) identity of MP cells.

To further characterize the MP cell population derived and expanded under our defined culture conditions, we performed transcriptome analysis by RNA sequencing (RNA-seq). For comparison, we analyzed the transcriptomes of undifferentiated hES cells, as well as of transient EC, EN, ME populations differentiated from hES cells. Cluster analysis of the RNA-seq data revealed that MP cells are more similar to ME cells than they are to EC, EN, and hES cells (Figure 4-6A and Table 4-1A and B). Comparison of expressed genes in MP and ME cell populations confirmed a high degree of similarity, with a correlation coefficient of 0.9522 (Figure 4-6B). Although this analysis revealed that MP cells are more similar to transient ME populations than they are to other cell populations examined, they are also distinct from ME cells. In contrast to ME cells, MP cells exhibit significantly lower levels of pluripotency regulators, including *POU5F1* (*OCT4*) and *SOX2*. Several established early mesodermal markers (*T*, *MIXL*) were significantly elevated in ME cells relative to MP cells, suggesting that MP cells have progressed beyond this transient and early ME phenotype.

During development as the ME germ layer matures, modulation of various signaling molecule pathways lead to its further specification into paraxial, intermediate, and lateral plate mesoderm (PM, IM, and LM, respectively) (Christ and Ordahl, 1995). Using established differentiation protocols for each of these sub-lineages (Figure 4-6C), I examined expression by qPCR of several mesodermal markers in MP cells relative to PM, IM, and LM. Interestingly, MP cells most closely resembled the mesodermal gene expression profile of IM cells (Figure 4-6D). In addition, we observed in the RNA-seq data that several IM markers (*CITED2*, *EYA1*, *GATA3*, *LHX1*, *SALL1*) were expressed in

MP cells (Table 4-1). Based on this gene expression analysis we speculated that MP

cells are most closely related to cells of intermediate mesoderm.

Figure 4-6.   Gene expression analysis reveals that MP cells have an intermediate mesodermal (IM) identity. RNA sequencing (RNA-seq) was used to analyze gene expression of MP cells. As a comparison, gene expression profiles were analyzed for hES (ES) cells and their differentiated progeny, mesoderm (ME), endoderm (EN) and ectoderm (EC). **A.** MP cells resemble mesodermally differentiated cells. Hierarchical clustering analysis was performed for all genes with detectable expression (RPKM [reads per kilobase per million mapped reads] values greater than 10) in one of the five cell populations. Table 4-1 provides the complete list of genes shared between MP and ME (A) and genes unique to MP (B). The complete RNA-seq data set for MP cells is provided in Table 4-2. **B.** Correlation of gene expression profiles. Genes with expression values (RPKM) expression between 10 and 1,500 were plotted for MP cells and mesoderm (ME). The correlation coefficient (R) for all expressed genes is 0.9522. **C.** Schematic depicted differentiation protocols to intermediate, lateral plate, and paraxial mesoderm (IM, LM, and PM, respectively) from hES cells. **D.** QPCR analysis of IM, LM, PM, and MP cells revealed that MP cells have a similar expression profile as IM cells. Abbreviations: ACT = Activin A, BMP = BMP4, CHR = CHIR98014, d = day, FGF = FGF2, IWP= IWP-2, RA = retinoic acid, VGF = VEGF.

A

18,147 genes

MP + ME

244 genes
Table 4-1A

MP only

140 genes
Table 4-1B

B

R = 0.9522

MP

ME

PDGFRA

POU5F1

SOX2

MIXL1

T

TBX6

Gray: no change ME vs MP
Purple: >2X in MP
Green: >2X in ME
Dark Blue: low in ME
Light Blue: absent in ME
Red: low in MP
Orange: absent in MP

C

ES
d0

ACT
FGF

BMP
CHR

BMP
CHR
RA

IM
d8

d3

d5

CHR

IWP

LM
d7

d3

FGF VGF SCF BMP

PM
d6

D

PDGFRA PAX1 TBX6 TCF15 MEOX1 NKX2.5 ISL1 LMO2 KDR PAX2 EYA1 SALL1 OSR1 LHX1 WT1 CITED2 PECAM1

MP
IM
PM
LM

0   100
% of max

MP cells are restricted to differentiate towards an intermediate mesoderm phenotype

Based on the above findings, I hypothesized that the differentiation potential of MP cells may be limited to cell types derived from IM, such as of the germ and renal lineages. Therefore, I tested the ability of MP cells to differentiate into cell types derived from LM (hematopoietic cells), PM (cardiomyocytes), and IM (renal progenitors). Adapting an established protocol for hematopoietic differentiation (Ng et al., 2008) (Figure 4-7A), I successfully differentiated hES cells into cells expressing *SOX17*, a marker of hemogenic endothelium, and CD34 and CD45, two cell surface markers commonly used to monitor the presence of hematopoietic cell populations (Figure 4-7B, C). In contrast, MP cells derived from three independent human pluripotent stem cell lines and manipulated in a similar manner failed to express these markers at detectable levels (Figure 4-7B, C).

Along similar lines, adapting an established protocol to derive cardiomyocytes (Lian et al., 2012) (Figure 4-7D), hES cells readily produced cardiac progenitors (CP) and subsequently cardiomyocytes (CM), as monitored by expression of *NKX2.5* and *ISL1* (Figure 4-7E). Cultures containing CM exhibited the characteristic contractile activity associated with such cells. In contrast, MP cells subjected to these same manipulations failed to express detectable levels of *NKX2.5* and *ISL1* (Figure 4-7E), and never produced contractile activity. Therefore, the MP cells were unable to differentiate into cells with hematopoietic or cardiogenic properties, derivatives of PM and LM, respectively.

Figure 4-7. MP cells are unable to differentiate to cell types derived from lateral plate and paraxial mesoderm. A. Schematic of the hematopoietic differentiation protocol. Cells were differentiated in a step-wise manner using the indicated growth factors and small molecules from undifferentiated ES cells or from MP cells to mesoderm (ME), endothelial cell (ENC) and subsequently to hematopoietic precursors (HP). Stage-specific marker genes and cell surface markers expressed during this differentiation process are indicated at the top. Abbreviations: FGF = FGF2, VGF = VEGF, SCF = Stem Cell Factor, BMP=BMP4. **B.** QPCR analysis of hES and MP cells differentiated towards hematopoietic precursors. Compared to hES cells, MP cells do not differentiate towards hematopoietic precursors, as indicated by the absence of *SOX17* expression. **C.** Flow cytometry analysis of hES and MP cells differentiated towards hematopoietic precursors for CD34 and CD45. While hESC cells can differentiate into CD34+CD35+ hematopoietic precursors, MP cells fail to differentiate generate cells positive for CD34 and CD45. **D.** Schematic of the cardiomyocyte differentiation protocol. Cells were differentiated in a step-wise manner using the indicated growth factors and small molecules from undifferentiated ES cells or from MP cells to mesoderm (ME), cardiac precursor (CP) and subsequently to cardiomyocyte (CM). Stage-specific marker genes expressed during this differentiation process are indicated at the top. Abbreviations: CHR = CHIR98014, IWP = IWP-2. **E.** QPCR analysis of MP cells differentiated towards cardiomyocytes. Compared to hES cells, MP cells do not differentiate towards cardiomyocytes, as indicated by the absence of *ISL1* and *NKX2.5* expression.
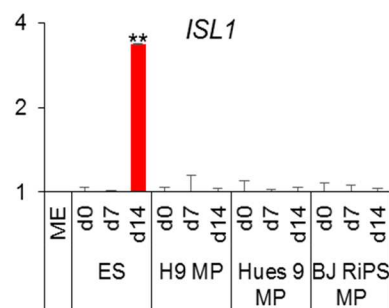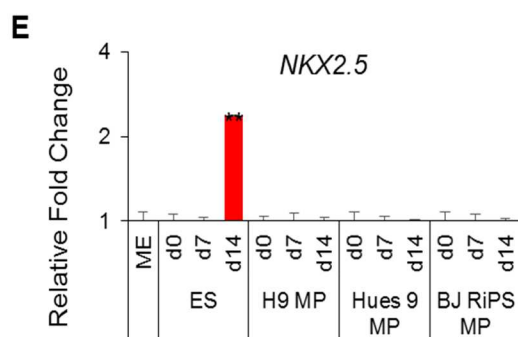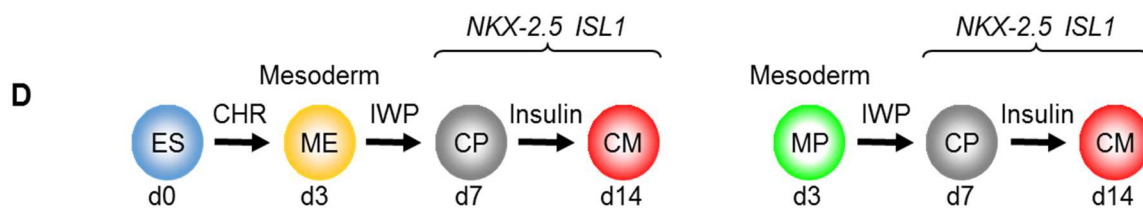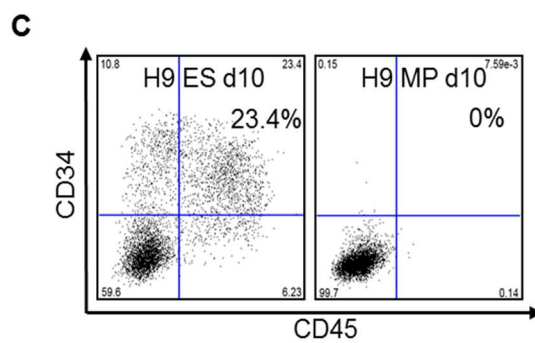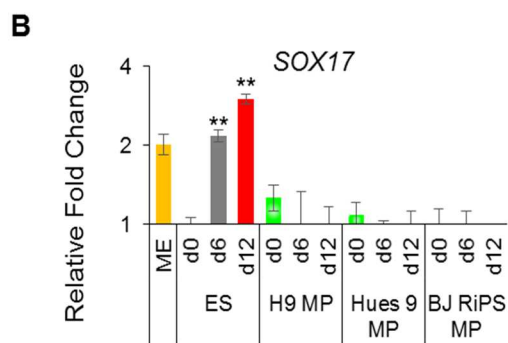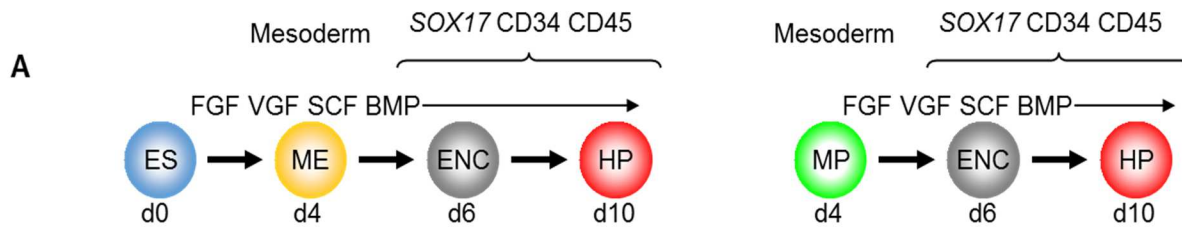
Since the MP cells described in this study failed to generate derivatives of PM and LM, I reasoned that these cells may differentiate into cell populations derived from IM, such as gonads and kidney. I first tested this feasibility by employing a method to induce germ cell differentiation from hPS cells (Figure 4-8A) (Kee and Reijo Pera, 2008). This protocol involves the addition of BMP (bone morphogenetic protein) 4, BMP7, and BMP8b to hPS differentiation medium. Notably, MP cells accrued transcriptional gene markers indicative of primordial germ cells, such as VASA, SCP1, STELLA, and DAZL, as measured by qPCR (Figure 4-8B). These results suggest that MP cells are capable of differentiating into cell types within the IM lineage.
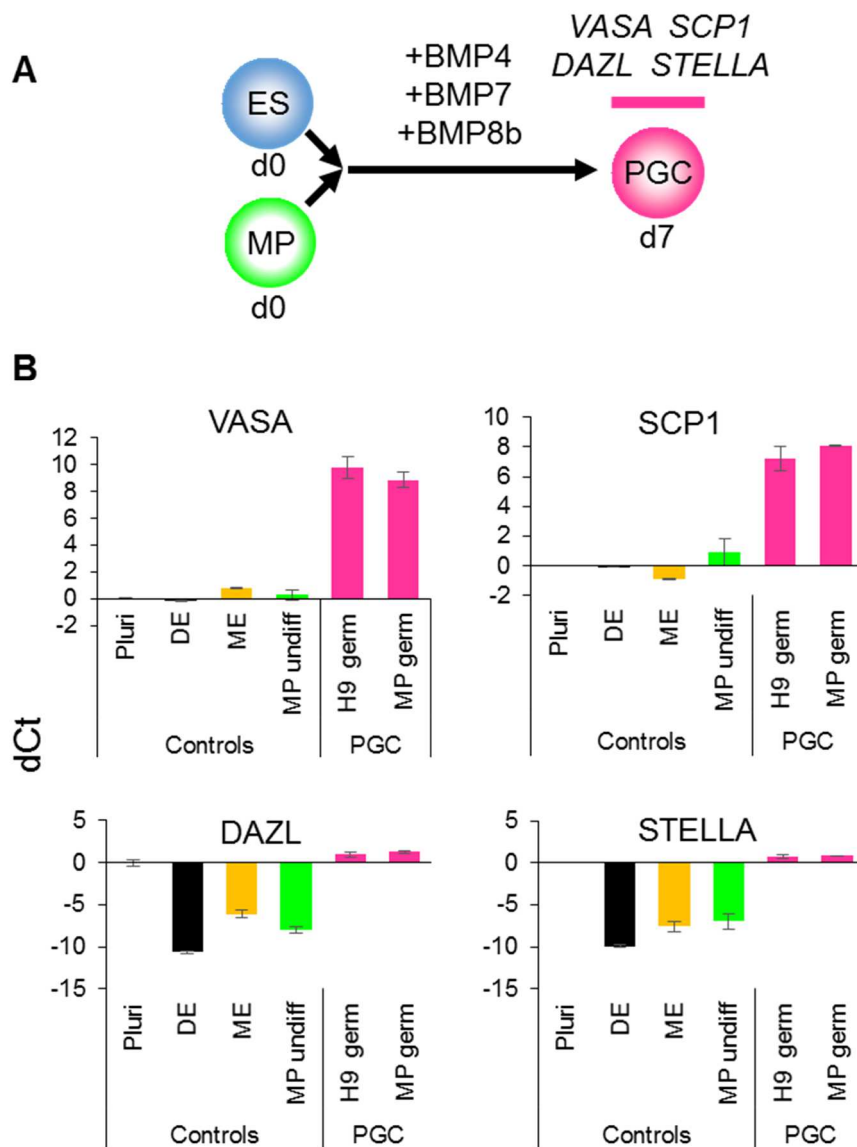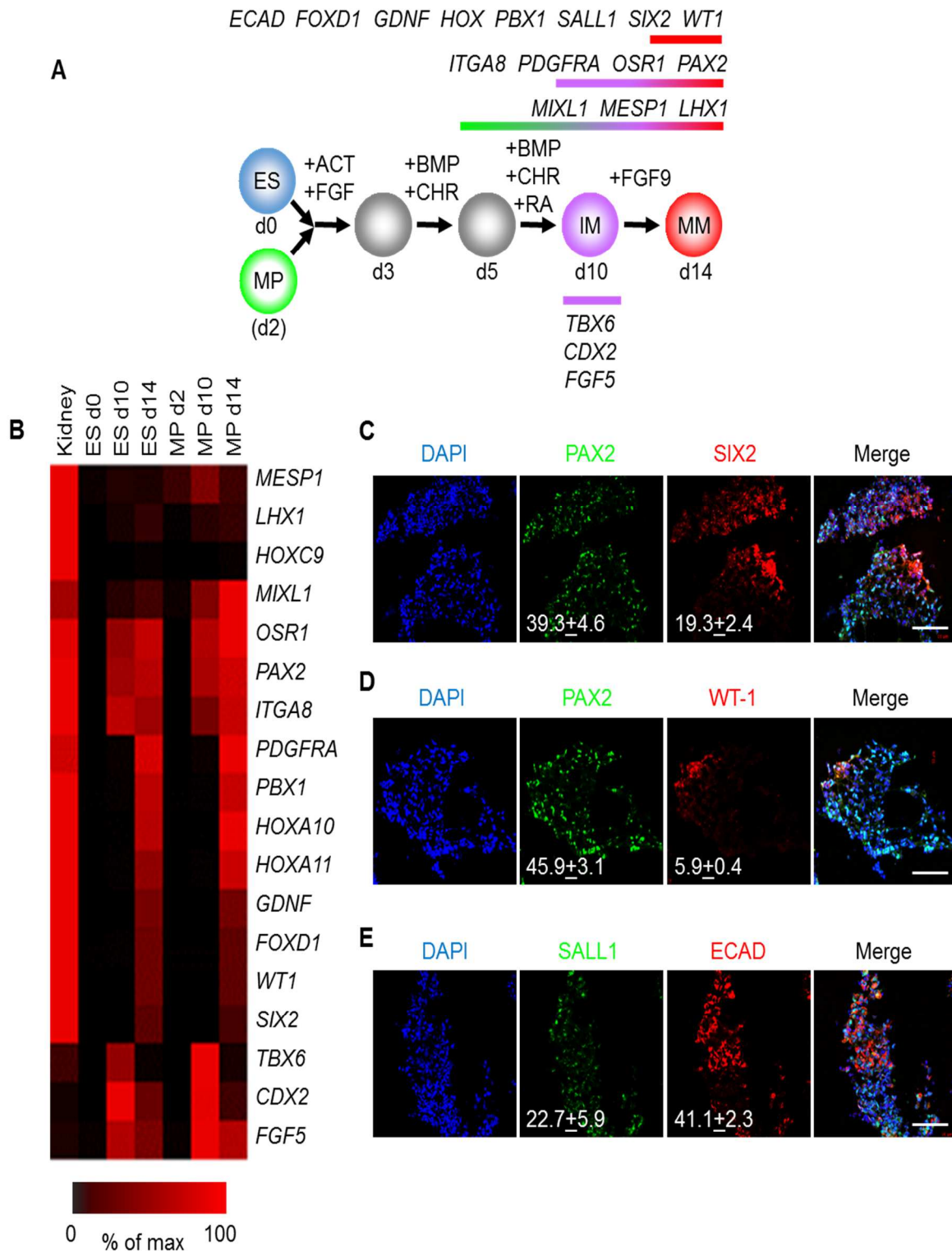
Figure 4-8. Differentiation of MP cells into primordial germ cells. A. Schematic of the differentiation protocol. Cells were differentiated in a step-wise manner using the indicated growth factors from undifferentiated ES cells or from MP cells to primordial germ cells (PGC). Stage-specific marker genes expressed by primordial germ cells are indicated at the top. **B.** Upon differentiation towards PGC, cells expressed genes associated with the germ cell lineage. QPCR was performed on ES and MP cells for the indicated genes at the final time point.

Since MP cells readily upregulated markers of primordial germ cells when

stimulated with BMPs, I hypothesized that MP cells could also be coaxed into other IM

derivatives, such as that of the renal lineage. To test this possibility, I employed a

published protocol to differentiate hES cells into renal progenitors (Figure 4-9A) (Taguchi et al., 2014b). This protocol employed several growth factors and small molecules to promote the differentiation of hES cells to IM and subsequently metanephric mesenchyme (MM). Importantly, MP cells efficiently acquired gene expression signatures associated with IM and MM as monitored by qPCR (Figure 4-9B). The gene expression profile of MP-derived MM exhibited a striking similarity to that of fetal kidney cells. *PAX2* and *SIX2* were upregulated at day 14 of renal differentiation, indicating commitment to the kidney lineage (Bush et al., 2014). Furthermore, immuno-fluorescence analysis demonstrated that a significant number of cells expressed IM and MM markers PAX2, SALL1, SIX2, WT1 and CDH1 (E-cadherin) (Figures 4-9C, D, E). These results suggested that MP cells are restricted to IM and effectively differentiate into cells expressing genes associated with a renal phenotype.

Figure 4-9. Differentiation of MP cells into metanephric mesenchyme. A. Schematic of the differentiation protocol. Cells were differentiated in a step-wise manner using the indicated growth factors and small molecules from undifferentiated ES cells or from MP cells to intermediate mesoderm (IM) and subsequently to metanephric mesenchyme (MM). Stage-specific marker genes expressed during this differentiation process are indicated at the top. Abbreviations: BMP = BMP4, CHR = CHIR98014, d = day, FGF = FGF2, RA = retinoic acid. **B.** Upon differentiation towards MM, cells expressed genes associated with kidney lineage. QPCR was performed on ES and MP cells for the indicated genes at various time points. Fetal kidney RNA (11 gestation weeks) was used as a control. The data is displayed as a heat map with black corresponding to minimal expression and red corresponding to maximal levels. **C-E.** Immunofluorescence analysis of MP cell-derived MM. MP cells were differentiated as depicted in panel A, fixed and stained for the indicated proteins and DNA (DAPI). Numbers refer to percentages of cells expressing the protein of interest. Standard deviation represents the variation between the fields of view used for counting (n=20). Scale bar = 100 μm

A

ECAD FOXD1 GDNF HOX PBX1 SALL1 SIX2 WT1

ITGA8 PDGFRA OSR1 PAX2

MIXL1 MESP1 LHX1

TBX6
CDX2
FGF5

B

C

D

E

To further assess the ability of the MP cells to generate cells with renal properties, I employed two rat explant assays that represent stringent measures of renal potential. In the first assay, rat embryonic kidneys were dissociated to single cells and re-aggregated to form kidney-like organoids (Davies et al., 2014; Unbekandt and Davies, 2010). These aggregation experiments were performed in the presence of either MP-derived MM cells (Figure 4-10A) or undifferentiated hES cells (control), thereby assessing the renal potential of these cells. The contribution of human cells to the re-aggregated rat kidneys is readily detected by staining for the human specific nuclear antigen (HuNu). In this assay, I consistently observed efficient incorporation of MP-derived MM cells into the kidney organoids (Figure 4-10B, Figure 4-11a). Interestingly, I primarily observed incorporation of these cells into the mesenchyme surrounding epithelial structures, which were visualized by staining with Dolichos biflorus lectin (DBA). In contrast, undifferentiated hES cells failed to incorporate into these kidney organoids (Figure 4-10C, Figure 4-11B) and instead were found adjacent to the organoid structures (Figure 4-11B, bottom row).

In a second assay, we co-cultured MP-derived MM cells with dissected embryonic rat spinal cords, a tissue that produces potent nephrogenic inductive signals (Figure 4-10D) (Gallegos et al., 2012; Kispert et al., 1998; Osafune et al., 2006). In this system, MP-derived MM cells readily acquired expression of markers associated with renal cell types, including CDH1, SIX2 and SALL1 (Figure 4-10E). In contrast, undifferentiated hES cells failed to express of SIX2 (Figure 4-10F), indicating that MM properties are required for efficient renal differentiation. Taken together, these studies demonstrate that MP cells efficiently generate cell types with renal characteristics.

Figure 4-10. Assessment of renal potential of MP cells. A. Schematic of a re-aggregation assay to test renal potential. MP cells were differentiated as depicted in Figure 7A and mixed with dissociated embryonic rat kidneys at a ratio of 7.5 : 92.5 and co-incubated for 4 days to form organoids in media-air interface co-culture. **B.** Representative images of re-aggregated kidney organoids. MP cells differentiated to MM are detected with the human specific nuclear antigen HuNu (green). Human cells are clearly integrated into renal organoids and surround epithelial structures labeled with the lectin DBA (red). Figure 8—figure supplement 1 provides additional images of MP cells incorporating into renal structures. Scale bar = 25 µm. **C.** Undifferentiated hES cells failed to integrate into renal organoids. Instead of MP cells, undifferentiated ES cells were mixed with dissociated embryonic rat kidneys. These cells failed to integrate into the renal organoid structures as indicated by the lack of HuNu staining. Figure 8—figure supplement 2 demonstrates that undifferentiated ES cells fail to incorporate into these structures. Scale bar = 25 µm. **D.** Schematic of spinal cord co-culture assay to assess renal differentiation potential of MP cells. MP cells were differentiated as depicted in Figure 7A and incubated in liquid-air interface cultures with rat embryonic spinal cord explants. **E.** Immuno-fluorescence analysis of markers expressed in renal progenitors. Four days after co-cultures were established, cells were fixed and stained for the indicated proteins (ECAD, SIX2 and SALL1) and for Lotus-tetragonolobus lectin (LTL). The dashed line indicates the boundary between human cells and the spinal cord (SC) explant. Scale bar = 100 µm. **F.** Undifferentiated hES cells failed to express SIX2 when co-cultured with embryonic rat spinal cords. Scale bar = 100 µm.
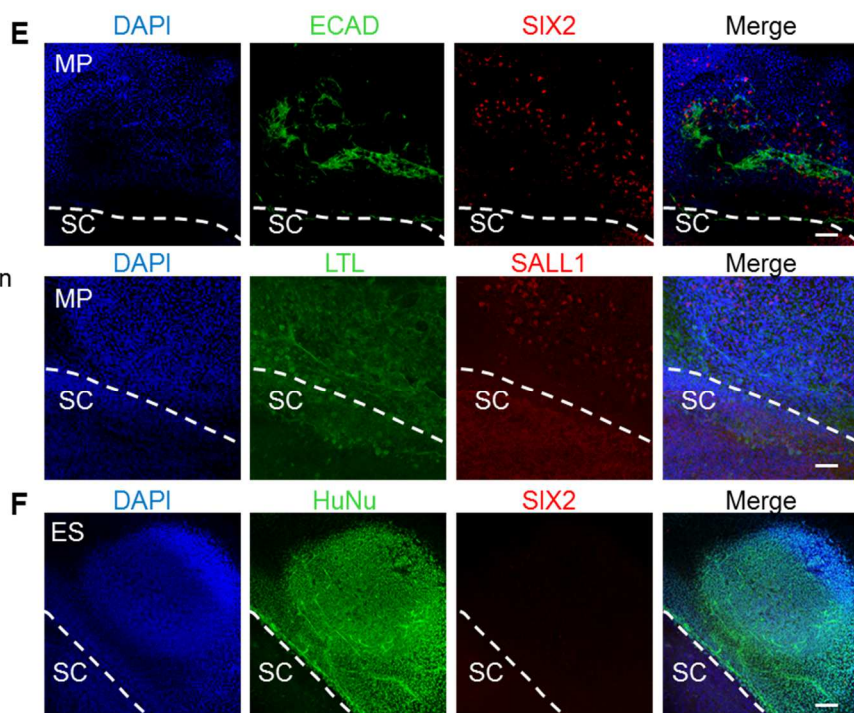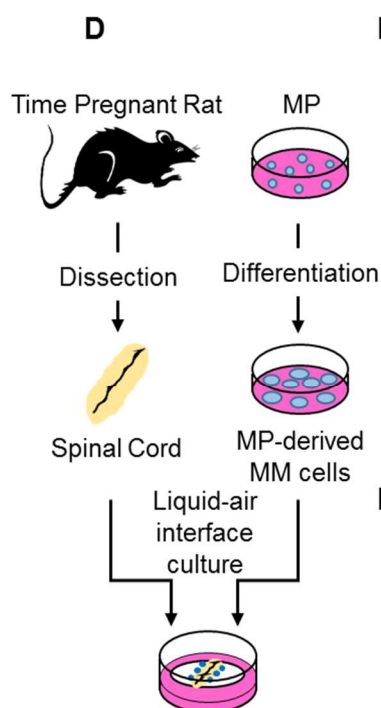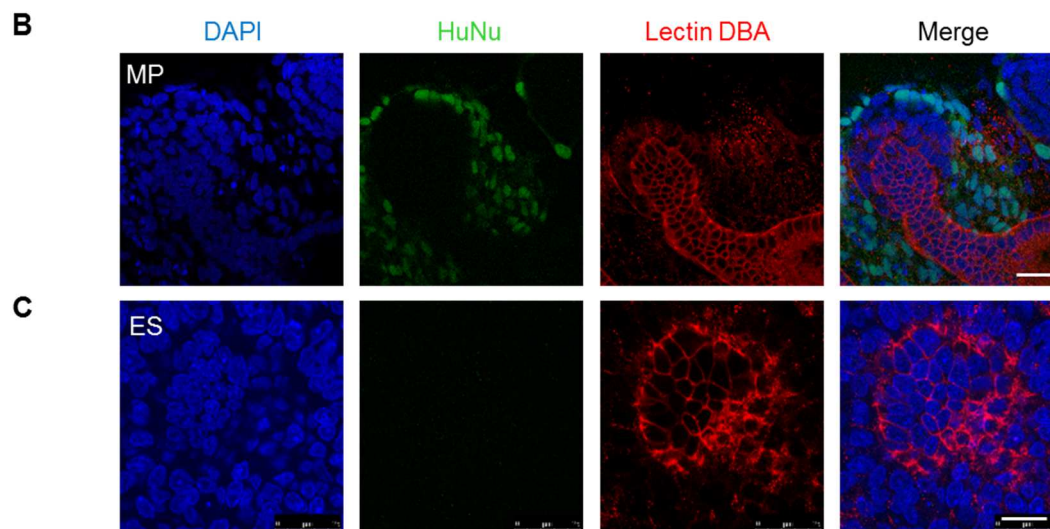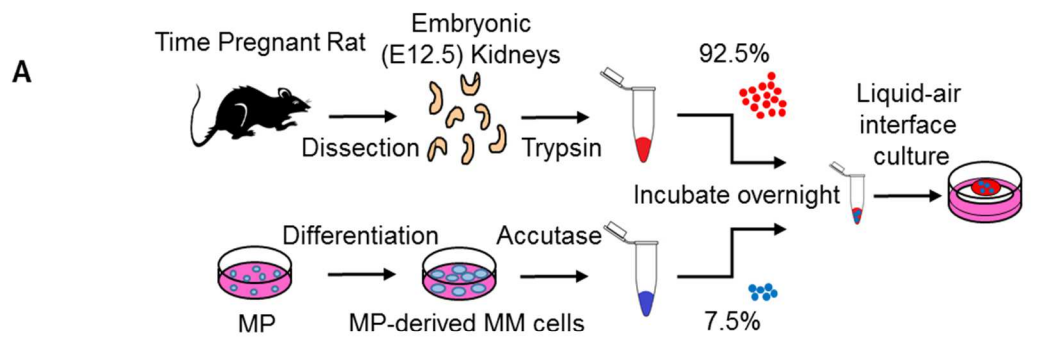
Figure 4-11. **Additional assessment of renal potential of MP cells. A.** Representative images of re-aggregated kidney organoids. MP cells differentiated to MM are detected with the human specific nuclear antigen HuNu (green). Human cells are clearly integrated into renal organoids and surround epithelial structures labeled with the lectin DBA (red). **B.** Undifferentiated hES cells failed to integrate into renal organoids. Unlike MP cells, undifferentiated ES cells failed to integrate into the renal organoid structures as indicated by the lack of HuNu staining. The last row of images demonstrates ES cells are present in the culture but are not incorporated into the renal aggregates. Scale bar = 25 µm.
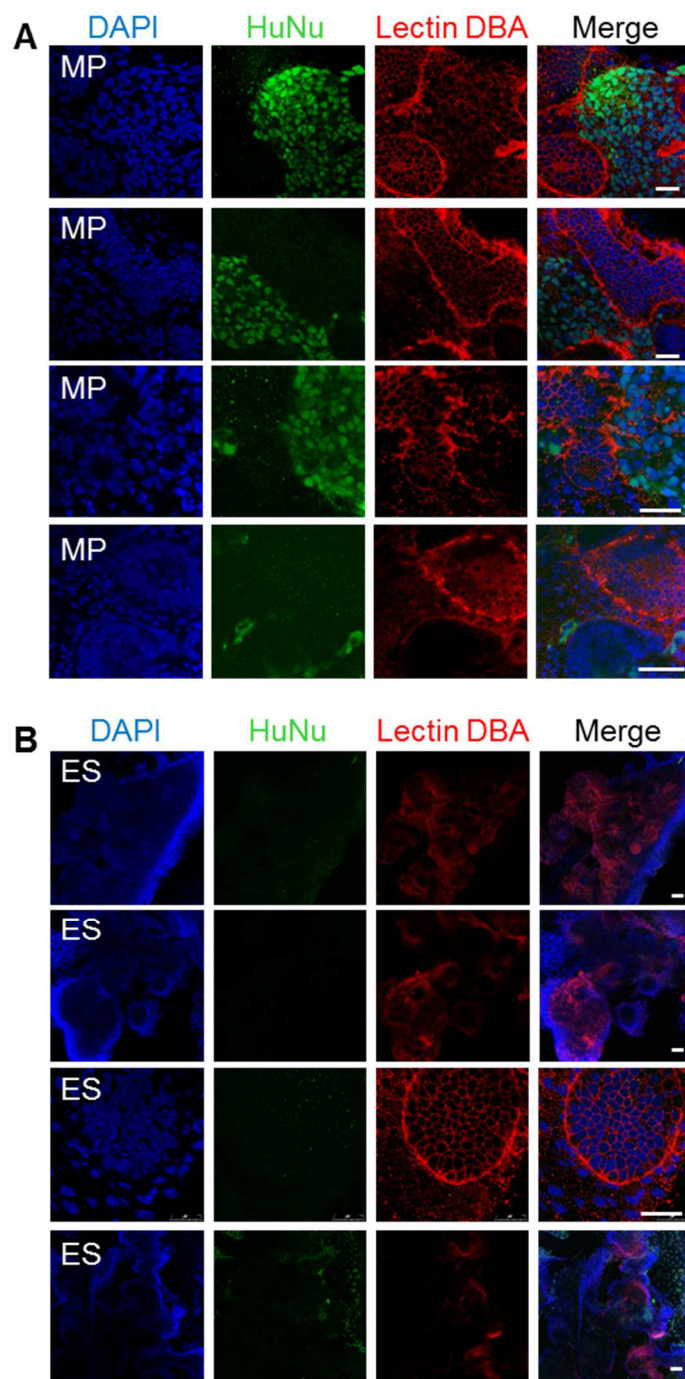
Discussion

In our mesoderm expansion study, I describe a novel progenitor cell population derived from hPS cells with the potential to differentiate into tissues of the intermediate mesodermal lineage. By using the arrayed cellular microenvironment (ACME) screening technology, I was able to simultaneously define and optimize derivation and expansion conditions for these mesodermal progenitor (MP) cells. Although it was our initial intention to produce a MP cell population with broad differentiation potential into all mesodermally-derived tissues, I made the surprising finding that the differentiation potential of these MP cells was restricted to the intermediate mesoderm (IM) lineage. Consequently, I was unable to coax MP cells to differentiate into cell types derived from paraxial mesoderm (PM) or intermediate mesoderm (IM), such as blood and cardiomyocytes. This exquisite lineage restriction was particularly surprising in light of the expression of multiple pan-mesodermal marker genes, such as *LHX1*, *MESP1* and *MIXL1*. Given their ability to differentiate into cell types with gene expression patterns associated with renal lineages, I hypothesize that this MP cell population is an *in vitro* counterpart to intermediate mesoderm.

Generation of expandable lineage restricted progenitor cell populations offers several advantages over the use of undifferentiated hPS cells in tissue engineering approaches. First, differentiated cultures derived directly from hPS cells often harbor undifferentiated cells, which retain the potential to seed tumor growth. Such tumor-initiating potential is problematic when cells are intended for transplantation to repair or replace damaged tissue. Based on our sub-cutaneous injections into immune-compromised mice, MP cells do not grow into teratomas, a defining property of undifferentiated pluripotent stem cells. Our gene expression analysis provides further evidence of this loss of pluripotency and hence of teratoma-seeding potential: MP cells

express nearly undetectable levels of pluripotency markers, such as *POU5F1/OCT4* and

SOX2, both of which show residual expression in mesodermally differentiated hPS cells.

Second, lineage-restricted progenitors require less elaborate manipulation to derive

more mature cell populations. In the case of the MP cells, early differentiation steps to

usher cells into a mesodermal lineage are no longer needed, thereby truncating

differentiation protocols to derive more mature cell populations. A third benefit for using

expanded progenitor cells is that such cultures are often quite homogenous. In contrast,

hPS cell cultures instructed to differentiate into a specific lineage generally contain other

cell types. Therefore, the yield of more mature cell types upon subsequent differentiation

is higher when starting with a homogenous, lineage restricted cell population than when

starting with undifferentiated hPS cells.

The conditions that I developed for the culture and expansion of MP cells were

fully defined and free from animal-derived components, which will be important when

cells are intended for therapeutic applications. Moreover, these optimized conditions are

robust as demonstrated by their ability to support derivation and expansion of MP cells

from two hES (H9 and Hues9) and one hiPS (RiPS) cell lines. Additionally, MP cells

grown in these optimized conditions can be frozen and thawed without any detectable

effect on proliferative capacity or differentiation potential. Finally, these optimized

conditions allow for near unlimited expansion (~10^{20}) to quantities necessary for drug

screening or regenerative medicine purposes (Chen et al., 2013).

Expandable lineage restricted cell populations have been developed for other

lineages, including the neural and endodermal lineages. Several protocols have been

described for the derivation of neural progenitor (NP) cells, which can proliferate

extensively and differentiate into all the neural lineages and supporting cells (neurons,

astrocytes, and oligodendrocytes) that compromise the central nervous system

(Chambers et al., 2009; Reubinoff et al., 2001; Shin et al., 2006). Endodermal progenitor (EP) cells represent another example of lineage restricted progenitor cells (Cheng et al., 2012). These cells retain the ability to differentiate into endodermally derived tissues, including liver and pancreas. Interestingly, differentiation into functional beta-cells is greatly improved when starting with EP cells compared to undifferentiated hPS cells.

Although both EP and MP cells exhibit restriction with respect to their developmental potency, MP cells are more severely restricted as they fail to produce certain mesodermally-derived cell populations, such as blood and heart muscle. We currently do not understand the mechanism by which the culture conditions defined for the derivation and expansion of MP cells lead to this highly restricted developmental potential. During embryogenesis, as the mesoderm emerges and migrates from the primitive streak it is further specified into paraxial, lateral plate, and intermediate mesoderm (PM, LM, and IM, respectively). Interestingly, both FGF and WNT/β-catenin signaling regulate this ME cell specification, migration, and proliferation (Aulehla and Pourquié, 2010; Ciruna and Rossant, 2001; Sweetman et al., 2008). Basic FGF is known to have a mitogenic effect on many different progenitor and stem cell culture systems, including both mouse and human models (Bianchi et al., 2003; Gospodarowicz et al., 1986; Gritti et al., 1995; Lindner and Reidy, 1991; Vescovi et al., 1993). It is therefore not surprising that hbFGF increased the expansion of both endoderm and mesoderm progenitor cells. WNT signaling is known to influence cytoskeletal polarity throughout the early embryo, distinguishing endoderm from mesoderm through complex regulatory interactions (Lindsley et al., 2006; Thorpe et al., 1997). Similarly, it is not unexpected that WNT activation at specific doses is involved in the expansion of both endoderm and mesoderm cells.

Along similar lines, modulation of the certain signaling pathways, such as WNT, can further refine and specify the differentiation potential of hPS cell-derived progenitors. For example, we previously showed that levels of WNT/β-catenin signaling instruct the positional identity of NPCs and, upon subsequent differentiation, of the resulting neuronal cell population (Moya et al., 2014). Specifically, high levels of WNT signaling instructed NP cells to adopt a posterior fate, consistent with WNT's role in posterior patterning during development. In a separate study, the level of WNT activation achieved through GSK3-β inhibition was found to directly influence the ME subtype of differentiating hPS cells (Mendjan et al., 2014). I speculate that in our *in vitro* MP cell culture system that continuous activation of the WNT and FGF signaling pathways are acting not only to stabilize the MP cell state but also to restrict its differentiation potential to cell types derived from the IM lineage.

The development of lineage-restricted progenitors also offers an opportunity to investigate mechanisms by which specific developmental stages can be paused. Recent studies to profile epigenetic changes during the differentiation of hPS cells to pancreatic beta cells indicate that specific chromosomal regions open during specific windows of differentiation, thereby conferring a certain development competence to sequentially acquire increased lineage restriction (Wang et al., 2015). In the future, the intermediate mesoderm restricted cell population described here can provide a further window into the mechanisms by which developmental competence is established and maintained.

Table 4-1. Related to Figure 4-6. Complete list of 244 genes with similar expression levels in MP cells and mesoderm (MP + ME).

AATF	DDX19A	JOSD2	PITHD1	TAF12
ABCD3	DENR	KAZN	PNO1	TAF9
ABCF3	DGCR2	KCNK17	POLR2B	TAOK2
ABCG2	DHX34	KHDRBS3	POLR2D	TCEB3
ACAT1	DIS3	KIAA0226L	POLR2J	TDG
ADAMTS15	DIS3L	KIAA1429	PRADC1	TENC1
AGPAT5	DKK1	LEF1	PRKAG1	TFAM
ALDH1A2	DLL3	LIPG	PRPF4	THEM4
ALG2	DNAJA1	LOC440925	PRPF6	THOC1
AP1AR	DNAJC25	LPAR6	PSMD6	THOC5
APEX1	DNAJC7	LRFN5	PSMD7	TIMM17A
APLNR	DONSON	LRRC55	PTDSS2	TM2D2
ATOH8	DRG2	LRRTM1	QTRTD1	TMEM70
ATP5F1	EEF1B2	LSG1	RAB35	TNFAIP2
BAG1	EGFLAM	MAD2L1	RARS	TNFAIP8L2
BAZ1A	EID1	MAD2L1BP	RASL10B	TNFRSF11B
BGN	EIF1AD	MAFA	RASSF9	TOE1
BTBD1	EIF2B1	MAP2K2	RBP1	TOMM34
BZW1	EMILIN1	MCM8	RCC1	TOPBP1
C14orf169	EMP2	MCOLN3	RFC2	TOR1B
C16orf53	ENOX2	MDFIC	RHOBTB2	TPRKB
C1orf151	ERLIN1	MESP2	RHOQ	TRAF2
C1orf174	EXOSC4	MINPP1	RNF20	TRMU
C1orf52	FAIM	MKI67IP	RPSA	TRPM7
C3orf14	FAM13A	MPHOSPH10	RRAGA	TRUB2
C5orf43	FAM181B	MSX1	SAC3D1	UBE2L3
C6orf204	FAM24B	MTA2	SALL1	UFD1L
C7orf16	FDX1L	MTRR	SAMD1	UNC5C
CAND1	FEN1	NBN	SAR1A	USP33
CANX	FRMD8	NCBP2	SDCCAG3	USP5
CAPRIN2	GABBR1	NDST1	SFXN2	UTP18
CCDC99	GLMN	NDUFS1	SKA1	WDR55
CCNE2	GLRX3	NHEJ1	SLC25A12	WDR81
CCNF	GOSR2	NOL8	SLC26A2	WNT5A
CCT6A	GRINL1A	NTS	SLC35E1	YBX1
CCT8	GRPEL1	NUBP1	SLC35G1	ZBTB2
CD44	GTF2H1	NUP50	SLIT2	ZDHHC6
CENPB	GTF3A	OBFC2B	SNAI1	ZFP64
CLPB	GYPC	OLFM1	SNAI2	ZMPSTE24

Table 4-1. Related to Figure 4-6. Complete list of 244 genes with similar expression levels in MP cells and mesoderm (MP + ME), continued

CMKLR1	HAT1	OLFML3	SOD1	ZNF100
CNPY2	HMGB1	PANK1	SP5	ZNF17
CNPY3	HMX1	PANX1	SP6	ZNF200
CNST	HNRNPA1	PC	SPATA5L1	ZNF286A
COMMD9	HOXB2	PCDHGC4	SPC25	ZNF347
CRABP2	IRX2	PDE3B	SSBP1	ZNF45
CWF19L1	IRX5	PGGT1B	STOML2	ZNF511
CYBASC3	ISCA1	PHAX	STRAP	ZNF639
DCBLD1	ISLR	PHLDA2	SUB1	ZNF668
DDI2	ISY1	PIP4K2B	TACR1	

Table 4-2. Related to Figure 4-6. Complete list of 140 genes expressed only in MP cells (MP only).

ACTA1	CHST11	GYPE	MMP2	RIPPLY1
ACTC1	CLSTN2	HAPLN1	MOGS	SCGB1A1
ADA	CNOT2	HAS2-AS1	MPST	SCYL1
ADAM12	COL1A2	HCN1	MSX2	SEMA3G
ADAMTS12	CREG1	HHIPL2	MYL4	SESN1
AEBP1	CRELD2	HS3ST3A1	MYLK3	SFRP5
ALPK2	CTNNB1	HSDL2	NFATC1	SPSB1
AMN1	DDB1	HSPA1B	NKX3-1	SRP54
AMOTL1	DGKI	HTRA1	NPPA	SVEP1
AP3S1	DNAJC14	IFI16	NRP1	TANC1
ARSK	DOK4	IL11	PAPPA	TFPI
ART5	DVL1	IL6	PCSK2	TMED7
ATP8B3	DYNC1I1	ISL1	PCYOX1	TMEM107
B2M	ECE1	ITGA8	PDGFRA	TMEM185A
BAMBI	EMILIN2	ITGA9	PDGFRB	TMF1
BIN1	FAM123C	JPH2	PGF	TNFAIP3
BMP4	FAM78A	KDELC1	PGM3	TNFRSF19
BMP5	FBN2	KIAA1462	PGM5	TNNT1
BMPER	FMOD	KIF26B	PHLDA3	TPK1
BSG	FN1	KLK6	PLCB1	TTC9C
C12orf23	FOXC2	KLK7	PLEC	TWIST1
C12orf35	FSHR	LAMC1	PMP22	VPS29
C6orf138	GNG11	LNPEP	PPP1R2	VSTM2L

Table 4-2. Related to Figure 4-6. Complete list of 140 genes expressed only in MP cells (MP only), continued.

C9orf21	GOLIM4	LRRC32	PSTPIP2	WDR20
CALU	GRAP2	LRRN4	PXDN	YIPF5
CBLN2	GREM1	MAB21L2	RASGRP1	ZAP70
CCNB1IP1	GSN	MAGEB3	RASGRP3	ZNF611
CHIC2	GYPB	MALT1	RGS4	ZNF702P

Table 4-3. Related to Figure 4-6. **RNA-seq data set of MP cells at passage 10.** This table provides the complete RNA-seq data set of MP cells at passage 10. Column A provides gene names. Values in column B are reads per kilobase per million mapped reads (RPKM).

Please see Supplementary File 2 published online at *ELife*.

Chapter 4, in part, has been submitted for publication. Kumar, Nathan; Richter, Jenna; Cutts, Josh; Bush, Kevin; Trujillo, Cleber; Nigam, Sanjay; Gaasterland, Terry; Brafman, David; Willert, Karl. "Generation of an expandable intermediate mesoderm restricted progenitor cell line from human pluripotent stem cells." I am the primary author and researcher.

Chapter 5. Conclusions

Discussion

Generating other lineage-restricted progenitor lines

During embryogenesis, progenitor specification is followed by expansion and subsequent differentiation, and the orchestrated balance between the two ultimately determines the final organ size (Thompson 1992). The delicate equilibrium is choreographed in vivo by signals provided within the developing organism. My work shows that these two steps, self-renewal and differentiation, can be effectively isolated in vitro, enabling the independent manipulation of each step. By systematically studying the effects of various components of the microenvironment, I identified culture conditions that allowed for amplification of restricted intermediate cell types without further differentiation. This approach fosters progenitor expansion to an extent that may even exceed that which occurs in normal in vivo development. Although I used the endodermal and mesodermal lineages as a model, amplification of progenitors by defining culture conditions to include optimal soluble and insoluble proteins could be translatable to various other cell types, facilitating progress for regenerative medicine as a whole.

Since the identification of self-renewal signals can be applied to intermediate cell types in any differentiation scheme, progenitors within all germ layers can theoretically be expanded without differentiation. In practice, however, I noticed that the simplified approach of optimizing soluble and insoluble proteins in the progenitor cell's microenvironment was not always sufficient to promote indefinite self-renewal while avoiding further differentiation, at least in the case of transient definitive endoderm cells. I cannot conclusively determine that it is impossible to generate self-renewing endoderm cells capable of subsequent differentiation, especially since other have claimed to do just that (Cheng et al., 2012; Hannan et al., 2013), but it is evident

that additional factors, such as glycans, other cytokines, or substrate rigidity and architecture, will be required to do so. Which factors are required and to what extent will depend on the cell type being amplified, making intelligent experimental design a necessary component to unravel the necessary cues for progenitor amplification.

Based on the results of my work, it does seem feasible that other mesodermally-restricted progenitor lines could be generated. In my approach, I looked for conditions that maximized the maintenance of the transient reporter *Brachyury* and discovered that these very conditions seemed to promote the expansion of intermediate mesoderm progenitor cells. As a slightly modified alternative to that approach, the focus could be shifted to the optimal maintenance of other gene markers within the mesodermal lineage, such as *PDGFRA* for paraxial mesoderm, *KDR* for lateral plate mesoderm, or more universal mesoderm genes such as *MESP1, MIXL1,* or *EOMES*. Even without reporter lines like the one used in this study, antibodies are readily available for the detection of these transcription factors, which could be carried out in the arrayed cellular microenvironment (ACME) format. Seeking culture conditions for the maintenance of these markers instead of the transient *Brachyury* gene would likely produce a different set of optimal ECMPs and GFs/SMs. Since these markers are less transient in their nature, the duration of the screen would potentially need to be elongated but the overarching design would be similar. Scaling up the results from these screens and characterizing the resultant cell populations would be key to discovering their in vitro potentials. Additionally, these screens could be carried out at later timepoints in paraxial or lateral plate differentiation protocols such that more mature mesodermally-restricted markers such as *NKX2.5*, *ISL1*, *TBX6*, *MEOX1*, *TCF15*, and *PAX1* became expressed before seeding the ACME screens. In these instances, it would be possible to optimize

culture conditions for maintenance of these later markers, and in doing so engineer culture conditions for expanding more specified progenitor lines within the mesodermal lineage.

Progenitor Cell Culture Benefits

Amplifying restricted intermediate progenitor cell types is desirable over pluripotent differentiation methods for several reasons. First, self-renewing, multipotent, non-tumorigenic progenitor stem cells could provide a feasible source for generating differentiated cells suitable for cellular therapy since they do not harbor undifferentiated cells capable of seeding tumor growth. Such tumor-promoting activity is precarious because cells intended to repair damaged tissue would in fact pose an entirely unhealthy tumorigenic risk. Secondly, expanded progenitor cells are typically homogenous in the character of cells within the population, making the yield of more mature cell types upon subsequent differentiation more efficient. Also, since early differentiation steps required to coax cells into a particular germ line are not needed, mature cell types can be derived with less manipulation of the starting population. Since stepwise differentiation of stem cells into specialized derivatives remains inefficient for several cell types, it will be necessary to expand progenitor cells, without differentiation, at some steps along the way to generate specialized cells in the quantities necessary for cell therapy. A third benefit of progenitor expansion is the systematic differentiation of various hPS lines without the need to establish individualized protocols, making these methods more streamlined and reliable for use in personalized regenerative medicine. Lastly, in this study I expanded restricted intermediate cell types in fully-defined, feeder-free culture systems, which is important if these cells are to be used for therapeutic applications. For these reasons, expansion of lineage-restricted or even individual cell type-

restricted progenitors is an enticing model for the advanced differentiation protocols that will be needed for regenerative medicine to become a reality.

Clinical Applications

Currently, MP cells could be used as a source for disease modeling and drug discovery. Treatment of disease can be complicated by our inability to preemptively study the mechanisms which play a role in exacerbating that disease. For this reason, disease modeling can greatly advance our ability to target diseases that remain elusive to treatment. Current animal models for studying diseases within the mesodermal lineage such as that of kidney failure are limited because of the inherent genetic variability that exists across species, making it difficult to fully mimic the human cell microenvironment. MP cells, on the other hand, could be of enormous use for the development of particular therapeutics targeted at human diseases such as kidney failure. Studying MP cells would provide a novel platform to identify potential drug molecules and to test their toxicity on human cells before entering the market. MP cells would serve as a legitimate source of human intermediate mesoderm cells and could be generated robustly across hPS cell lines, potentially making it widely applicable for disease modeling and drug discovery.

Furthermore, MP cells could be utilized as a source for regenerative medicine therapies such as tissue transplantation. Using MP cells as a source of transplantable tissue is feasible in theory but would require additional studies to make it practically functional. Since MP cells are seemingly homogenous, can be expanded virtually indefinitely without tumorigenicity and still retain their differentiation potential towards intermediate mesoderm cell types, they provide a promising source for cell therapy. With that said, although MP cells can be induced to express gene markers for the kidney and gonad tissues, additional factors would be needed to

make the specialized cells actually useful in vivo. It is likely that 3D scaffolding and the complex interplay between neighboring cell types would require further optimization before these cells can be practically used in regenerative medicine applications. However, this particular study provides a genuinely solid foundation from which to build towards that ultimate goal.

Conclusion

In my studies, I focused on expansion of progenitors in order to take advantage of these potential benefits. In doing so, I noticed that so far, most attention has focused on the soluble signals responsible for fostering expansion of intermediate cell types or directing differentiation from one stage to the next. Here I aspired to amplify or renew distinct progenitors at the stages of transient endoderm or mesoderm by also optimizing the insoluble substrate upon which the cells grow. Interestingly, I discovered that the effects of soluble signals could be augmented or diminished by the insoluble extracellular matrix components in a cell's surroundings. This dependence on insoluble protein substrates and the need to develop fully-defined culture systems for clinical applications highlights the importance of selecting appropriate matrix components for manipulating cells in vitro. Our work demonstrates this crucial impact of the extracellular matrix milieu on determining the self-renewal and differentiation fate of a stem cell.

In summary, I describe a fully-defined, scalable culture system to reproducibly and efficiently generate intermediate mesoderm progenitor cell lines from hPSCs. Intermediate mesoderm progenitor cells self-renew virtually indefinitely and can be subsequently stimulated to form kidney and gonad tissues. Importantly, these progenitor cells are non-tumorigenic, reflecting their potential use in cell replacement therapies. Our work defies the belief that hPSCs must be used as the starting point

for directed differentiation protocols. Rather, the progenitor cell lines I generated

serve as an intermediate between pluripotent stem cells and more differentiated

mesodermal tissues. These lines will provide novel experimental platforms to

investigate the natural processes of mesodermal differentiation and a safer, more

efficient starting point for cell replacement therapies aimed at treating widespread

human disorders including kidney failure.

Appendix

Regulation of endodermal differentiation of human embryonic stem cells through integrin-ECM interactions

DA Brafman*,1, C Phung[1], N Kumar[2] and K Willert*,1

Many cellular responses during development are regulated by interactions between integrin receptors and extracellular matrix proteins (ECMPs). Although the majority of recent studies in human embryonic stem cell (hESC) differentiation have focused on the role of growth factors, such as FGF, TGFβ, and WNT, relatively little is known about the role of ECMP-integrin signaling in this process. Moreover, current strategies to direct hESC differentiation into various lineages are inefficient and have yet to produce functionally mature cells *in vitro*. This suggests that additional factors, such as ECMPs, are required for the efficient differentiation of hESCs. Using a high-throughput multifactorial cellular array technology, we investigated the effect of hundreds of ECMP combinations and concentrations on differentiation of several hPSC lines to definitive endoderm (DE), an early embryonic cell population fated to give rise to internal organs such as the lung, liver, pancreas, stomach, and intestine. From this screen we identified fibronectin (FN) and vitronectin (VTN) as ECMP components that promoted DE differentiation. Analysis of integrin expression revealed that differentiation toward DE led to an increase in FN-binding integrin α5 (ITGA5) and VTN-binding integrin αV (ITGAV). Conditional short hairpin RNA-mediated knockdown of ITGA5 and ITGAV disrupted hESC differentiation toward DE. Finally, fluorescence-based cell sorting for ITGA5 and ITGAV significantly enriched cells with gene expression signatures associated with DE, demonstrating that these cell surface proteins permit isolation and enrichment of DE from hESCs. These data provide evidence that FN and VTN promote endoderm differentiation of hESCs through interaction with ITGA5 and ITGAV, and that ECMP-integrin interactions are required for hESC differentiation into functionally mature cells.
Cell Death and Differentiation (2013) **20**, 369–381; doi:10.1038/cdd.2012.138; published online 16 November 2012

Human embryonic stem cells (hESCs), with their ability to differentiate into mature cell types, represent a novel system to study human development and disease, and assess safety and efficacy of drugs before clinical trials. In addition, these cells provide an unlimited source of 'raw material' for regenerative medicine therapies of many incurable diseases, including diabetes and heart disease. However, applications of hESCs in basic research, pharmaceutical, and regenerative medicine are hampered by the lack of well-defined conditions for their directed differentiation and insufficient methods for the purification of lineage-specific cell types from heterogeneous cell populations. Cells derived from definitive endoderm (DE), including those comprising the gut, lung, and pancreas, are of significant interest for many regenerative medicine purposes. Previous studies have identified conditions to generate DE from hESCs through growth factor or small molecule modulation of various soluble signaling pathways including TGFβ, Wnt and AKT/PI3K.[1–4] However, most DE differentiation protocols yield heterogeneous cell populations,[4] suggesting that additional factors, such as

extracellular matrix proteins (ECMPs), are required for the specification of hESCs to specific fates.

While many studies have focused on the roles of signaling molecules in the differentiation of hESCs, relatively little is known about the role of ECMPs and their interactions with integrins in controlling hESC fate. In mammals, 24 heterodimeric integrin receptors consisting of one of 18 α-subunits and one of 8 β-subunits have been identified. In addition to mediating binding to specific ECMPs, which provide a scaffold for cell growth,[5,6] activation of integrins through interactions with local ECMPs influence cellular processes during embryonic development, including cell survival, proliferation, motility and differentiation. Furthermore, the bidirectional (i.e. inside-out and outside-in) nature of integrin signaling serves as a link between the extracellular and intracellular environments and in turn modulates various downstream signaling pathways and components, such as MEK–ERK, PI3-kinase, and SRC.[7] Moreover, many of these downstream pathways have previously been implicated in regulating hESC self-renewal, proliferation, and differentiation.[7]

Therefore, the study of ECMP-integrin signaling is important in understanding the mechanisms that control hESC differentiation.

Current endodermal differentiation strategies involve guiding hESCs through sequential, staged protocols that mimic early embryonic signaling events known to control primitive streak formation and gastrulation. However, these protocols are often variable and inefficient, yielding only 30–40% cells expressing endodermal markers, such as SOX17. A potential strategy for improving hESC differentiation efficiency involves a two-pronged approach in which hESCs are differentiated to DE and then isolated and enriched using cell surface markers. This strategy not only relies on developing methods for improving the efficiency of DE differentiation from hESCs but also on methods for isolating endodermal cells from heterogeneous differentiating hESC cultures.

The majority of hESC differentiation protocols utilize poorly defined matrices, such as Matrigel (MGEL, BD Biosciences, San Jose, CA, USA), which is a protein mixture produced by EHS mouse sarcoma cells. While such protein extracts provide extracellular components necessary to support cell adhesion, they fail to mimic the specialized microenvironments to which cells are exposed *in vivo*. In this study, we employed a high-throughput combinatorial ECMP array platform to identify fibronectin (FN) and vitronectin (VTN) as components that improve differentiation of hESCs to DE. Furthermore, we show that the integrin receptors that engage FN and VTN are required for hESC differentiation to DE. Finally, we identified a novel DE integrin 'signature' that allows for fluorescence-based cell sorting methods to purify endodermal progeny from differentiating hESC cultures. Thus, our studies demonstrate the utility of investigating ECMP-integrin interactions to improve of hESC differentiation.
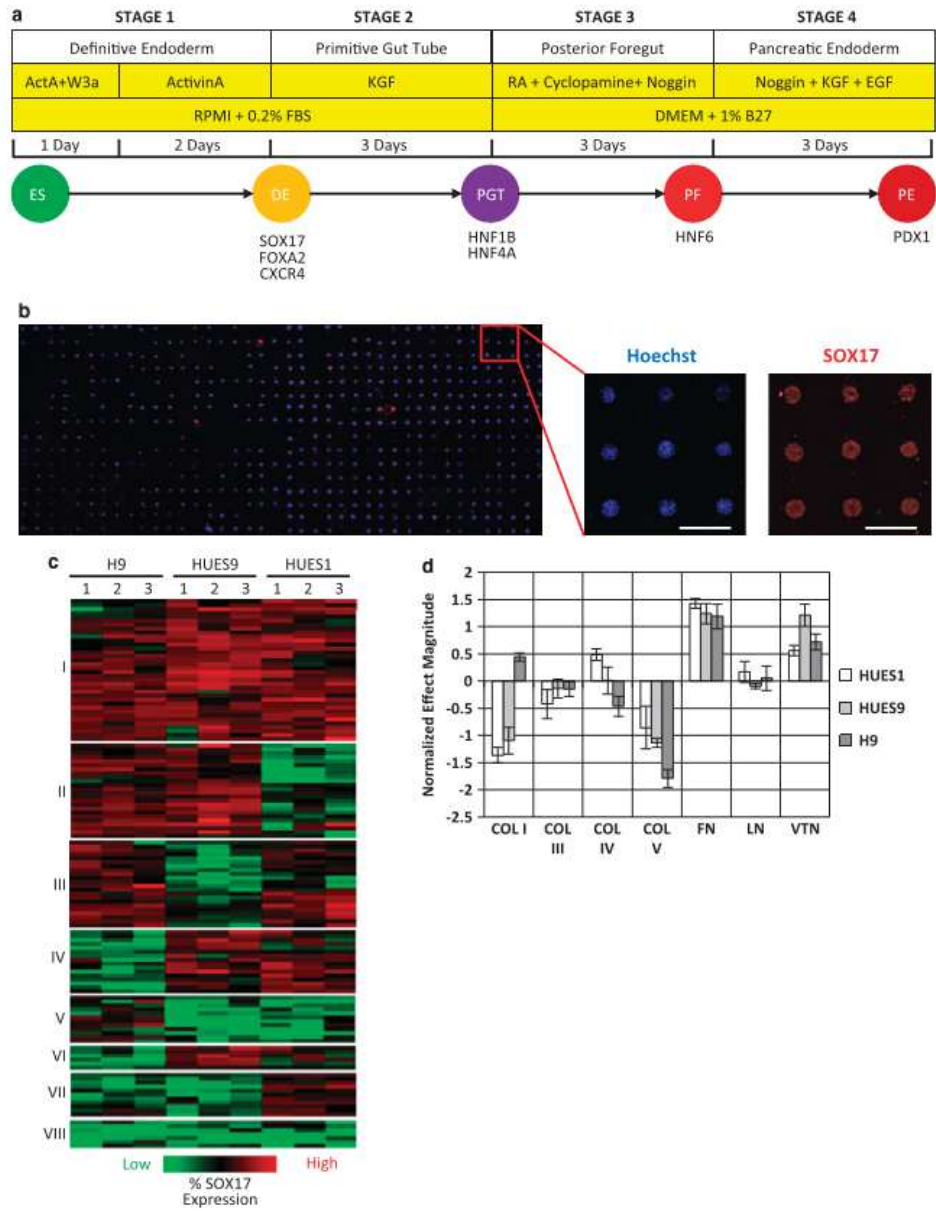
Results

High-throughput cellular microarray screen to identify matrix components that promote endodermal differentiation. In an effort to further define and optimize current differentiation protocols of hESCs, we chose to examine the staged differentiation protocol toward pancreatic endoderm (PE, Figure 1a), the first stage of which involves Wnt3a and Activin A treatment to differentiate hESCs to DE,[2,8,9] as assessed by expression of SOX17, FOXA2, and CXCR4. Although certain hESC lines, such as CyT49, efficiently differentiate into DE,[2,8,9] other cell lines yield variable amounts of cells expressing DE marker genes, ranging from 32–65% (Supplementary Figure 1), suggesting that additional factors are required for DE differentiation. We sought to investigate to what extent the extracellular milieu, specifically ECMPs, affects endodermal differentiation of three hESC lines, H9, HUES1, and HUES9. We employed a cellular microarray screening platform previously developed in our laboratory.[10–13] All possible combinations of seven ECMPs, collagen I (COL I), collagen III (COL III), collagen IV (COL IV), collagen V (COL V), FN, laminin (LN) and VTN were printed on arrays as described (see Materials and Methods). For comparison we included MGEL (BD Biosciences), which is commonly employed in differentiation protocols of adherent hESC cultures. These arrays were seeded with hESCs, the medium was supplemented with Wnt3a and Activin A to promote endodermal differentiation, and cells were fixed, stained, and imaged for the DE marker SOX17 and DNA (Hoechst Stain 33342) (Figure 1b).

Hierarchical clustering of data sets revealed eight well-defined clusters (Figure 1c; for raw data see Supplementary Table 1), representing ECMP combinations that either promoted high normalized SOX17 expression in all three hESC lines tested (Cluster I), two out of three hESC lines tested (clusters II, III, and IV), one out of the three hESC lines tested (cluster V, VI, VII), or in none of the hESC lines tested (cluster VIII). Analysis of the Pearson correlation coefficient between independent array experiments demonstrated the consistent effects of ECMP combinations within each hESC line but also revealed that the efficiency of some ECMP conditions in promoting DE differentiation was cell line-specific (Supplementary Figures 2a and b). To identify the ECMPs that most effectively promoted DE formation, we performed a full factorial analysis,[14] which revealed FN and VTN as the most common DE promoting ECMPs (Figure 1d). Other ECMPs had either no effect (e.g. LN) or negative effects (e.g. COL V) on DE differentiation (Figure 1d).

FN and VTN promote endodermal differentiation. To confirm that FN and VTN promoted DE differentiation of hESCs we compared their effects to that of MGEL in conventional cell culture formats. HUES9 hESCs were plated on MGEL and the combination of FN and VTN (FN + VTN) and differentiated to DE. Immunofluorescent (IF) staining demonstrated that FN + VTN caused a statistically significant increase in the percentage of cells expressing the DE marker SOX17 (Figure 2a). Moreover, culture on FN + VTN increased the total number of SOX17 + cells, as well as the total cell number (Figure 2b). Flow cytometry revealed that culture on FN + VTN produced an increase in the percentage of cells expressing the DE marker CXCR4 (Figure 2c). Finally, quantitative PCR (qPCR; Figure 2d) of DE markers *SOX17*, *FOXA2*, and *CXCR4* showed that FN + VTN increased the efficiency of DE differentiation relative to MGEL. We also observed that FN + VTN resulted in increased DE differentiation in two additional hESC lines, HUES1 and H9 (Supplementary Figures 3a and b). Finally, our analysis revealed that FN + VTN increased the efficiency

Figure 1 High-throughput ECMP screen reveals the influence of ECMPs in DE differentiation. (a) Schematic of the four stage differentiation protocol from hESC (ES), to DE, PGT, posterior PF, and finally PE. The soluble factors and culture media used at each stage are shown. (b) hESCs (H9, HUES1, HUES9) were cultured on ECMP arrays using previously published DE differentiation conditions.[8] On day 3, arrays were fixed and stained with Hoechst and an antibody to SOX17, a marker for DE (scale bar = 450 μm). (c) Heat map representing the cell number normalized SOX17 expression of each ECMP combination (rows) for each independent array experiment. Three independent array experiments were performed with each hESC line. Columns were mean normalized and scaled to one unit S.D. Hierarchical clustering of ECMP conditions was performed using Pearson correlation coefficient as a similarity metric. Clustering segregated ECMP combinations into eight groups based on the normalized SOX17 expression induced in each hESC line. (d) Magnitude of the main effects from a full factorial analysis of the ECMP array data reveals that specific ECMP components, FN and VTN, have largest positive effects on DE differentiation efficiency (n = 3 independent array experiments; error bars, S.E.M.)

a

	STAGE 1	STAGE 2	STAGE 3	STAGE 4
	Definitive Endoderm	Primitive Gut Tube	Posterior Foregut	Pancreatic Endoderm
ActA+W3a	ActivinA	KGF	RA + Cyclopamine+ Noggin	Noggin + KGF + EGF
	RPMI + 0.2% FBS		DMEM + 1% B27	
1 Day	2 Days	3 Days	3 Days	3 Days

ES → OE → PGT → PF → PE

OE: SOX17 FOXA2 CXCR4
PGT: HNF1B HNF4A
PF: HNF6
PE: PDX1

b

Hoechst   SOX17

c

H9   HUES9   HUES1
1 2 3   1 2 3   1 2 3

I
II
III
IV
V
VI
VII
VIII

Low — High
% SOX17 Expression

d

Normalized Effect Magnitude

COL I, COL III, COL IV, COL V, FN, LN, VTN
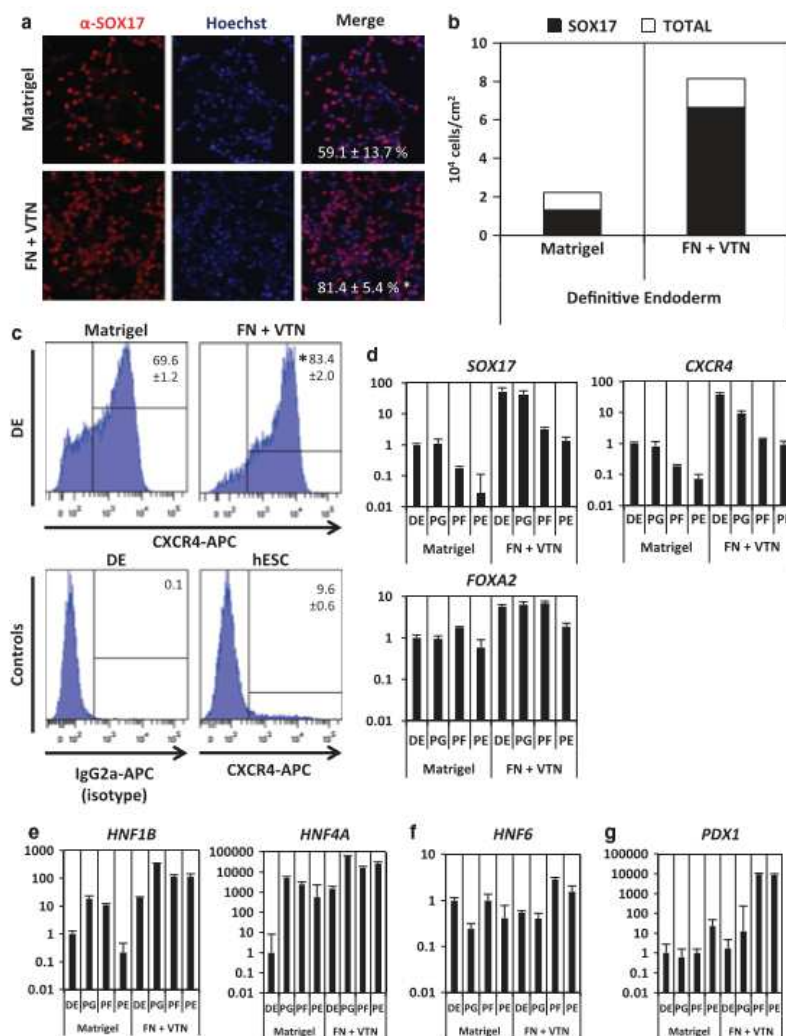
□ HUES1
▨ HUES9
▨ H9

Figure 2 ECMPs improve efficiency of hESC differentiation to DE, PGT, PF endoderm, and PE. HESCs were cultured on MGEL and FN and VTN (FN + VTN) using previously published protocols.[2,8,9] (a) Representative images of αSOX17 immunofluorescence of HUES9 hESCs differentiated to DE on MGEL and FN + VTN (mean ± S.E.M.). (b) Quantification of HUES9 hESCs stained by SOX17 cells out of total cell number (*n* = 3; mean ± S.E.M.). (c) Flow cytometric analysis of CXCR4 expression of HUES9 hESCs differentiated to DE on MGEL and FN and VTN (FN + VTN). Gene expression analysis for markers of (d) DE (SOX17, FOXA2, CXCR4), (e) PGT (HNF1β, HNF4α), and (f and g) PF and PE (HNF6, PDX1) of HUES9 hESCs differentiated to DE, PGT, PF, and PE on MGEL and FN + VTN. (*n* = 3; error bars, S.E.M.). Asterisks indicate statistical significance relative to MGEL as determined by a two tail *t*-test

of DE differentiation over that observed when hESCs were differentiated on either ECMP alone (FN, VTN) or on MGEL (Supplementary Figures 3c and d).

To address whether culture on FN + VTN improved differentiation of hESC to more mature endodermal lineages, HUES9 were cultured on FN + VTN and MGEL and

differentiated to primitive gut tube (PGT), posterior foregut (PF), and pancreatic endoderm (PE) using previously published protocols (Figure 1a).[9] Expression of *HNF1β* and *HNF4α*, markers of both pancreas and liver development, was higher in cells differentiated on FN + VTN compared with those differentiated on MGEL (Figure 2e). Expression of the PF marker *HNF6* (Figure 2f) and the PE marker *PDX1* (Figure 2g) was higher in FN + VTN *versus* MGEL cultures. These results demonstrate that culture on FN + VTN increases differentiation efficiency toward endodermal lineages.

Integrin expression in hESC differentiation. Having established that FN and VTN were critical ECMP components to promote DE differentiation, we studied the role of integrin receptors in hESC differentiation. HESCs were differentiated to the three germ layers—endoderm, mesoderm, and ectoderm—using previously established protocols[2,15,16] and analyzed for integrin gene expression. Hierarchical clustering of integrin gene expression revealed specific integrin 'signatures' that defined each differentiated cell population, with a set of integrin genes (*ITGA4, ITGA5* (integrin α5), *ITGA7, ITGAV* (integrin αV), *ITGB2, ITGB5*) being upregulated in cells expressing endodermal markers (*SOX17, FOXA2, CXCR4*) relative to cells expressing either mesodermal (*SMA, ACTC1*) or ectodermal (*SOX1, SOX2*) marker genes (Figure 3a). Importantly, among these integrins, ITGA4, ITGA5, ITGAV, and ITGB5 encode subunits of heterodimeric integrin receptors that bind FN and VTN.[17–21]

As ITGA5 is required for hESC binding to FN and ITGAV, and ITGB5 are required for binding to VTN,[22] we investigated the expression levels of these integrin subunits as hESCs differentiate to DE. A time course of hESCs differentiating to DE revealed that *ITGA5* and *ITGAV* expression is upregulated in a dynamically similar manner to that of *SOX17* (Figure 3b). Furthermore, expression of *ITGB5* is also upregulated as cells differentiate to DE (Figure 3c), suggesting that hESCs display functional FN and VTN receptors as they differentiate to DE. By contrast, expression of the gene encoding subunits of the LN receptor, *ITGA6*, is significantly downregulated during endoderm differentiation of (Supplementary Figure 4a).

Using flow cytometry, we confirmed that expression of these three integrin receptors, detected by antibodies that bind ITGA5 (CD49e), ITGAV (CD51), and ITGB5, is increased in DE *versus* undifferentiated hESCs (Figures 3c and d). In comparison, flow cytometry of ITGA6 and ITGB1, integrin subunits that comprise the LN receptor, were either downregulated or unchanged as hESCs differentiated to DE (Supplementary Figures 4b and c). Taken together, these results suggest that hESCs differentiating to DE significantly upregulate cell surface expression of the subunits that comprise the integrin receptors that bind FN and VTN, the two ECMP components that we identified in our cellular microarray screen to promote DE differentiation.

Knockdown of ITGA5 and ITGAV impairs endoderm formation. To determine to what extent expression of the FN and VTN integrin receptors is functionally important during endodermal differentiation, we used a short hairpin RNA (shRNA) approach to knockdown expression of either

ITGA5 or ITGAV. HESCs stably harboring doxycycline (DOX) inducible shRNAs (Figure 4a) to either gene—referred to as ITGA5[shRNA] or ITGAV[shRNA] hESCs—were treated for 3 days with DOX (1 μg/ml) before induction of endodermal differentiation (see flowchart in Figure 4b). DOX treatment of either ITGA5[shRNA] or ITGAV[shRNA] hESCs and DE led to a significant increase in expression of red fluorescent protein (Supplementary Figure 5a), the expression of which was driven from the same DOX-inducible promoter as the shRNAs. QPCR analysis confirmed that expression of *ITGA5* and *ITGAV* was significantly decreased in DOX-treated undifferentiated hESC and DE cell populations (Figures 4c and d). Flow cytometry revealed that cell surface protein expression of ITGA5 and ITGAV was decreased in DOX-treated DE cell populations (Figures 4e and f). We confirmed that DOX treatment of ITGA5[shRNA] hESCs had no effect on *ITGAV* gene (Supplementary Figure 5b) or cell surface protein expression (Figure 4e). Similarly, DOX treatment of ITGAV[shRNA] hESCs had no effect on *ITGA5* gene (Supplementary Figure 5c) or cell surface protein expression (Figure 4f). Additionally, DOX treatment alone was not responsible for decreases in integrin expression as DOX treatment of wild-type hESCs had no effect on ITGA5 or ITGAV expression (Supplementary Figure 5d). Importantly, expression of the endodermal marker genes, *SOX17, FOXA2,* and *CXCR4*, was significantly decreased in hESC-derived DE in which *ITGA5* or *ITGAV* expression was knocked-down by the shRNAs (Figures 4c and d). Furthermore, flow cytometry revealed that CXCR4 cell surface expression was almost absent in DOX-treated DE cells (Figures 4e and f). IF analysis demonstrated that knockdown of either ITGA5 or ITGAV resulted in a significant reduction in SOX17 or FOXA2 staining at DE (Figures 4g and h). These results suggest that expression of FN and VN integrin receptors ITGA5 and ITGAV is necessary for differentiation of hESCs to DE.

ITGA5 and ITGAV as cell surface markers for the isolation of endodermal progeny from differentiating hESCs. As increases in ITGA5 (CD49e) and ITGAV (CD51) expression correlate with endodermal differentiation, we tested whether cell separation by flow cytometry for these integrin receptors could be employed to isolate cells with endodermal gene expression signatures (Figure 5a). HESC-derived DE was sorted for ITGA5 (CD49e) and ITGAV (CD51) (Figure 5b) and analyzed for expression of SOX17 (Figure 5c and Supplementary Figure 6). This analysis revealed that double-positive ITGA5(CD49e)[+]/ITGAV (CD51)[+] cells expressed higher amounts of the DE maker gene *SOX17* than single-positive ITGA5(CD49e)[+]/ITGAV (CD51)[−] or ITGA5(CD49e)[−]/ITGAV(CD51)[+] cells or double-negative ITGA5(CD49e)[−]/ITGAV(CD51)[−] cells (Supplementary Figure 6). Furthermore, expression of additional DE marker genes *FOXA2* and *CXCR4* was increased in double-positive cells compared with double-negative cells (Figure 5c). We next investigated if double-positive ITGA5(CD49e)[+]/ITGAV(CD51)[+] were capable of differentiating into more mature endodermal progeny. Double-positive ITGA5(CD49e)[+]/ITGAV(CD51)[+] and double-negative ITGA5(CD49e)[−]/ITGAV(CD51)[−] cells were replated
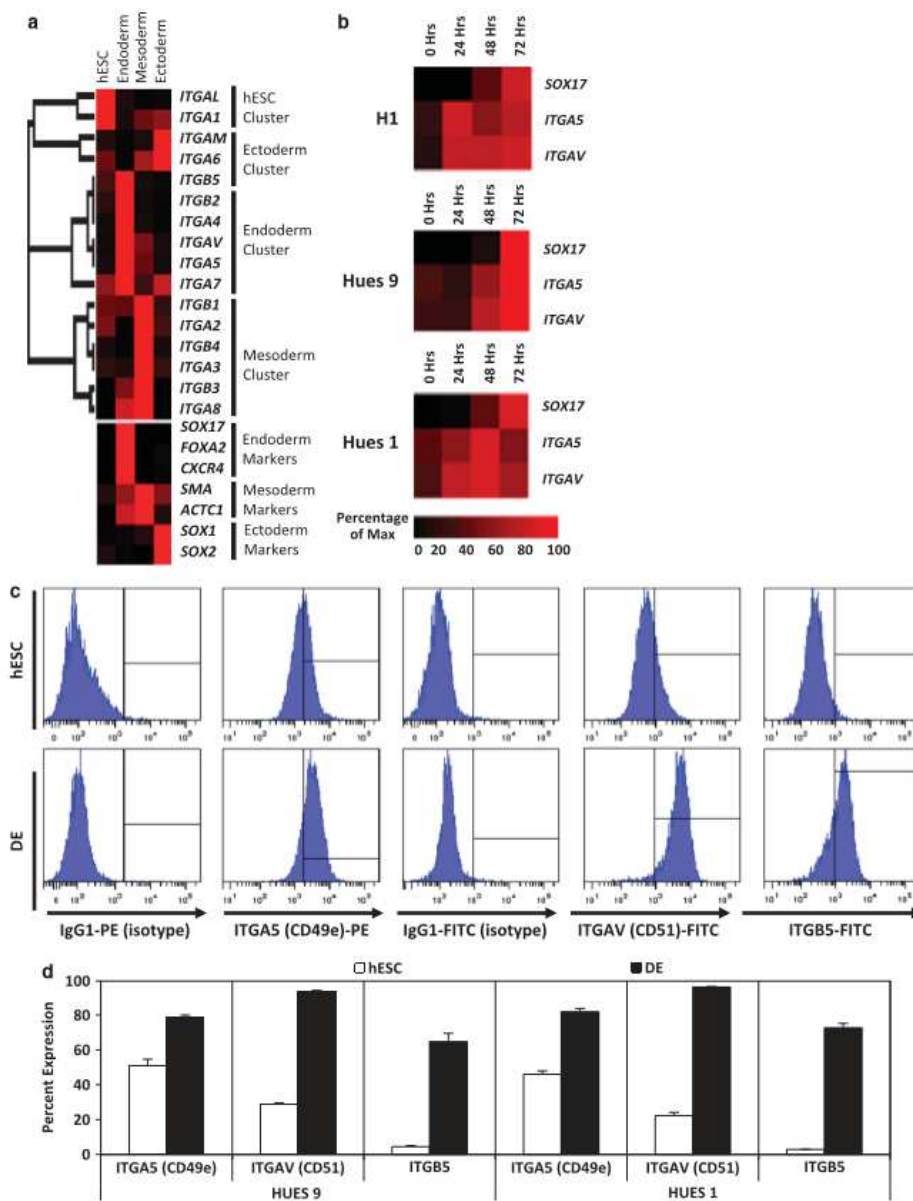
after cell sorting and differentiated to PGT. Subsequent gene expression analysis revealed that expression of *HNF1β* and *HNF4α*, markers of pancreas and liver development, were enriched in the ITGA5(CD49e)⁺/ITGAV(CD51)⁺ population relative to the ITGA5(CD49e)⁻/ITGAV(CD51)⁻ population (Figure 5d). Therefore, cell enrichment strategies for ITGA5 (CD49e) and ITGAV (CD51) significantly increase the yield of cells with DE gene expression patterns from differentiating hESC cultures.

Remodeling of the extracellular matrix during endodermal differentiation. In addition to exploring the effects of exogenous ECMP on DE formation, we wanted to investigate the role of endogenous ECMP production and remodeling during endodermal differentiation. To that end, we measured endogenous *ECMP* gene expression of hESCs differentiated to DE (Figure 6a). In general, expression of endogenous ECMPs increased as cells differentiated to DE on MGEL and FN + VTN substrates. Specifically, we observed a statistically significant increased expression of several COLs (*COL4A2, COL5A1, COL6A1, COL7A1, COL8A1, COL11A1, COL12A1*), *FN1, VTN*, and LN subunits (*LAMA3, LAMAB1, LAMAB3*) as hESCs differentiated to DE.

Previous studies have shown ECMP degradation and proteolysis have a critical role in endoderm development and cell differentiation.[23,24] Therefore, we wanted to determine if ECM remodeling and degradation through the action of matrix metalloproteinases (MMPs) was required for differentiation of hESCs to DE. While expression of *MMP* 1, 3, 7, 10, 12, or 13 was not detected in hESCs or DE (data not shown), we observed a statistically significant increased expression of *MMP* 2, 8, 9, 14, and 15 during DE differentiation (Figure 6b). To test whether MMP activity was required for DE differentiation, we treated cells with broad-spectrum small molecule inhibitors of MMP (Baritasmat, Marimastat, CP471474) and the glycoprotein tissue inhibitor of metalloproteinases (TIMP1) during DE differentiation. Gene expression analysis of DE markers *SOX17, FOXA2*, and *CXCR4* revealed that MMP inhibition does not inhibit formation of DE (Figure 6c). Therefore, even though we observe changes in the composition of the extracellular environment during DE differentiation, including endogenous deposition of ECMPs and secretion of MMPs, pharmacological inhibition of MMPs does not appear to disrupt endodermal differentiation of hESCs.

Discussion

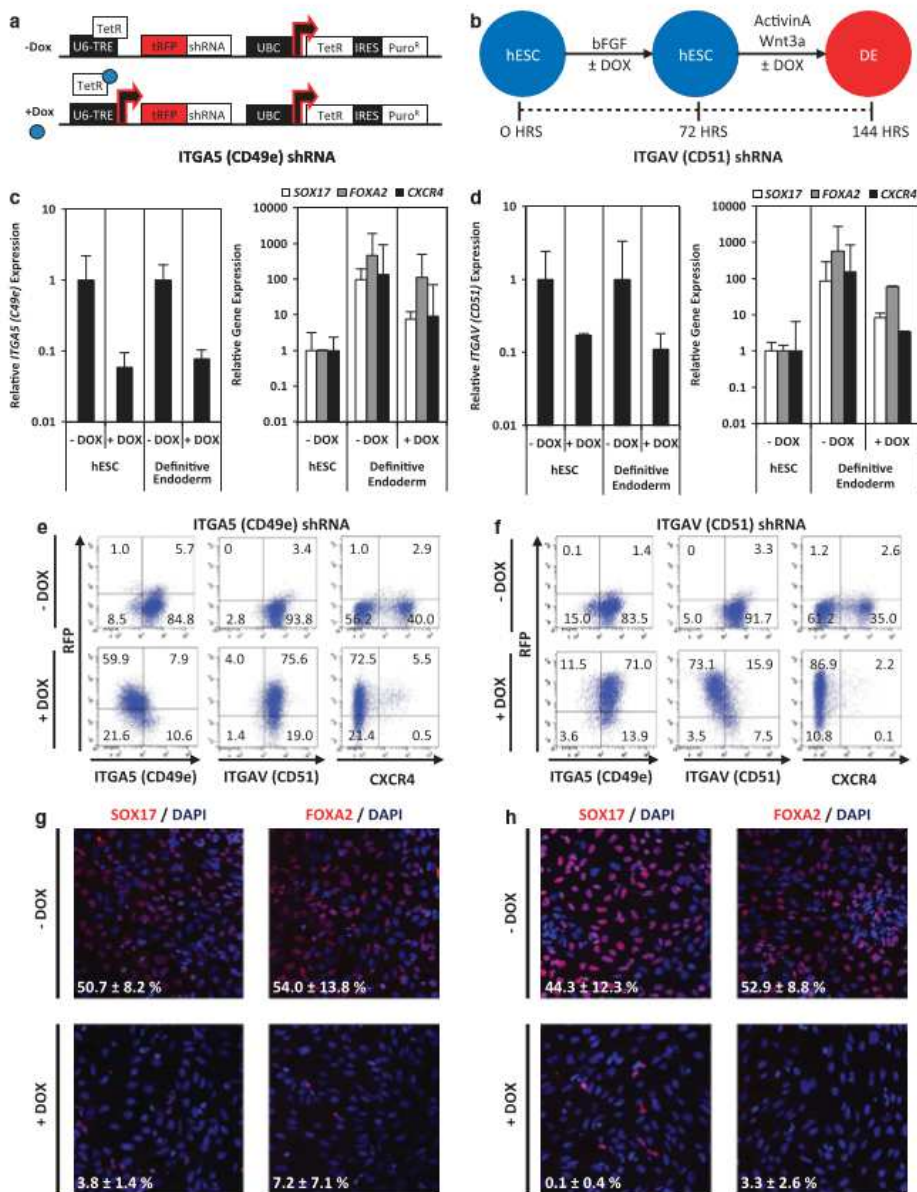The selection of the appropriate extracellular matrix is critical for hESC self-renewal and proliferation,[13,22] and here we show that the ECMP composition also potently influences hESC differentiation to DE. By systematically screening hundreds of ECMP combinations, we identified two ECMPs, FN, and VTN, which significantly improve the efficiency of hESC differentiation to DE, thereby overcoming the need for poorly defined and non-human biological components, such as MGEL, in the manipulation of hESCs.

While certain studies have explored the role of physical properties of the microenvironment, including three-dimensional culture[25] and substrate rigidity,[26] we focused our analysis on the role of the ECM in differentiation and found that changes in the composition of the ECM profoundly affected the differentiation of hESCs to endoderm. It is particularly important to note that the effects of the growth factors inducing DE (Wnt3a and Activin A) are significantly influenced by ECMP composition. Our results suggest that appropriately defining the ECMP substrate in addition to the soluble signaling molecule environment is critical for improving the differentiation of hESCs to specific lineages.

The differentiation of hESCs to DE resembles that of primitive streak formation and gastrulation where cells invaginate and generate mesendodermal cell populations. These movements of epiblast cells require several growth factor signaling pathways, as well as an ECM. In this process the ECM does not merely function as a scaffold through which cells migrate. Rather, as determined by computational and optical methods, migrating cells move in concert with the ECM with little cellular movement relative to the ECM.[27] This study supports the notion that the ECM has a more active role in development than previously appreciated and further underscores the importance of performing screens to identify optimal ECM compositions that promote specific developmental processes.

Consistent with our identification of FN and VTN as critical components that promote endodermal differentiation in cell culture, several studies in model organisms have provided compelling evidence that these ECM components are critical constituents of the microenvironment guiding the processes of primitive streak formation and gastrulation. For example, injection of agents that disrupt integrin-FN interactions, such as RGDS peptides or antibodies and Fab' fragments directed against FN, into chick embryos perturb gastrulation movements.[28] Such microinjection experiments in frog embryos have led to similar observations.[29] Mice lacking FN-binding integrins die early in development and fail to extend the anterior–posterior axis.[30–32] Earlier defects, such as during gastrulation, are likely not uncovered due to rescue by maternally contributed FN message and protein. Together, countless studies in a variety of model organisms support the concept that the ECM, and specifically FN, has an

Figure 3 Expression of integrin genes in hESC differentiation. (a) HUES9 hESCs were differentiated *in vitro* to the three germ layers (ectoderm, endoderm, and mesoderm) as previously described.[2,15,16] QPCR analysis of integrin gene expression was performed. The data is displayed as a heat map where black corresponds to minimum expression levels and red corresponds to maximum levels. Hierarchical clustering of integrin gene expression resulted in segregation of integrins into four groups based on their expression levels in hESCs or germ layer-specific cell types. (b) Time course of DE marker *SOX17* and FN/VTN specific subunits *ITGA5 (CD49e)* and *ITGAV (CD51)* gene expression during hESC (H1, HUES1, and HUES9) differentiation to DE. This analysis reveals that *SOX17*, *ITGA5 (CD49e)*, and *ITGAV (CD51)* gene expression increase in a dynamically similar manner. (c) Representative flow cytometry histograms of cell surface protein expression of FN/VTN specific subunits ITGA5 (CD49e), ITGAV (CD51), and ITGB5 in hESCs and DE. (d) Quantification of percentage of cell surface protein expression of ITGA5⁺ (CD49e⁺), ITGAV⁺ (CD51⁺), and ITGB5⁺ hESCs and DE (HUES9 and HUES1; n = 3; error bars, S.E.M.)

a ITGA5 (CD49e) shRNA

b ITGAV (CD51) shRNA

c

d

e ITGA5 (CD49e) shRNA

f ITGAV (CD51) shRNA

g SOX17 / DAPI   FOXA2 / DAPI

h SOX17 / DAPI   FOXA2 / DAPI

important and instructive function in early embryogenesis. However, it should be stressed that in our studies only the initial matrix compositions are specified. Cells exposed to these ECMPs remodel the underlying matrix and begin secreting their own ECMPs. Even so, the observed cellular responses are a result of their exposure to the initial composition of the ECM.

Previous studies demonstrated that undifferentiated hESCs express a variety of integrins, including integrins α1, 2, 3, 5, 6, 7, 11, E, and V, and β1, 2, 3, and 5.[33–35] We extended these studies by examining integrin gene expression in undifferentiated hESCs and hESC differentiated to each of the three primitive germ layers—endoderm, mesoderm, and ectoderm. This analysis revealed a specific integrin 'signature' that was unique to each of these cell populations. Specifically, we found that *ITGA5* and *ITGAV* gene expression was highly upregulated and *ITGA6* expression was significantly down-regulated in the endodermal lineage. Treatment with specific integrin blocking antibodies revealed that blocking ITGA5 impaired adhesion to FN, blocking ITGAV and ITGB5 reduced the binding to VTN, and blocking ITGA6 inhibited binding to LN.[22] Furthermore, ITGA6 binding to LN has been implicated as having a critical role in the self-renewal and maintenance of pluripotent hESCs.[36] In this study, we implemented an inducible shRNA system to demonstrate that knockdown of ITGA5 and ITGAV impaired endoderm formation. During development, integrin switching, rapid changes in the proportions of specific integrin subunits expressed at the cell surface, has been implicated as a mechanism that regulates cell differentiation.[37,38] Together our results suggest a possible mechanism in which hESCs differentiating to DE undergo an integrin switch from an ITGA6 signature which favors binding LN, and thereby maintenance of pluripotency, to an ITGA5 and ITGAV signature, which allows for interaction with FN and VTN and subsequent differentiation to DE.

Mouse models have been used extensively to interrogate integrin expression and functionality during embryonic development.[37,39,40] Interestingly, mouse embryos stained for different integrin subunits at E6.5 revealed that Itga5 expression was mainly restricted to endoderm,[41] which is consistent with the ITGA5 expression patterns that we identified in hESC-derived DE. Furthermore, Itga5 and ItgaV are widely expressed during development of many organs of endodermal origin, such as the pancreas, liver, and lungs.[42–44] Knockout of Itga5 or ItgaV resulted in embryonic lethality,[32,45] while tissue specific deletion of Itga5 or ItgaV resulted in vasculature and neuronal defects.[18,32,45,46] Therefore, the novel findings presented here, which demonstrate knockdown of ITGA5 and ITGAV in hESCs impaired endoderm formation in hESCs, suggests that similar integrin knockdown strategies

in hESCs can be used to interrogate the function of various integrin-ECMP interactions during the earliest stages of human development.

Current hESC differentiation protocols are insufficient in creating pure cell populations, which are required for understanding human development and creating disease relevant models. Therefore, developing sorting strategies for flow cytometry-based isolation of highly pure populations of cells from differentiating hESC cultures is of particular interest.[47–50] By investigating the role of integrin-ECMP interactions in hESC differentiation to DE, we identified a panel of novel surface integrins, ITGA5 (CD49e) and ITGAV (CD51), that allow for the FACS-based isolation of endodermal cells. In the future, similar integrin 'signatures' could be developed that would permit the isolation of lineage committed cells from mixed differentiated hESC cultures.

Materials and Methods

Arrayed cellular microenvironment fabrication. Arrayed cellular microenvironment (ACME) slides were fabricated as previously described. Briefly, glass slides were cleaned, silanized, and then functionalized with a polyacrylamide gel layer. Stock solutions of human COL I, COl III, COl IV, COl V, FN, LN (Sigma-Aldrich, St Louis, MO, USA) and VTN (EMD-Millipore, Billerica, MA, USA) were prepared in an ECMP-printing buffer (200 mM acetate, 10 mM EDTA, 40% (v/v) glycerol, and 0.5% (v/v) triton-X-100 in MQH2O, with pH adjusted to 4.9 using glacial acetic acid). All ECMP combinations were premixed at a constant protein concentration of 250 µg/ml in polypropylene 384-well plates. SMP 3.0 spotting pins (Telechem Corp., Atlanta, GA, USA) were washed with 90% ethanol. All printings were performed with a SpotArray 24 (Perkin-Elmer, Waltham, MA, USA) at room temperature (RT) with 65% relative humidity. The printing conditions were a 1000-ms inking time and a 250-ms stamping time. To control for variability, each ECMP combination was printed in replicates of five spots. Each spot had a diameter of 150–200 µm, and neighboring microenvironments were separated by a center-to-center distance of 450 µm. A single slide carried 6400 spots arranged in sixteen 20 × 20 matrices so that one slide carried 1280 unique ECMP conditions. Slides were inspected manually under a light microscope for consistent and uniform ECMP deposition. ECMP spotting was characterized using general protein stain (SYPRO Ruby gel stain, Life Technologies, Carlsbad, CA, USA) or protein specific antibodies (Sigma-Aldrich) as previously described. A single slide from each batch of printed arrays was seeded with HEK-293 (2.5 × 10^5 cells per slide) to ensure that each ECMP spot supported cell adhesion.

Cells and culture conditions. The following media were used: mouse embryonic fibroblast (MEF) (1 × high glucose DMEM, 10% fetal bovine serum (FBS), 1% (v/v) L-glutamine penicillin/streptomycin); H9/WA09 hESCs (1 × DMEM-F12, 20% (v/v) Knockout Serum Replacement, 1% (v/v) non-essential amino acids, 0.5% (v/v) glutamine, 120 µM 2-mercaptoethanol (Sigma-Aldrich)); HUES1 and nine hESCs (1 × Knockout DMEM, 10% (v/v) Knockout Serum Replacement, 10% (v/v) human plasmanate (Chapin Healthcare, Anaheim, CA, USA), 1% (v/v) non-essential amino acids, 1% (v/v) penicillin/streptomycin, 1% (v/v) Gluta-MAX, 55 µM 2-mercaptoethanol (Sigma-Aldrich)). All media components are from Life Technologies unless indicated otherwise. H9, HUES9, and HUES1 hESC lines were maintained on feeder layers of mitotically inactivated MEFs (2 × 10^4/cm²; Millipore). All hESC cultures were supplemented with 30 ng/ml bFGF (Life Technologies). MEF-CM was produced by culturing the appropriate

Figure 4 Expression of FN and VTN receptors integrin α5 (ITGA5) and integrin αv (ITGAV) is required for DE formation. (a) DOX-inducible shRNAs targeting ITGA5 (CD49e) and ITGAV (CD51) were introduced into hESCs (HUES9) using lenti-viral gene transduction. HESCs were selected with Puromycin until stable hESC lines were established. (b) ITGA5[shRNA] and ITGAV[shRNA] hESCs were treated with DOX for 72 h before induction of endoderm differentiation. QPCR analysis of DOX treated (c) ITGA5[shRNA] and (d) ITGAV[shRNA] hESCs revealed that expression of *ITGA5 (CD49e)* and *ITGAV (CD51)*, respectively, was decreased in both hESCs and DE. Expression of endoderm genes (*SOX17, FOXA2,* and *CXCR4*) was also decreased in DOX-treated hESCs (n = 3; error bars, S.E.M). Flow cytometric analysis of (e) ITGA5[shRNA] and (f) ITGAV[shRNA] hESCs revealed that cell surface protein expression of ITGA5 (CD49e) and ITGAV (CD51), respectively, was decreased in DOX-treated hESCs compared with untreated cells. Analysis also revealed that ITGAV (CD51) and ITGA5 (CD49e) cell surface protein expression was unchanged in DOX-treated ITGA5[shRNA] and ITGAV[shRNA] hESCs, respectively. Cell surface protein expression of the endoderm marker CXCR4 was also decreased in DOX-treated hESCs. Immunofluorescence of DOX treated (g) ITGA5[shRNA] and (h) ITGAV[shRNA] hESCs revealed that protein expression of endoderm markers SOX17 and FOXA2 decreased during DOX treatment (mean ± S.E.M)
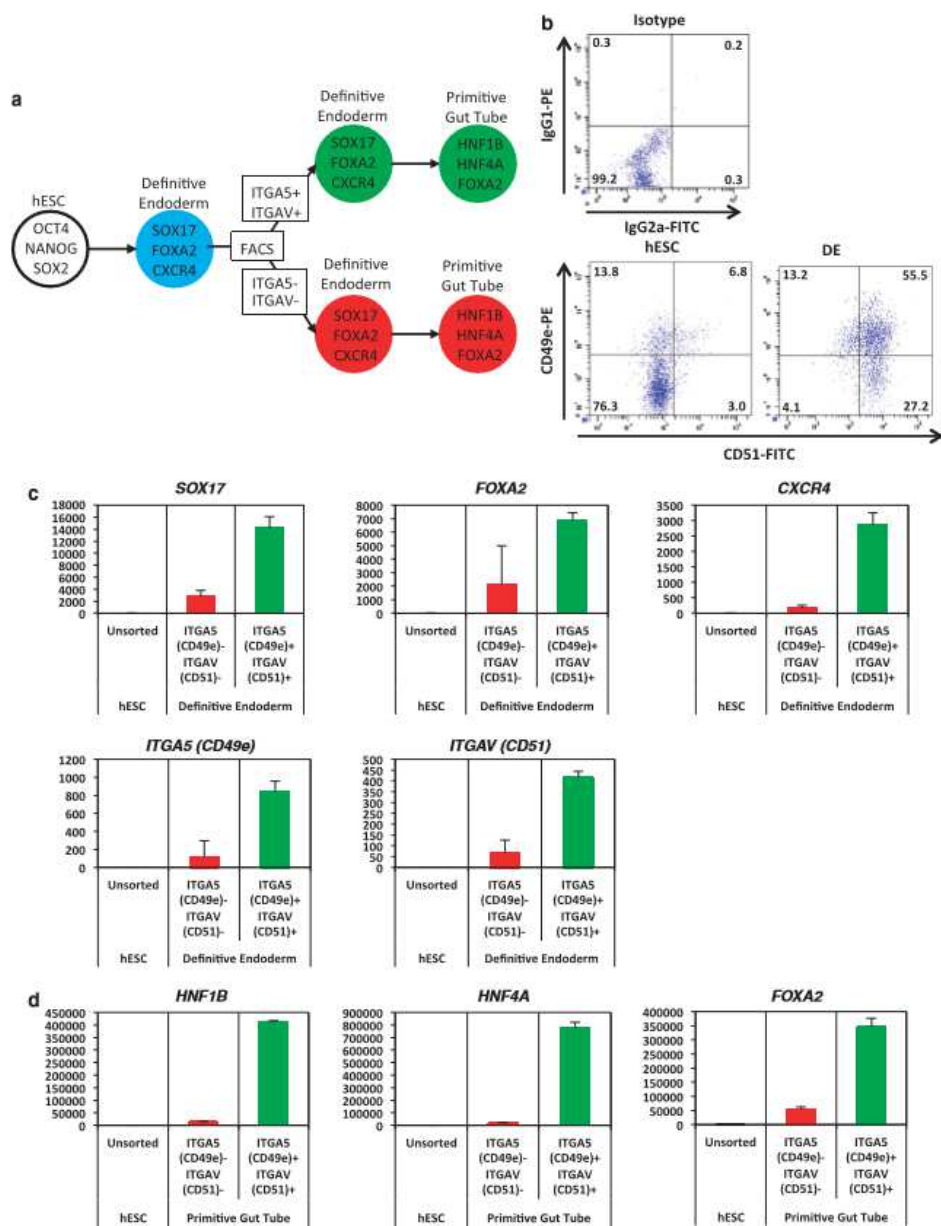
hESC medium on MEFs for 24 h. Cells were routinely passaged with Acutase (Millipore), washed, and replated at a density 4.25 × 10⁴/cm²).

Endoderm induction on ACME slides. Before their use, slides were soaked in PBS while being exposed to UVC germicidal radiation in a sterile flow hood for 10 min. Before seeding onto the ACME slides, hESCs were cultured for two passages on MGEL (BD) with MEF-CM supplemented with 30 ng/ml bFGF to remove residual feeder cells. HESCs were then acutase-passaged onto the ACME slides (5.0 × 105 cells per slide) and allowed to settle on the spots for 18 h. Array slides were then gently washed twice with RPMI (Life Technologies) to remove cell debris and residual hESC media. The medium was then changed to RPMI supplemented with 1% (w/v) Gluta-MAX and 100 ng/ml recombinant human Activin A (R&D Systems, Minneapolis, MN, USA). Cells were cultured for 3 days, with FBS concentrations at 0% for the first day and 0.2% for the second and third days. Cultures were supplemented with 30 ng/ml purified mouse Wnt3a for the first day.

Endoderm induction on defined ECMPs. H9, HUES9 and HUES1 were cultured on MGEL (BD) with MEF-CM supplemented with 30 ng/ml bFGF for 2 passages to remove residual MEFs. The human ECMP-coated plates were prepared by coating tissue culture plates in the ECMP (diluted in 10 mM acetic acid) overnight, followed by air drying. 10 μg of total protein was plated per cm² of culture dish surface. Human ECMP-coated plates were used immediately after air drying. HESCs were passaged at a density of 2.5 × 10⁵ cells/ml onto human ECMP or MGEL-coated plates in order to achieve confluency the following day. HESCs were then gently washed twice with RPMI (Life Technologies) to remove cell debris and residual hESC media. The medium was then changed to RPMI supplemented with 1% (w/v) Gluta-MAX and 100 ng/ml recombinant human Activin A (R&D Systems). Cells were cultured for 3 days, with FBS concentrations at 0% for the first day and 0.2% for the second and third days. Cultures were supplemented with 30 ng/ml purified mouse Wnt3a for the first day. For further differentiation to PGT, the medium was changed to RPMI with 0.2% FBS
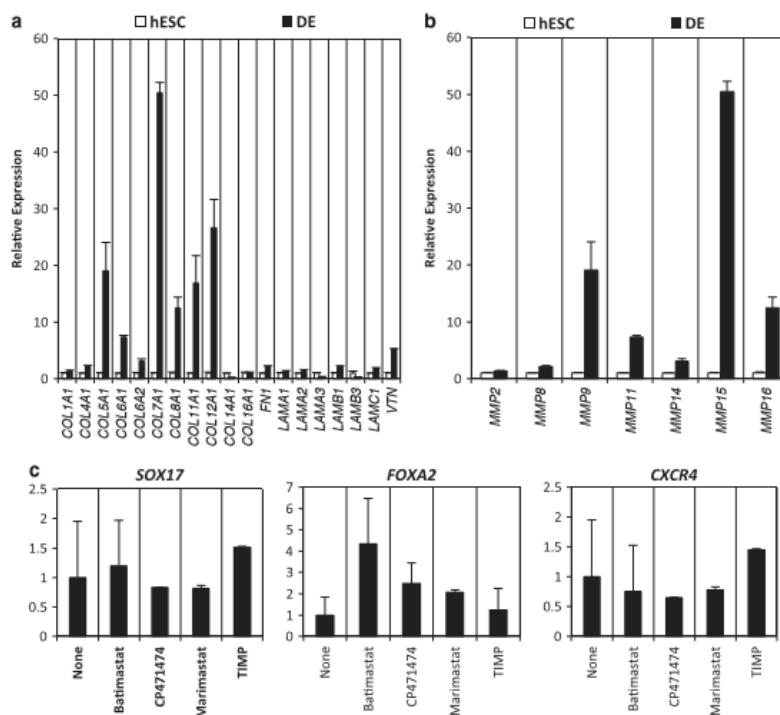
Figure 6 Remodeling of the exogenous extracellular matrix (ECM) during hESC differentiation to DE. QPCR analysis of (a) endogenous ECMP encoding genes and (b) matrix metalloproteinase (MMP) gene expression during hESC differentiation to DE. (c) hESCs were differentiated to DE in the presence of broad-spectrum inhibitors of MMP (Baritasmat, Marimastat, and CP471474) and TIMP1. QPCR analysis of DE markers SOX17, FOXA2, and CXCR4 revealed that MMP inhibition had no effect on DE differentiation

Figure 5 Purification of endoderm progeny from differentiating hESCs using the cell surface molecules Integrin α5 (ITGA5/CD49e) and integrin αv (ITGAV/CD51). (a) HESC-differentiated DE cells were sorted based on levels of ITGA5 (CD49e) and ITGAV (CD51) expression. ITGA5 (CD49e) ⁺/ITGAV (CD51) ⁺ and ITGA5 (CD49e) ⁻/ITGAV (CD51) ⁻ were replated and further differentiated *in vitro* to PGT cells. (b) Flow cytometry shows that that the expression of ITGA5 (CD49e) and ITGAV (CD51) changes during hESC differentiation to DE. (c) HESC-differentiated DE cells were sorted based on levels of ITGA5 (CD49e) and ITGAV (CD51) expression. Gene expression analysis reveals that the expression of endodermal markers *SOX17*, *FOXA2*, and *CXCR4* were highly enriched in the ITGA5 (CD49e) ⁺/ITGAV (CD51) ⁺ cells (n=3; error bars, S.E.M.). (d) Expression of PGT markers HNF1β, HNF4α, and *FOXA2* was enriched in *in vitro* differentiated ITGA5 (CD49e) ⁺/ITGAV (CD51) ⁺ cells (n=3; error bars, S.E.M.)

supplemented with 50 ng/ml recombinant human KGF (R&D Systems) for 3 days. For differentiation to PF endoderm, the medium was changed to DMEM with 1 × B27 (Life Technologies), 50 ng/ml recombinant human Noggin (R&D Systems), 0.25 μM KAAD-cyclopamine (Tocris Biosciences, Bristol, UK), and 2 μM retinoic acid (Sigma-Aldrich) for 3 days. Finally, for differentiation to PE the medium was changed to DMEM with 1 × B27 (Invitrogen) supplemented with 50 ng/ml recombinant human Noggin, 50 ng/ml recombinant human KGF, and 50 ng/ml recombinant human EGF (R&D Systems) and for 3 days.

Ectoderm and mesoderm differentiation. To differentiate hESCs to ectoderm we modified several previously published protocols.[9,15,51] To initiate ectoderm differentiation, hPSCs were cultured on MGEL in MEF-CM supplemented with 30 ng/ml FGF2. Cells were then detached with treatment with acutase (Millipore) for 5 min and resuspended in ectoderm embryoid body (EB) media (10% FBS/1% N2/1% B27/DMEM:F12) supplemented with 5 μM Y-267632 (Stemgent, Cambridge, MA, USA), 50 ng/ml recombinant mouse Noggin (R&D Systems), 0.5 μM Dorsomorphin (Tocris Biosciences). Next, 7.5 × 10^5 cells were pipetted to each well of several 6-well ultra low attachment plates (Corning, Lowell, MA, USA). The plates were then placed on an orbital shaker set at 95 r.p.m. in a 37 °C/5% CO_2 tissue culture incubator. The next day, the cells formed spherical clusters and the media was changed to ectoderm EB media without FBS supplemented with 50 ng/ml recombinant mouse Noggin and 0.5 μM Dorsomorphin. The media was subsequently changed every other day. After 5 days in suspension culture, the EBs were then transferred to a 10-cm dish coated (3 × 6 wells per 10 cm dish) with growth factor reduced MGEL (1 : 25 in KnockOut DMEM; BD Biosciences) for attachment. The plated EBs were cultured in ectoderm EB media without FBS supplemented with 50 ng/ml recombinant mouse Noggin and 0.5 μM Dorsomorphin for an additional 3 days. To differentiate hESC to mesoderm, we modified several previously published protocols.[16,52] To initiate mesoderm differentiation, hPSCs were cultured on MGEL in MEF-CM supplemented with 30 ng/ml FGF2 until they reached 60% confluency. Cells were then gently washed with RMPI media to remove residual hESC media. The medium was then changed to RPMI supplemented with 0.5% B27 supplement. Cells were cultured for 5 days supplemented with 100 ng/ml recombinant human Activin A (R&D systems) for the first day, and 10 ng/ml BMP4 for days 2–5.

Immunofluorescence. ACME slides and cultures were gently washed twice with staining buffer (PBS w/ 1% (w/v) BSA) before fixation. Cultures were then fixed for 15 min at RT with fresh paraformaldeyde (4% (w/v)). The cultures were washed twice with staining buffer and permeabilized with 0.2% (w/v) triton-X-100 in stain buffer for 20 min at 4 °C. Cultures were then washed twice with staining buffer. Primary antibodies were incubated overnight at 4 °C and then washed twice with stain buffer at RT. Secondary antibodies were incubated at RT for 1 h. Antibodies used are listed in Supplementary Table 2. Nucleic acids were stained for DNA with Hoechst 33342 (2 μg/ml; Life Technologies) for 5 min at RT. Imaging of was performed using an automated confocal microscope (Olympus Fluoview 1000 (Olympus America, Center Valley, PA, USA) with motorized stage and incubation chamber. Images of ACME slides were quantified using GenePix software (MDS Analytical Technologies, Molecular Devices, Sunnyvale, CA, USA). Quantification of additional images was performed by counting a minimum of nine fields at × 20 magnification.

Flow cytometry and cell replating. Cells were dissociated Acutase (Millipore) for 5 min at 37 °C, triturated, and passed through a 40 μm cell strainer. Cells were then washed twice with FACS buffer (PBS, 10 mM EDTA, and 2% FBS) and resuspended at a maximum concentration of 5 × 10^6 cells per 100 μl. One test volume of antibody was added for each 100 μl cell suspension (Supplementary Table 2). Cells were stained for 30 min on ice, washed, and resuspended in stain buffer. Cells were analyzed and sorted with a FACSCanto or FACSAria (BD Biosciences). FACS data was analyzed with FACSDiva software (BD Biosciences). For replating experiments, DE cells were stained with CD49e and CD51 and sorted into FACS buffer with 10 nm Y27632 (Stemgent). Sorted cells were replated at a density of 1 × 10^5 cells/cm^2 in stage 2 PGT media with 10 nM Y27632 and differentiated for 4 days.

MMP inhibition during endoderm differentiation. Before endoderm differentiation, hESC were treated with 0.5 μM Batimastat (Tocris Biosciences), 0.5 μM CP471474 (Tocris Biosciences), 0.5 μM Marimastat (Tocris Biosciences), or recombinant 130 nM human TIMP1 for 48 h. The medium was then changed to

RPMI supplemented with 1% (v/v) Gluta-MAX and 100 ng/ml recombinant human Activin A (R&D Systems). Cells were cultured for 3 days, with FBS concentrations at 0% for the first day and 0.2% for the second and third days. Cultures were supplemented with 30 ng/ml purified mouse Wnt3a for the first day. MMP inhibition continued throughout the duration of endoderm differentiation.

Quantitative PCR. RNA was isolated from cells using TRIzol (Life Technologies), and treated with DNase I (Life Technologies) to remove traces of DNA. Reverse transcription was performed by means of qScript cDNA Supermix (Quanta Biosciences, Gaithersburg, MA, USA). QPCR was carried out using TaqMan probes (Life Technologies) and TaqMan Fast Universal PCR Master Mix (Life Technologies) on a 7900HT Real Time PCR machine (Life Technologies), with a 10-min gradient to 95 °C followed by 40 cycles at 95 °C for 15 s and 60 °C for 1 min. Taqman gene expression assay primers (Life Technologies; Supplementary Table 3) were used. Gene expression was normalized to 18S rRNA levels. Delta C_t values were calculated as $C_t^{target} - C_t^{18s}$. All experiments were performed with three technical replicates. Relative fold changes in gene expression were calculated using the $2^{-\Delta\Delta C_t}$ method.[53] Data are presented as the average of the biological replicates ± S.E.M.

Generation of inducible shRNA hESCs. The lenti constructs that were used to generate the inducible shRNA lines were obtained from Open Biosystems (ITGA5:1334333, ITGAV:133468). High titer lenti virus was produced as previously described.[54,55] HUES9 hESCs were infected overnight with lenti virus and treated with puromycin (0.5 μg/ml) for 2 weeks.

Statistical analysis. For statistical analysis, unpaired t-test were used and a P-value < 0.05 was considered statistically significant. All values were presented as mean ± S.E.M. unless otherwise noted. For each ACME experiment, the ratio (R) of the log$_2$ of the SOX17 signal and the DNA signal was calculated for each spot. From this a differentiation z-score was calculated for each spot $Z_{DIF} = (R_i - \mu_{DIF})/\sigma_{DIF}$, where R_i was the ratio for the spot, μ_{DIF} was the average of the rations for all spots on each array, and σ_{DIF} was the S.D. of the ratios for all spots on each array. Differentiation z-scores from replication spots ($n = 5$ per ECMP condition) were averaged for each ECMP condition on the array. The replicate average z-scores were displayed in a heat map with rows corresponding to individual ECMP conditions and columns representing independent array experiments. For each array experiment, all columns were mean-centered and normalized to one unit S.D. The rows were clustered using Pearson correlations as a metric of similarity.[56] All clustering was performed using Gene Cluster.[56] The results were displayed using a color code with red and green representing an increase and decrease, respectively, relative to the global mean. All heat maps were created using Tree View.[56] Normalized effect magnitudes were calculated as previously described.[14]

Conflict of Interest

The authors declare no conflict of interest.

Author contributions

DAB and KW designed the experiments. DAB, CP, and NK performed the experiments. DAB, CP, and KW analyzed the results. DAB and KW wrote the manuscript.

1. Borowiak M, Maehr R, Chen S, Chen AE, Tang W, Fox JL et al. Small molecules efficiently direct endodermal differentiation of mouse and human embryonic stem cells. Cell Stem Cell 2009; 4: 348–358.
2. D'Amour KA, Agulnick AD, Eliazer S, Kelly OG, Kroon E, Baetge EE. Efficient differentiation of human embryonic stem cells to definitive endoderm. Nat Biotechnol 2005; 23: 1534–1541.
3. McLean AB, D'Amour KA, Jones KL, Krishnamoorthy M, Kulik MJ, Reynolds DM et al. Activin a efficiently specifies definitive endoderm from human embryonic stem cells only when phosphatidylinositol 3-kinase signaling is suppressed. Stem Cells 2007; 25: 29–38.

4. Osafune K, Caron L, Borowiak M, Martinez RJ, Fitz-Gerald CS, Sato Y et al. Marked differences in differentiation propensity among human embryonic stem cell lines. Nat Biotechnol 2008; 26: 313–315.
5. Berrier AL, Yamada KM. Cell-matrix adhesion. J Cell Physiol 2007; 213: 565–573.
6. Humphries JD, Byron A, Humphries MJ. Integrin ligands at a glance. J Cell Sci 2006; 119: 3901–3903.
7. Prowse AB, Chong F, Gray PP, Munro TP. Stem cell integrins: implications for ex-vivo culture and cellular therapies. Stem Cell Res 2011; 6: 1–12.
8. Kroon E, Martinson LA, Kadoya K, Bang AG, Kelly OG, Eliazer S et al. Pancreatic endoderm derived from human embryonic stem cells generates glucose-responsive insulin-secreting cells in vivo. Nat Biotechnol 2008; 26: 443–452.
9. Schulz TC, Young HY, Agulnick AD, Babin MJ, Baetge EE, Bang AG et al. A scalable system for production of functional pancreatic progenitors from human embryonic stem cells. PLoS One 2012; 7: e37004.
10. Brafman DA, Chang CW, Fernandez A, Willert K, Varghese S, Chien S. Long-term human pluripotent stem cell self-renewal on synthetic polymer surfaces. Biomaterials 2010; 31: 9135–9144.
11. Brafman DA, Chien S, Willert K. Arrayed cellular microenvironments for identifying culture and differentiation conditions for stem, primary and rare cell populations. Nat Protoc 2012; 7: 703–717.
12. Brafman DA, de Minicis S, Seki E, Shah KD, Teng D, Brenner D et al. Investigating the role of the extracellular environment in modulating hepatic stellate cell biology with arrayed combinatorial microenvironments. Integr Biol 2009; 1: 513–524.
13. Brafman DA, Shah KD, Fellner T, Chien S, Willert K. Defining long-term maintenance conditions of human embryonic stem cells with arrayed cellular microenvironment technology. Stem Cells Dev 2009; 18: 1141–1154.
14. Box G et al. Statistics for Experimenters. 1st edn. Wiley: New York, 1978.
15. Chambers SM, Fasano CA, Papapetrou EP, Tomishima M, Sadelain M, Studer L. Highly efficient neural conversion of human ES and iPS cells by dual inhibition of SMAD signaling. Nat Biotechnol 2009; 27: 275–280.
16. Yang L, Soonpaa MH, Adler ED, Roepke TK, Kattman SJ, Kennedy M et al. Human cardiovascular progenitor cells develop from a KDR + embryonic-stem-cell-derived population. Nature 2008; 453: 524–528.
17. Huang X, Griffiths M, Wu J, Farese RV Jr, Sheppard D. Normal development, wound healing, and adenovirus susceptibility in beta5-deficient mice. Mol Cell Biol 2000; 20: 755–759.
18. McCarty JH, Lacy-Hulbert A, Charest A, Bronson RT, Crowley D, Housman D et al. Selective ablation of alphav integrins in the central nervous system leads to cerebral hemorrhage, seizures, axonal degeneration and premature death. Development 2005; 132: 165–176.
19. Munger JS, Huang X, Kawakatsu H, Griffiths MJ, Dalton SL, Wu J et al. The integrin alpha v beta 6 binds and activates latent TGF beta 1: a mechanism for regulating pulmonary inflammation and fibrosis. Cell 1999; 96: 319–328.
20. Yang JT, Hynes RO. Fibronectin receptor functions in embryonic cells deficient in alpha 5 beta 1 integrin can be replaced by alpha V integrins. Mol Biol Cell 1996; 7: 1737–1748.
21. Yang JT, Rayburn H, Hynes RO. Cell adhesion events mediated by alpha 4 integrins are essential in placental and cardiac development. Development 1995; 121: 549–560.
22. Braam SR, Zeinstra L, Litjens S, Ward-van Oostwaard D, van den Brink S, van Laake L et al. Recombinant vitronectin is a functionally defined substrate that supports human embryonic stem cell self-renewal via alphavbeta5 integrin. Stem Cells 2008; 26: 2257–2265.
23. Behrendtsen O, Alexander CM, Werb Z. Cooperative interactions between extracellular matrix, integrins and parathyroid hormone-related peptide regulate parietal endoderm differentiation in mouse embryos. Development 1995; 121: 4137–4148.
24. Behrendtsen O, Werb Z. Metalloproteinases regulate parietal endoderm differentiating and migrating in cultured mouse embryos. Dev Dyn 1997; 208: 255–265.
25. Chen SS, Fitzgerald W, Zimmerberg J, Kleinman HK, Margolis L. Cell-cell and cell-extracellular matrix interactions regulate embryonic stem cell differentiation. Stem Cells 2007; 25: 553–561.
26. Engler AJ, Sen S, Sweeney HL, Discher DE. Matrix elasticity directs stem cell lineage specification. Cell 2006; 126: 677–689.
27. Zamir EA, Rongish BJ, Little CD. The ECM moves during primitive streak formation – computation of ECM versus cellular motion. PLoS Biol 2008; 6: e247.
28. Brown AJ, Sanders EJ. Interactions between mesoderm cells and the extracellular matrix following gastrulation in the chick embryo. J Cell Sci 1991; 99(Part 2): 431–441.
29. Boucaut JC, Darribere T, Li SD, Boulekbache H, Yamada KM, Thiery JP et al. Evidence for the role of fibronectin in amphibian gastrulation. J Embryol Exp Morphol 1985; 89(Suppl): 211–227.
30. George EL, Georges-Labouesse EN, Patel-King RS, Rayburn H, Hynes RO. Defects in mesoderm, neural tube and vascular development in mouse embryos lacking fibronectin. Development 1993; 119: 1079–1091.
31. Takahashi S, Leiss M, Moser M, Ohashi T, Kitao T, Heckmann D et al. The RGD motif in fibronectin is essential for development but dispensable for fibril assembly. J Cell Biol 2007; 178: 167–178.
32. Yang JT, Rayburn H, Hynes RO. Embryonic mesodermal defects in alpha 5 integrin-deficient mice. Development 1993; 119: 1093–1105.
33. Alavi SM, Rodina M, Viveiros AT, Cosson J, Gela D, Boryshpolets S et al. Effects of osmolality on sperm morphology, motility and flagellar wave parameters in Northern pike (Esox lucius L.). Theriogenology 2009; 72: 32–43.
34. Prowse AB, Doran MR, Cooper-White JJ, Chong F, Munro TP, Fitzpatrick J et al. Long term culture of human embryonic stem cells on recombinant vitronectin in ascorbate free media. Biomaterials 2010; 31: 8281–8288.
35. Rowland TJ, Miller LM, Blaschke AJ, Doss EL, Bonham AJ, Hikita ST et al. Roles of integrins in human induced pluripotent stem cell growth on Matrigel and vitronectin. Stem Cells Dev 2010; 19: 1231–1240.
36. Xu C et al. Feeder-free growth of undifferentiated human embryonic stem cells. Nat Biotechnol 2001; 19: 971–974.
37. Meighan CM, Schwarzbauer JE. Temporal and spatial regulation of integrins during development. Curr Opin Cell Biol 2008; 20: 520–524.
38. Zaidel-Bar R, Geiger B. The switchable integrin adhesome. J Cell Sci 2010; 123: 1385–1388.
39. Bokel C, Brown NH. Integrins in development: moving on, responding to, and sticking to the extracellular matrix. Dev Cell 2002; 3: 311–321.
40. Hynes RO. Integrins: bidirectional, allosteric signaling machines. Cell 2002; 110: 673–687.
41. Liu J, He X, Corbett SA, Lowry SF, Graham AM, Fässler R et al. Integrins are required for the differentiation of visceral endoderm. J Cell Sci 2009; 122: 233–242.
42. Coraux C, Delplanque A, Hinnrasky J, Peault B, Puchelle E, Gaillard D. Distribution of integrins during human fetal lung development. J Histochem Cytochem 1998; 46: 803–810.
43. Shiojiri N, Sugiyama Y. Immunolocalization of extracellular matrix components and integrins during mouse liver development. Hepatology 2004; 40: 346–355.
44. Wang R, Li J, Lyte K, Yashpal NK, Fellows F, Goodyer CG. Role for beta1 integrin and its associated alpha3, alpha5, and alpha6 subunits in development of the human fetal pancreas. Diabetes 2005; 54: 2080–2089.
45. van der Flier A, Badu-Nkansah K, Whittaker CA, Crowley D, Bronson RT, Lacy-Hulbert A et al. Endothelial alpha5 and alphav integrins cooperate in remodeling of the vasculature during development. Development 2010; 137: 2439–2449.
46. Marchetti G, Escuin S, van der Flier A, De Arcangelis A, Hynes RO, Georges-Labouesse E et al. Integrin alpha5beta1 is necessary for regulation of radial migration of cortical neurons during mouse brain development. Eur J Neurosci 2010; 31: 399–409.
47. Dubois NC, Craft AM, Sharma P, Elliott DA, Stanley EG, Elefanty AG et al. SIRPA is a specific cell-surface marker for isolating cardiomyocytes derived from human pluripotent stem cells. Nat Biotechnol 2011; 29: 1011–1018.
48. Elliott DA, Braam SR, Koutsis K, Ng ES, Jenny R, Lagerqvist EL et al. NKX2-5(eGFP/w) hESCs for isolation of human cardiac progenitors and cardiomyocytes. Nat Methods 2011; 8: 1037–1040.
49. Wang P, Rodriguez RT, Wang J, Ghodasara A, Kim SK. Targeting SOX17 in human embryonic stem cells creates unique strategies for isolating and analyzing developing endoderm. Cell Stem Cell 2011; 8: 335–346.
50. Yuan SH, Martin J, Elia J, Flippin J, Paramban RI, Hefferan MP et al. Cell-surface marker signatures for the isolation of neural stem cells, glia and neurons derived from human pluripotent stem cells. PLoS One 2011; 6: e17540.
51. Watanabe K, Kamiya D, Nishiyama A, Katayama T, Nozaki S, Kawasaki H et al. Directed differentiation of telencephalic precursors from embryonic stem cells. Nat Neurosci 2005; 8: 288–296.
52. Laflamme MA, Chen KY, Naumova AV, Muskheli V, Fugate JA, Dupras SK et al. Cardiomyocytes derived from human embryonic stem cells in pro-survival factors enhance function of infarcted rat hearts. Nat Biotechnol 2007; 25: 1015–1024.
53. VanGuilder HD, Vrana KE, Freeman WM. Twenty-five years of quantitative PCR for gene expression analysis. Biotechniques 2008; 44: 619–626.
54. Miyoshi H et al. Development of a self-inactivating lentivirus vector. J Virol 1998; 72: 8150–8157.
55. Zufferey R, Dull T, Mandel RJ, Bukovsky A, Quiroz D, Naldini L et al. Self-inactivating lentivirus vector for safe and efficient in vivo gene delivery. J Virol 1998; 72: 9873–9880.
56. Eisen MB, Spellman PT, Brown PO, Botstein D. Cluster analysis and display of genome-wide expression patterns. Proc Natl Acad Sci USA 1998; 95: 14863–14868.

Supplementary Information accompanies the paper on Cell Death and Differentiation website (http://www.nature.com/cdd)

References

Abdi, H., and Williams, L.J. (2010). Principal component analysis. Wiley Interdiscip. Rev. Comput. Stat. *2*, 433–459.

Ang, S.L., Wierda, A., Wong, D., Stevens, K.A., Cascio, S., Rossant, J., and Zaret, K.S. (1993). The formation and maintenance of the definitive endoderm lineage in the mouse: involvement of HNF3/forkhead proteins. Dev. Camb. Engl. *119*, 1301–1315.

Aulehla, A., and Pourquié, O. (2010). Signaling gradients during paraxial mesoderm development. Cold Spring Harb. Perspect. Biol. *2*, a000869.

Basma, H., Soto-Gutiérrez, A., Yannam, G.R., Liu, L., Ito, R., Yamamoto, T., Ellis, E., Carson, S.D., Sato, S., Chen, Y. (2009). Differentiation and transplantation of human embryonic stem cell-derived hepatocytes. Gastroenterology *136*, 990–999.

Beddington, R.S.P., and Smith, J.C. (1993). Control of vertebrate gastrulation: inducing signals and responding genes. Curr. Opin. Genet. Dev. *3*, 655–661.

Berrier, A.L., and Yamada, K.M. (2007). Cell–matrix adhesion. J. Cell. Physiol. *213*, 565–573.

Bianchi, G., Banfi, A., Mastrogiacomo, M., Notaro, R., Luzzatto, L., Cancedda, R., and Quarto, R. (2003). Ex vivo enrichment of mesenchymal cell progenitors by fibroblast growth factor 2. Exp. Cell Res. *287*, 98–105.

Blanpain, C., Lowry, W.E., Geoghegan, A., Polak, L., and Fuchs, E. (2004). Self-renewal, multipotency, and the existence of two cell populations within an epithelial stem cell niche. Cell *118*, 635–648.

Bone, H.K., Nelson, A.S., Goldring, C.E., Tosh, D., and Welham, M.J. (2011). A novel chemically directed route for the generation of definitive endoderm from human embryonic stem cells based on inhibition of GSK-3. J. Cell Sci. *124*, 1992–2000.

Borowiak, M., Maehr, R., Chen, S., Chen, A.E., Tang, W., Fox, J.L., Schreiber, S.L., and Melton, D.A. (2009). Small Molecules Efficiently Direct Endodermal Differentiation of Mouse and Human Embryonic Stem Cells. Cell Stem Cell *4*, 348–358.

Braam, S.R., Zeinstra, L., Litjens, S., Ward-van Oostwaard, D., van den Brink, S., van Laake, L., Lebrin, F., Kats, P., Hochstenbach, R., Passier, R. (2008). Recombinant Vitronectin Is a Functionally Defined Substrate That Supports Human Embryonic Stem Cell Self-Renewal via αVβ5 Integrin. STEM CELLS *26*, 2257–2265.

Brafman, D.A., de Minicis, S., Seki, E., Shah, K.D., Teng, D., Brenner, D., Willert, K., and Chien, S. (2009a). Investigating the role of the extracellular environment in modulating hepatic stellate cell biology with arrayed combinatorial microenvironments. Integr. Biol. *1*, 513–524.

Brafman, D.A., Shah, K.D., Fellner, T., Chien, S., and Willert, K. (2009b). Defining long-term maintenance conditions of human embryonic stem cells with arrayed cellular microenvironment technology. Stem Cells Dev *18*, 1141–1154.

Brafman, D.A., Chang, C.W., Fernandez, A., Willert, K., Varghese, S., and Chien, S. (2010). Long-term human pluripotent stem cell self-renewal on synthetic polymer surfaces. Biomaterials *31*, 9135–9144.

Brafman, D.A., Chien, S., and Willert, K. (2012). Arrayed cellular microenvironments for identifying culture and differentiation conditions for stem, primary and rare cell populations. Nat Protoc *7*, 703–717.

Brafman, D.A., Phung, C., Kumar, N., and Willert, K. (2013). Regulation of endodermal differentiation of human embryonic stem cells through integrin-ECM interactions. Cell Death Differ. *20*, 369–381.

Bush, K.T., Martovetsky, G., and Nigam, S.K. (2014). Relevance of ureteric bud development and branching to tissue engineering, regeneration and repair in acute and chronic kidney disease. Curr. Opin. Organ Transplant. *19*, 153–161.

Chambers, I., and Smith, A. (2004). Self-renewal of teratocarcinoma and embryonic stem cells. Oncogene *23*, 7150–7160.

Chambers, S.M., Fasano, C.A., Papapetrou, E.P., Tomishima, M., Sadelain, M., and Studer, L. (2009). Highly efficient neural conversion of human ES and iPS cells by dual inhibition of SMAD signaling. Nat. Biotechnol. *27*, 275–280.

Chen, G., Gulbranson, D.R., Hou, Z., Bolin, J.M., Ruotti, V., Probasco, M.D., Smuga-Otto, K., Howden, S.E., Diol, N.R., Propson, N.E. (2011). Chemically defined conditions for human iPSC derivation and culture. Nat Methods *8*, 424–429.

Chen, K.-D., Li, Y.-S., Kim, M., Li, S., Yuan, S., Chien, S., and Shyy, J.Y.-J. (1999). Mechanotransduction in Response to Shear Stress ROLES OF RECEPTOR TYROSINE KINASES, INTEGRINS, AND Shc. J. Biol. Chem. *274*, 18393–18400.

Chen, S., Borowiak, M., Fox, J.L., Maehr, R., Osafune, K., Davidow, L., Lam, K., Peng, L.F., Schreiber, S.L., Rubin, L.L. (2009). A small molecule that directs differentiation of human ESCs into the pancreatic lineage. Nat. Chem. Biol. *5*, 258–265.

Chen, S.S., Fitzgerald, W., Zimmerberg, J., Kleinman, H.K., and Margolis, L. (2007). Cell-Cell and Cell-Extracellular Matrix Interactions Regulate Embryonic Stem Cell Differentiation. STEM CELLS *25*, 553–561.

Chen, Y.-S., Lin, W.-C., and Miller, C. (2013). The Role of Complementary and Alternative Medicine in Regenerative Medicine. Evid.-Based Complement. Altern. Med. ECAM *2013*.

Cheng, X., Ying, L., Lu, L., Galvão, A.M., Mills, J.A., Lin, H.C., Kotton, D.N., Shen, S.S., Nostro, M.C., Choi, J.K. (2012). Self-Renewing Endodermal Progenitor Lines Generated from Human Pluripotent Stem Cells. Cell Stem Cell *10*, 371–384.

Christ, B., and Ordahl, C.P. (1995). Early stages of chick somite development. Anat. Embryol. (Berl.) *191*, 381–396.

Ciruna, B., and Rossant, J. (2001). FGF signaling regulates mesoderm cell fate specification and morphogenetic movement at the primitive streak. Dev. Cell *1*, 37–49.

Conlon, F.L., Lyons, K.M., Takaesu, N., Barth, K.S., Kispert, A., Herrmann, B., and Robertson, E.J. (1994). A primary requirement for nodal in the formation and maintenance of the primitive streak in the mouse. Dev. Camb. Engl. *120*, 1919–1928.

Cormier, J.T., Nieden, N.I.Z., Rancourt, D.E., and Kallos, M.S. (2006). Expansion of Undifferentiated Murine Embryonic Stem Cells as Aggregates in Suspension Culture Bioreactors. Tissue Eng. *12*, 3233–3245.

D'Amour, K.A., Agulnick, A.D., Eliazer, S., Kelly, O.G., Kroon, E., and Baetge, E.E. (2005). Efficient differentiation of human embryonic stem cells to definitive endoderm. Nat. Biotechnol. *23*, 1534–1541.

D'Amour, K.A., Bang, A.G., Eliazer, S., Kelly, O.G., Agulnick, A.D., Smart, N.G., Moorman, M.A., Kroon, E., Carpenter, M.K., and Baetge, E.E. (2006). Production of pancreatic hormone–expressing endocrine cells from human embryonic stem cells. Nat. Biotechnol. *24*, 1392–1401.

Davies, J.A., Unbekandt, M., Ineson, J., Lusis, M., and Little, M.H. (2012). Dissociation of embryonic kidney followed by re-aggregation as a method for chimeric analysis. Methods Mol Biol *886*, 135–146.

Davies, J.A., Chang, C.-H., Lawrence, M.L., Mills, C.G., and Mullins, J.J. (2014). Engineered kidneys: principles, progress, and prospects. Adv. Regen. Biol. *1*.

Engler, A.J., Sen, S., Sweeney, H.L., and Discher, D.E. (2006). Matrix Elasticity Directs Stem Cell Lineage Specification. Cell *126*, 677–689.

Eshghi, S., and Schaffer, D.V. (2008). Engineering microenvironments to control stem cell fate and function. In StemBook, (Cambridge (MA): Harvard Stem Cell Institute),.

Evseenko, D., Zhu, Y., Schenke-Layland, K., Kuo, J., Latour, B., Ge, S., Scholes, J., Dravid, G., Li, X., MacLellan, W.R. (2010). Mapping the first stages of mesoderm commitment during differentiation of human embryonic stem cells. Proc Natl Acad Sci U A *107*, 13742–13747.

Falk, A., Koch, P., Kesavan, J., Takashima, Y., Ladewig, J., Alexander, M., Wiskow, O., Tailor, J., Trotter, M., Pollard, S. (2012). Capture of Neuroepithelial-Like Stem

Cells from Pluripotent Stem Cells Provides a Versatile System for In Vitro Production of Human Neurons. PLoS ONE *7*, e29597.

Faust, C., and Magnuson, T. (1993). Genetic control of gastrulation in the mouse. Curr. Opin. Genet. Dev. *3*, 491–498.

Flaim, C.J., Chien, S., and Bhatia, S.N. (2005). An extracellular matrix microarray for probing cellular differentiation. Nat Methods *2*, 119–125.

Gallegos, T.F., Kouznetsova, V., Kudlicka, K., Sweeney, D.E., Bush, K.T., Willert, K., Farquhar, M.G., and Nigam, S.K. (2012). A protein kinase A and Wnt-dependent network regulating an intermediate stage in epithelial tubulogenesis during kidney development. Dev. Biol. *364*, 11–21.

Gospodarowicz, D., Neufeld, G., and Schweigerer, L. (1986). Molecular and biological characterization of fibroblast growth factor, an angiogenic factor which also controls the proliferation and differentiation of mesoderm and neuroectoderm derived cells. Cell Differ. *19*, 1–17.

Gouon-Evans, V., Boussemart, L., Gadue, P., Nierhoff, D., Koehler, C.I., Kubo, A., Shafritz, D.A., and Keller, G. (2006). BMP-4 is required for hepatic specification of mouse embryonic stem cell-derived definitive endoderm. Nat. Biotechnol. *24*, 1402–1411.

Gritti, A., Cova, L., Parati, E.A., Galli, R., and Vescovi, A.L. (1995). Basic fibroblast growth factor supports the proliferation of epidermal growth factor-generated neuronal precursor cells of the adult mouse CNS. Neurosci. Lett. *185*, 151–154.

Hannan, N.R.F., Fordham, R.P., Syed, Y.A., Moignard, V., Berry, A., Bautista, R., Hanley, N.A., Jensen, K.B., and Vallier, L. (2013). Generation of Multipotent Foregut Stem Cells from Human Pluripotent Stem Cells. Stem Cell Rep. *1*, 293–306.

Hay, D.C., Fletcher, J., Payne, C., Terrace, J.D., Gallagher, R.C.J., Snoeys, J., Black, J.R., Wojtacha, D., Samuel, K., Hannoun, Z. (2008). Highly efficient differentiation of hESCs to functional hepatic endoderm requires ActivinA and Wnt3a signaling. Proc. Natl. Acad. Sci. *105*, 12301–12306.

Hentze, H., Soong, P.L., Wang, S.T., Phillips, B.W., Putti, T.C., and Dunn, N.R. (2009). Teratoma formation by human embryonic stem cells: evaluation of essential parameters for future safety studies. Stem Cell Res. *2*, 198–210.

Hoveizi, E., Khodadadi, S., Tavakol, S., Karima, O., and Nasiri-Khalili, M.A. (2014). Small molecules differentiate definitive endoderm from human induced pluripotent stem cells on PCL scaffold. Appl. Biochem. Biotechnol. *173*, 1727–1736.

Humphries, J.D., Byron, A., and Humphries, M.J. (2006). Integrin ligands at a glance. J. Cell Sci. *119*, 3901–3903.

James, D., Nam, H., Seandel, M., Nolan, D., Janovitz, T., Tomishima, M., Studer, L., Lee, G., Lyden, D., Benezra, R. (2010). Expansion and maintenance of human embryonic stem cell-derived endothelial cells by TGFβ inhibition is Id1 dependent. Nat. Biotechnol. *28*, 161–166.

Jiang, W., Zhang, D., Bursac, N., and Zhang, Y. (2013). WNT3 is a biomarker capable of predicting the definitive endoderm differentiation potential of hESCs. Stem Cell Rep. *1*, 46–52.

Jones, D.L., and Wagers, A.J. (2008). No place like home: anatomy and function of the stem cell niche. Nat. Rev. Mol. Cell Biol. *9*, 11–21.

Kallos, M.S., and Behie, L.A. (1999). Inoculation and growth conditions for high-cell-density expansion of mammalian neural stem cells in suspension bioreactors. Biotechnol. Bioeng. *63*, 473–483.

Kee, K., and Reijo Pera, R.A. (2008). Human germ cell lineage differentiation from embryonic stem cells. CSH Protoc. *2008*, pdb.prot5048.

Kelly, O.G., Chan, M.Y., Martinson, L.A., Kadoya, K., Ostertag, T.M., Ross, K.G., Richardson, M., Carpenter, M.K., D'Amour, K.A., Kroon, E. (2011). Cell-surface markers for the isolation of pancreatic cell types derived from human embryonic stem cells. Nat. Biotechnol. *29*, 750–756.

Kirkeby, A., Grealish, S., Wolf, D.A., Nelander, J., Wood, J., Lundblad, M., Lindvall, O., and Parmar, M. (2012). Generation of Regionally Specified Neural Progenitors and Functional Neurons from Human Embryonic Stem Cells under Defined Conditions. Cell Rep. *1*, 703–714.

Kispert, A., Vainio, S., and McMahon, A.P. (1998). Wnt-4 is a mesenchymal signal for epithelial transformation of metanephric mesenchyme in the developing kidney. Development *125*, 4225–4234.

Kita-Matsuo, H., Barcova, M., Prigozhina, N., Salomonis, N., Wei, K., Jacot, J.G., Nelson, B., Spiering, S., Haverslag, R., Kim, C. (2009). Lentiviral vectors and protocols for creation of stable hESC lines for fluorescent tracking and drug resistance selection of cardiomyocytes. PLoS One *4*, e5046.

Krawetz, R., Taiani, J.T., Liu, S., Meng, G., Li, X., Kallos, M.S., and Rancourt, D.E. (2009). Large-Scale Expansion of Pluripotent Human Embryonic Stem Cells in Stirred-Suspension Bioreactors. Tissue Eng. Part C Methods *16*, 573–582.

Kroon, E., Martinson, L.A., Kadoya, K., Bang, A.G., Kelly, O.G., Eliazer, S., Young, H., Richardson, M., Smart, N.G., Cunningham, J. (2008). Pancreatic endoderm derived from human embryonic stem cells generates glucose-responsive insulin-secreting cells in vivo. Nat. Biotechnol. *26*, 443–452.

Kubo, A., Shinozaki, K., Shannon, J.M., Kouskoff, V., Kennedy, M., Woo, S., Fehling, H.J., and Keller, G. (2004). Development of definitive endoderm from embryonic stem cells in culture. Development *131*, 1651–1662.

Lawson, A., and Schoenwolf, G.C. (2003). Epiblast and primitive-streak origins of the endoderm in the gastrulating chick embryo. Development *130*, 3491–3501.

Ledran, M.H., Krassowska, A., Armstrong, L., Dimmick, I., Renström, J., Lang, R., Yung, S., Santibanez-Coref, M., Dzierzak, E., Stojkovic, M. (2008). Efficient Hematopoietic Differentiation of Human Embryonic Stem Cells on Stromal Cells Derived from Hematopoietic Niches. Cell Stem Cell *3*, 85–98.

Li, L., and Xie, T. (2005). STEM CELL NICHE: Structure and Function. Annu. Rev. Cell Dev. Biol. *21*, 605–631.

Lian, X., Hsiao, C., Wilson, G., Zhu, K., Hazeltine, L.B., Azarin, S.M., Raval, K.K., Zhang, J., Kamp, T.J., and Palecek, S.P. (2012). Robust cardiomyocyte differentiation from human pluripotent stem cells via temporal modulation of canonical Wnt signaling. Proc Natl Acad Sci U A *109*, E1848–E1857.

Lian, X., Zhang, J., Azarin, S.M., Zhu, K., Hazeltine, L.B., Bao, X., Hsiao, C., Kamp, T.J., and Palecek, S.P. (2013). Directed cardiomyocyte differentiation from human pluripotent stem cells by modulating Wnt/β-catenin signaling under fully defined conditions. Nat. Protoc. *8*, 162–175.

Lindner, V., and Reidy, M.A. (1991). Proliferation of smooth muscle cells after vascular injury is inhibited by an antibody against basic fibroblast growth factor. Proc. Natl. Acad. Sci. *88*, 3739–3743.

Lindsley, R.C., Gill, J.G., Kyba, M., Murphy, T.L., and Murphy, K.M. (2006). Canonical Wnt signaling is required for development of embryonic stem cell-derived mesoderm. Development *133*, 3787–3796.

Lorences, E.P., and Fry, S.C. (1991). Absolute measurement of cell expansion in plant cell suspension cultures. Plant Cell Tissue Organ Cult. *24*, 211–215.

Lowry, W.E., and Richter, L. (2007). Signaling in adult stem cells. Front. Biosci. J. Virtual Libr. *12*, 3911–3927.

Martovetsky, G., Tee, J.B., and Nigam, S.K. (2013). Hepatocyte nuclear factors 4α and 1α regulate kidney developmental expression of drug-metabolizing enzymes and drug transporters. Mol. Pharmacol. *84*, 808–823.

Mendjan, S., Mascetti, V.L., Ortmann, D., Ortiz, M., Karjosukarso, D.W., Ng, Y., Moreau, T., and Pedersen, R.A. (2014). NANOG and CDX2 pattern distinct subtypes of human mesoderm during exit from pluripotency. Cell Stem Cell *15*, 310–325.

Molofsky, A.V., Pardal, R., and Morrison, S.J. (2004). Diverse mechanisms regulate stem cell self-renewal. Curr. Opin. Cell Biol. *16*, 700–707.

Moore, K.A., and Lemischka, I.R. (2006). Stem cells and their niches. Science *311*, 1880–1885.

Morrison, S.J., and Spradling, A.C. (2008). Stem Cells and Niches: Mechanisms That Promote Stem Cell Maintenance throughout Life. Cell *132*, 598–611.

Moya, N., Cutts, J., Gaasterland, T., Willert, K., and Brafman, D.A. (2014). Endogenous WNT Signaling Regulates hPSC-Derived Neural Progenitor Cell Heterogeneity and Specifies Their Regional Identity. Stem Cell Rep. *3*, 1015–1028.

Murry, C.E., and Keller, G. (2008). Differentiation of embryonic stem cells to clinically relevant populations: lessons from embryonic development. Cell *132*, 661–680.

Naujok, O., Diekmann, U., and Lenzen, S. (2014). The generation of definitive endoderm from human embryonic stem cells is initially independent from activin A but requires canonical Wnt-signaling. Stem Cell Rev. *10*, 480–493.

Ng, E.S., Davis, R., Stanley, E.G., and Elefanty, A.G. (2008). A protocol describing the use of a recombinant protein-based, animal product-free medium (APEL) for human embryonic stem cell differentiation as spin embryoid bodies. Nat. Protoc. *3*, 768–776.

Nostro, M.C., Sarangi, F., Ogawa, S., Holtzinger, A., Corneo, B., Li, X., Micallef, S.J., Park, I.-H., Basford, C., Wheeler, M.B. (2011). Stage-specific signaling through TGFβ family members and WNT regulates patterning and pancreatic specification of human pluripotent stem cells. Development *138*, 861–871.

Olmer, R., Lange, A., Selzer, S., Kasper, C., Haverich, A., Martin, U., and Zweigerdt, R. (2012). Suspension culture of human pluripotent stem cells in controlled, stirred bioreactors. Tissue Eng. Part C Methods *18*, 772–784.

Osafune, K., Takasato, M., Kispert, A., Asashima, M., and Nishinakamura, R. (2006). Identification of multipotent progenitors in the embryonic mouse kidney by a novel colony-forming assay. Development *133*, 151–161.

Prowse, A.B.J., Chong, F., Gray, P.P., and Munro, T.P. (2011). Stem cell integrins: Implications for ex-vivo culture and cellular therapies. Stem Cell Res. *6*, 1–12.

Ra'em, T., and Cohen, S. (2012). Microenvironment design for stem cell fate determination. Adv. Biochem. Eng. Biotechnol. *126*, 227–262.

Reubinoff, B.E., Itsykson, P., Turetsky, T., Pera, M.F., Reinhartz, E., Itzik, A., and Ben-Hur, T. (2001). Neural progenitors from human embryonic stem cells. Nat. Biotechnol. *19*, 1134–1140.

Rho, J.-Y., Yu, K., Han, J.-S., Chae, J.-I., Koo, D.-B., Yoon, H.-S., Moon, S.-Y., Lee, K.-K., and Han, Y.-M. (2006). Transcriptional profiling of the developmentally important signalling pathways in human embryonic stem cells. Hum. Reprod. Oxf. Engl. *21*, 405–412.

Rivera-Pérez, J.A., and Magnuson, T. (2005). Primitive streak formation in mice is preceded by localized activation of Brachyury and Wnt3. Dev. Biol. *288*, 363–371.

Ross, J., Busch, J., Mintz, E., Ng, D., Stanley, A., Brafman, D., Sutton, V.R., Van den Veyver, I., and Willert, K. (2014). A rare human syndrome provides genetic evidence that WNT signaling is required for reprogramming of fibroblasts to induced pluripotent stem cells. Cell Rep *9*, 1770–1780.

Saini, V., Marchese, A., and Majetschak, M. (2010). CXC Chemokine Receptor 4 Is a Cell Surface Receptor for Extracellular Ubiquitin. J. Biol. Chem. *285*, 15566–15576.

Sasaki, H., and Hogan, B.L. (1993). Differential expression of multiple fork head related genes during gastrulation and axial pattern formation in the mouse embryo. Dev. Camb. Engl. *118*, 47–59.

Scadden, D.T. (2006). The stem-cell niche as an entity of action. Nature *441*, 1075–1079.

Schofield, R. (1978). The relationship between the spleen colony-forming cell and the haemopoietic stem cell. Blood Cells *4*, 7–25.

Schulz, T.C., Young, H.Y., Agulnick, A.D., Babin, M.J., Baetge, E.E., Bang, A.G., Bhoumik, A., Cepa, I., Cesario, R.M., Haakmeester, C. (2012). A Scalable System for Production of Functional Pancreatic Progenitors from Human Embryonic Stem Cells. PLoS ONE *7*, e37004.

Shin, S., Mitalipova, M., Noggle, S., Tibbitts, D., Venable, A., Rao, R., and Stice, S.L. (2006). Long-term proliferation of human embryonic stem cell-derived neuroepithelial cells using defined adherent culture conditions. Stem Cells Dayt. Ohio *24*, 125–138.

Sneddon, J.B., Borowiak, M., and Melton, D.A. (2012). Self-renewal of embryonic-stem-cell-derived progenitors by organ-matched mesenchyme. Nature *491*, 765–768.

Spence, J.R., Mayhew, C.N., Rankin, S.A., Kuhar, M.F., Vallance, J.E., Tolle, K., Hoskins, E.E., Kalinichenko, V.V., Wells, S.I., Zorn, A.M. (2011). Directed differentiation of human pluripotent stem cells into intestinal tissue in vitro. Nature *470*, 105–109.

Steiner, D., Khaner, H., Cohen, M., Even-Ram, S., Gil, Y., Itsykson, P., Turetsky, T., Idelson, M., Aizenman, E., Ram, R. (2010). Derivation, propagation and controlled differentiation of human embryonic stem cells in suspension. Nat. Biotechnol. *28*, 361–364.

Sweetman, D., Wagstaff, L., Cooper, O., Weijer, C., and Münsterberg, A. (2008). The migration of paraxial and lateral plate mesoderm cells emerging from the late primitive streak is controlled by different Wnt signals. BMC Dev. Biol. *8*, 63.

Taguchi, A., Kaku, Y., Ohmori, T., Sharmin, S., Ogawa, M., Sasaki, H., and Nishinakamura, R. (2014a). Redefining the in vivo origin of metanephric nephron

progenitors enables generation of complex kidney structures from pluripotent stem cells. Cell Stem Cell *14*, 53–67.

Taguchi, A., Kaku, Y., Ohmori, T., Sharmin, S., Ogawa, M., Sasaki, H., and Nishinakamura, R. (2014b). Redefining the in vivo origin of metanephric nephron progenitors enables generation of complex kidney structures from pluripotent stem cells. Cell Stem Cell *14*, 53–67.

Takeuchi, H., Nakatsuji, N., and Suemori, H. (2014). Endodermal differentiation of human pluripotent stem cells to insulin-producing cells in 3D culture. Sci. Rep. *4*.

Tam, P.P., and Behringer, R.R. (1997). Mouse gastrulation: the formation of a mammalian body plan. Mech. Dev. *68*, 3–25.

Tam, P.P., Parameswaran, M., Kinder, S.J., and Weinberger, R.P. (1997). The allocation of epiblast cells to the embryonic heart and other mesodermal lineages: the role of ingression and tissue movement during gastrulation. Development *124*, 1631–1642.

Thomson, J.A., Itskovitz-Eldor, J., Shapiro, S.S., Waknitz, M.A., Swiergiel, J.J., Marshall, V.S., and Jones, J.M. (1998). Embryonic stem cell lines derived from human blastocysts. Science *282*, 1145–1147.

Thorpe, C.J., Schlesinger, A., Carter, J.C., and Bowerman, B. (1997). Wnt Signaling Polarizes an Early C. elegans Blastomere to Distinguish Endoderm from Mesoderm. Cell *90*, 695–705.

Touboul, T., Hannan, N.R.F., Corbineau, S., Martinez, A., Martinet, C., Branchereau, S., Mainot, S., Strick-Marchand, H., Pedersen, R., Di Santo, J. (2010). Generation of functional hepatocytes from human embryonic stem cells under chemically defined conditions that recapitulate liver development. Hepatology *51*, 1754–1765.

Trapnell, C., Roberts, A., Goff, L., Pertea, G., Kim, D., Kelley, D.R., Pimentel, H., Salzberg, S.L., Rinn, J.L., and Pachter, L. (2012). Differential gene and transcript expression analysis of RNA-seq experiments with TopHat and Cufflinks. Nat. Protoc. *7*, 562–578.

Trapnell, C., Hendrickson, D.G., Sauvageau, M., Goff, L., Rinn, J.L., and Pachter, L. (2013). Differential analysis of gene regulation at transcript resolution with RNA-seq. Nat. Biotechnol. *31*, 46–53.

Unbekandt, M., and Davies, J.A. (2010). Dissociation of embryonic kidneys followed by reaggregation allows the formation of renal tissues. Kidney Int. *77*, 407–416.

VanGuilder, H.D., Vrana, K.E., and Freeman, W.M. (2008). Twenty-five years of quantitative PCR for gene expression analysis. Biotechniques *44*, 619–626.

Vescovi, A.L., Reynolds, B.A., Fraser, D.D., and Weiss, S. (1993). bFGF regulates the proliferative fate of unipotent (neuronal) and bipotent (neuronal/astroglial) EGF-generated CNS progenitor cells. Neuron *11*, 951–966.

Viotti, M., Foley, A.C., and Hadjantonakis, A.-K. (2014). Gutsy moves in mice: cellular and molecular dynamics of endoderm morphogenesis. Philos. Trans. R. Soc. Lond. B Biol. Sci. *369*, 20130547.

Wang, P., Alvarez-Perez, J.-C., Felsenfeld, D.P., Liu, H., Sivendran, S., Bender, A., Kumar, A., Sanchez, R., Scott, D.K., Garcia-Ocaña, A. (2015). A high-throughput chemical screen reveals that harmine-mediated inhibition of DYRK1A increases human pancreatic beta cell replication. Nat. Med. *21*, 383–388.

Wang, Y., Chou, B.-K., Dowey, S., He, C., Gerecht, S., and Cheng, L. (2013). Scalable expansion of human induced pluripotent stem cells in the defined xeno-free E8 medium under adherent and suspension culture conditions. Stem Cell Res. *11*, 1103–1116.

Warren, L., Manos, P.D., Ahfeldt, T., Loh, Y.H., Li, H., Lau, F., Ebina, W., Mandal, P.K., Smith, Z.D., Meissner, A. (2010). Highly efficient reprogramming to pluripotency and directed differentiation of human cells with synthetic modified mRNA. Cell Stem Cell *7*, 618–630.

Weissman, I.L. (2000). Stem cells: units of development, units of regeneration, and units in evolution. Cell *100*, 157–168.

Wilson, P.G., and Stice, S.S. (2006). Development and differentiation of neural rosettes derived from human embryonic stem cells. Stem Cell Rev. *2*, 67–77.

Xi, J., Liu, Y., Liu, H., Chen, H., Emborg, M.E., and Zhang, S.-C. (2012). Specification of Midbrain Dopamine Neurons from Primate Pluripotent Stem Cells. STEM CELLS *30*, 1655–1663.

Yang, L., Soonpaa, M.H., Adler, E.D., Roepke, T.K., Kattman, S.J., Kennedy, M., Henckaerts, E., Bonham, K., Abbott, G.W., Linden, R.M. (2008). Human cardiovascular progenitor cells develop from a KDR+ embryonic-stem-cell-derived population. Nature *453*, 524–528.

Yasunaga, M., Tada, S., Torikai-Nishikawa, S., Nakano, Y., Okada, M., Jakt, L.M., Nishikawa, S., Chiba, T., Era, T., and Nishikawa, S.-I. (2005). Induction and monitoring of definitive and visceral endoderm differentiation of mouse ES cells. Nat. Biotechnol. *23*, 1542–1550.

Zandstra, P.W., Eaves, C.J., and Piret, J.M. (1994). Expansion of hematopoietic progenitor cell populations in stirred suspension bioreactors of normal human bone marrow cells. Biotechnol. Nat. Publ. Co. *12*, 909–914.

Zhu, S., Wurdak, H., Wang, J., Lyssiotis, C.A., Peters, E.C., Cho, C.Y., Wu, X., and Schultz, P.G. (2009). A Small Molecule Primes Embryonic Stem Cells for Differentiation. Cell Stem Cell *4*, 416–426.

Zorn, A.M., and Wells, J.M. (2009). Vertebrate endoderm development and organ formation. Annu. Rev. Cell Dev. Biol. *25*, 221–251.

Zuk, P.A., Zhu, M., Ashjian, P., Ugarte, D.A.D., Huang, J.I., Mizuno, H., Alfonso, Z.C., Fraser, J.K., Benhaim, P., and Hedrick, M.H. (2002). Human Adipose Tissue Is a Source of Multipotent Stem Cells. Mol. Biol. Cell *13*, 4279–4295.

Zweigerdt, R., Olmer, R., Singh, H., Haverich, A., and Martin, U. (2011). Scalable expansion of human pluripotent stem cells in suspension culture. Nat. Protoc. *6*, 689–700.

Wiley: Statistics for Experimenters: Design, Innovation, and Discovery, 2nd Edition - George E. P. Box, J. Stuart Hunter, William G. Hunter.

On growth and form : Thompson, D'Arcy Wentworth, 1860-1948 : Free Download & Streaming.